Modelling and Simulation of Trickle-Bed Reactors Using Computational Fluid Dynamics: a State-of-The-Art Review

Yining Wang,[1,2] Jinwen Chen[1] and Faical Larachi[2]*

1. CanmetENERGY, Natural Resources Canada, Devon, Alberta, Canada, T9G 1A8

2. Department of Chemical Engineering, Laval University, Quebec, Quebec, Canada, G1V 0A6

Trickle-bed reactors (TBRs), which accommodate the flow of gas and liquid phases through packed beds of catalysts, host a variety of gas–liquid–solid catalytic reactions, particularly in the petroleum/petrochemical industry. The multiphase flow hydrodynamics in TBRs are complex and directly affect the overall reactor performance in terms of reactant conversion and product yield and selectivity. Non-ideal flow behaviours, such as flow maldistribution, channelling or partial catalyst wetting may significantly reduce the effectiveness of the reactor. However, conventional TBR modelling approaches cannot properly account for these non-ideal behaviours owing to the complex coupling between fluid dynamics and chemical kinetics. Recent advances in the application of computational fluid dynamics (CFD) to three-phase TBR systems have shown promise of achieving a deeper understanding of the interactions between multiphase fluid dynamics and chemical reactions. This study is intended to give a state-of-the-art overview of the progress achieved in the field of CFD simulation of TBRs over the past two decades. The fundamental modelling framework of multiphase flow in TBRs, advances in important constitutive models, and the application of CFD models are discussed in detail. Directions for future research are suggested.

RÉSUMÉ Les lits fixes arrosés à co-courant descendant de gaz et de liquide sont le siège d'innombrables processus catalytiques triphasiques, en particulier dans le domaine du raffinage pétrolier et de la pétrochimie. Les caractères polyphasique et non-idéal de leur hydrodynamique ont des répercussions importantes sur la conversion chimique, la productivité et la sélectivité. Ceci se traduit par l'entremise de la maldistribution des fluides, le mouillage partiel du catalyseur ou des écoulements préférentiels qui peuvent être déterminants en ce qui a trait à l'efficacité du réacteur. La mise en équation rigoureuse de ces non-idéalités et des couplages réaction-hydrodynamique a longtemps résisté aux approches de conceptualisation dites « conventionnelles ». Cette revue de synthèse s'attarde par conséquent à discuter les récentes avancées dans l'utilisation de la mécanique des fluides numérique comme outil « émergent et non-conventionnel » de description quantitative et fine des écoulements et des réactions catalytiques, et de leur interaction au sein de ces réacteurs. Spécifiquement, nous discuterons de la pertinence des différentes approches multi-fluides mises en œuvre, des relations constitutives développées et de l'utilisation de la mécanique des fluides numérique pour des applications pratiques des lits fixes arrosés. Nous suggérerons en guise d'épilogue de nouvelles directions de recherche dans ce domaine.

Keywords: trickle-bed reactor, computational fluid dynamics, multiphase hydrodynamics, constitutive equations

Mots clés: Lit fixe arrosé, mécanique des fluides numérique, hydrodynamique polyphasique, équations constitutives

INTRODUCTION

Trickle-bed reactors (TBRs) house packed beds of catalyst particles in which co-current downward flow of gas and liquid phases is the most common mode of operation. TBRs have achieved widespread commercial acceptance in many gas–liquid–solid catalytic industrial applications. They are mainly employed in the petroleum industry (for hydrocracking, hydrotreating, alkylation, etc.), the petrochemical industry, and the chemical industry (for hydrogenation of aldehydes, reactive amination, liquid-phase oxidation, etc.). TBRs are also used for the catalytic abatement of aqueous biocidal compounds in

*Author to whom correspondence may be addressed.
E-mail address: faical.larachi@gch.ulaval.ca
Can. J. Chem. Eng. 9999:1–45, 2012

DOI 10.1002/cjce.20702
Published online in Wiley Online Library (wileyonlinelibrary.com).

bio- and electro-chemical processing (Satterfield, 1975; Meyers, 1996; Dudukovic et al., 1999; Gladden et al., 2005; Anadon et al., 2006).

Improvements in TBR effectiveness and utilisation based on fundamental understanding can both reduce operation costs and increase process sustainability while meeting increasingly stringent environmental regulations (Bansal et al., 2005; Maiti and Nigam, 2007). The prospect of technological improvements continues to drive researchers and developers to enhance knowledge of TBRs and improve the understanding of the physicochemical phenomena involved in TBR operation. These pursuits have been subjects of longstanding interest (Iliuta et al., 1999a; Gladden et al., 2005).

TBRs have advantages in terms of cost and simplicity, but fully understanding the complex hydrodynamics inside these gas–liquid/solid multiphase reactors is challenging. Two-phase frictional pressure drop, liquid holdup and degree of wetting are some of the essential parameters for designing these reactors. Accordingly, the overall performance of a TBR is a complex function of reaction kinetics, operating pressure and temperature and flow hydrodynamics (including flow maldistribution, channelling, degree of catalyst wetting). In addition, due to complex interphase interactions, TBR scale-up is very sensitive to fluid dynamics and simple scaling rules often fail to provide proper design. In fact, the complex hydrodynamics of TBRs have inhibited the development of first-principle design procedures (by rigorously solving the complete phasic holdup-velocity field). Therefore, in the past several decades, various conventional reactor-modelling approaches have been proposed to characterise the complex non-ideal flow and mixing patterns in TBRs by introducing simplified flow assumptions (such as macromixing and micromixing). However, the use of these assumptions makes such approaches inappropriate as a design/diagnostic tool for TBR operations under the conditions outside their range of validity. In addition, without resolving the local velocity fields, conventional modelling approaches are unable to account for some important design factors (such as flow maldistribution, channelling and the influence of reactor internals). For trickle-flow operations, local flow and liquid holdup distribution are interrelated with operating and design variables in a very complex manner. Therefore, development of detailed multiphase fluid dynamic models is essential to capture the complex hydrodynamic interactions in TBRs and is beneficial for reliable and efficient reactor design.

The past two decades have witnessed widespread adoption of computational fluid dynamics (CFD) simulation methods in the realm of multiphase flows, in particular for providing refined and local analyses of phase flow distributions, transport and reactions in TBRs. In principle, the performance of TBRs as multiphase reactors can be predicted by solving the complete multidimensional flow equations coupled with chemical species transport, reaction kinetics and kinetics of phase change. Efforts aimed at developing CFD hydrodynamic modelling of (cold) TBRs remains by far the most eloquent. Some progress is being made in developing coupled multiphysics or reactive flow TBR computational models. Because of their first-principle foundations and ability to capture local phenomena, CFD-inspired TBR models are particularly powerful complements to experimental studies when such studies are impracticable due to a lack of appropriate instrumentation or are unaffordable due to the scale or operating severity of the unit to be scrutinised. Far more sophisticated than conventional models, CFD-based TBR models can specifically account for local geometrical variations and capture their repercussions on flow maldistribution, the formation of local hot spots, as well as the influence of reactor internals and inlet distributors. Historically, it is worthy of mention that the successes scored by multiphase flow CFD approaches have been partly attributed to the evolving maturity acquired in single-phase flow modelling and simulation. However, a number of the remaining numerical and physical modelling challenges are exclusive to the CFD analysis of trickle-bed (multiphase) flow systems (Sundaresan, 2000; Ranade et al., 2011). Among these challenges, it suffices to mention particle-scale partial wetting and interactive drag forces between flowing gas and liquid phases and their linkages to the bed structure.

A great number of review articles have been published in the open literature during the past several decades. Table 1 gives a chronological summary of review papers on TBRs, covering various aspects of three-phase TBRs (such as hydrodynamics, chemical kinetics, mass and heat transfer). Some of these review articles have also addressed the hydrodynamic and reactor modelling of TBR systems (Crine and L'Homme, 1983; Ramachandran et al., 1987; Attou and Boyer, 1999; Carbonell, 2000; Iliuta and Larachi, 2005d; Mederos et al., 2009b). However, up to now not a single review article devoted to the modelling and simulation of TBRs using a CFD approach has appeared in the open literature. The authors of the present study believe that a systematic review of the past and ongoing progress in this challenging research field is of great importance for future research efforts and that such a review is timely. Accordingly, the present study is intended to provide a state-of-the-art review of multiphase CFD simulation in the field of TBRs. Our review discusses the fundamental modelling framework of multiphase flow in TBRs, the key advances in important auxiliary model components, as well as the application of multiphase CFD models in analysing TBR performance. It is hoped that this review will stimulate additional research and development activities on the CFD modelling of TBRs.

PHYSICAL DESCRIPTION AND FLOW PATTERNS IN TBRs

The operation of TBRs involves a variety of gas–liquid flow interactions reflected in the form of flow regimes ranging from low- and high-interaction gas-continuous patterns to high-interaction liquid-continuous patterns. Identification of flow regime is an important task as different flow regimes may connote different levels of momentum, heat and mass transfer (Gunjal et al., 2005a).

In a TBR, four basic flow regimes may be encountered, depending on the flow rates of the gas and liquid phases, the properties of flowing fluids and the size and shape of stationary packing (Wammes et al., 1990; Gianetto and Specchia, 1992; Reinecke and Mewes, 1997; Attou and Boyer, 1999; Gunjal et al., 2005a). These regimes are illustrated schematically in Figure 1 (Reinecke and Mewes, 1997; Attou and Boyer, 1999). At low liquid and gas flow rates the liquid trickles over the packing and the gas phase is the continuous phase occupying the remaining voids. This regime, coined trickle-flow regime (Figure 1a), features partially or totally wet catalyst particles, depending on the flow rate and structure of the liquid flow. At the microscopic or particle level, the liquid flow textures in a bed consist of several features (Hartley and Murgatroyd, 1964; Charpentier et al., 1968a,b; Zimmerman and Ng, 1986; Maiti et al., 2006; Mederos et al., 2009b): liquid film flow, rivulets over the particles, pendular structures, liquid-filled channels and liquid-filled pockets (Figure 2). Pendular structures form at the contact points between packing particles, while liquid pockets may widen to spread over several contiguous pores. The

Table 1. Summary of literature reviews on trickle-bed reactors

Period	Refs.	Title
1960s	Østergaard (1968)	Gas–liquid–particle operations in chemical reaction engineering
1970s	Satterfield (1975)	Trickle-bed reactors
	Charpentier (1976)	Recent progress in two-phase gas–liquid mass transfer in packed beds
	Goto et al. (1977)	Trickle-bed oxidation reactors
	Hofmann (1978)	Multiphase catalytic packed-bed reactors
	Charpentier (1978)	Gas–liquid reactors
	Gianetto et al. (1978)	Hydrodynamics and solid–liquid contacting effectiveness in trickle-bed reactors
	Charpentier (1979)	Hydrodynamics of two-phase flow through porous media
1980s	Baldi (1981a)	Design and scale-up of trickle-bed reactors: solid–liquid contacting effectiveness
	Baldi (1981b)	Heat transfer in gas–liquid–solid reactors
	Baldi (1981c)	Hydrodynamics of multiphase reactors
	Herskowitz and Smith (1983)	Trickle-bed reactors—a review
	Crine and L'Homme (1983)	Recent trends in the modelling of catalytic trickle-bed reactors
	Mills and Dudukovic (1984)	A comparison of current models for isothermal trickle-bed reactors: application of a model reaction system
	Hanika and Stanek (1986)	Operation and design of trickle-bed reactors
	Charpentier (1986)	Mass transfer in fixed-bed reactors
	Dudukovic and Mills (1986)	Contacting and hydrodynamics in trickle-bed reactors
	Gianetto and Berruti (1986)	Modelling of trickle-bed reactors
	Ng and Chu (1987)	Trickle-bed reactors
	Ramachandran et al. (1987)	Recent advances in the analysis and design of trickle-bed reactors
	Lemcoff et al. (1988)	Effectiveness factor of partially wetted catalyst particles—evaluation and application to the modelling of trickle bed reactors
1990s	Zhukova et al. (1990)	Modelling and design of industrial reactors with a stationary bed of catalyst and two-phase gas–liquid flow—a review
	Sie (1999)	Scale effects in laboratory and pilot-plant reactors for trickle flow processes
	de Santos et al. (1991)	Mechanics of gas–liquid flow in packed-bed contactors
	Gianetto and Specchia (1992)	Trickle-bed reactors—state of art and perspectives
	Saroha and Nigam (1996)	Trickle-bed reactors
	Al-Dahhan et al. (1997)	High-pressure trickle-bed reactors: a review
	Sie and Krishna (1998)	Process development and scale up: III. Scale-up and scale-down of trickle bed processes
	Attou and Boyer (1999)	Hydrodynamics of gas–liquid–solid trickle-bed reactors: a critical review
2000s	Carbonell (2000)	Multiphase flow models in packed beds
	Maiti et al. (2004)	Trickle-bed reactors: liquid distribution and flow texture
	Iliuta and Larachi (2005d)	Modelling the hydrodynamics of gas–liquid packed beds via slit models: a review
	Nigam and Larachi (2005)	Process intensification in trickle-bed reactors
	Maiti et al. (2006)	Hysteresis in trickle-bed reactors: a review
	Maiti and Nigam (2007)	Gas–liquid distributors for trickle-bed reactors: a review
	Mederos et al. (2009a)	Review on criteria to ensure ideal behaviours in trickle-bed reactors
	Mary et al. (2009)	Trickle-bed laboratory reactors for kinetic studies
	Mederos et al. (2009b)	Steady-state and dynamic reactor models for hydrotreatment of oil fractions: a review

relative proportions of these structures are modulated by factors, such as fluid properties and flow rates, the distribution of inlet fluids, the size and shape of packing and the corresponding wettability and the packing and start-up schemes (Ravindra et al., 1997; Sederman and Gladden, 2001; Maiti et al., 2004).

The pulse-flow regime supplants trickle flow by increasing one of the phasic flow rates, provided the flow rate of the other phase is sufficient (Figure 1b). This regime features alternating gas-rich and liquid-rich structures traveling with more or less coherent frequencies and velocities. The onset of the pulse-flow regime can equally be viewed as an outcome of a statistically large number of single-pore pulsatile occurrences (Sicardi and Hofmann, 1980; Blok et al., 1983; Ng, 1986), or, complementarily, as a critical state where the stability of steady-state liquid and gas flow cannot be sustained (Grosser et al., 1988).

The spray (or mist) flow regime substitutes one of the two previous regimes at relatively high gas and low-liquid flow rates in which liquid entrainment in the form of droplets is imposed by strong shearing action by the gas phase (Figure 1c). Low gas flow rates and high liquid flow rates turn liquid into the continuous phase hosting a downward flow of gas in the form of (dispersed) bubbles (Figure 1d).

In the design or scale-up of TBRs, it is of importance to predict which flow regime dominates for a specified set of operating conditions. A simplistic though pragmatic approach categorises the dichotomy of the above flow patterns based on the interaction intensity between gas and liquid, namely, low-interaction and high-interaction regimes. The latter include pulse, spray and bubble/dispersed bubble flow regimes, whereas the former refers to a trickle-flow regime. In industrial practice, trickling and pulsing flow patterns are by far the most commonly encountered (Figure 3). Elucidating the characteristics of the hydrodynamics in these flow regimes and the transition between them has been a subject of ongoing interest (Iliuta et al., 1999b; Gladden et al., 2005). In the literature, up to now the CFD application in trickle-bed systems has been largely limited to the trickling-flow regime. A few researchers have also attempted to address the prediction of trickling-to-pulsing regime by coupling CFD approach and

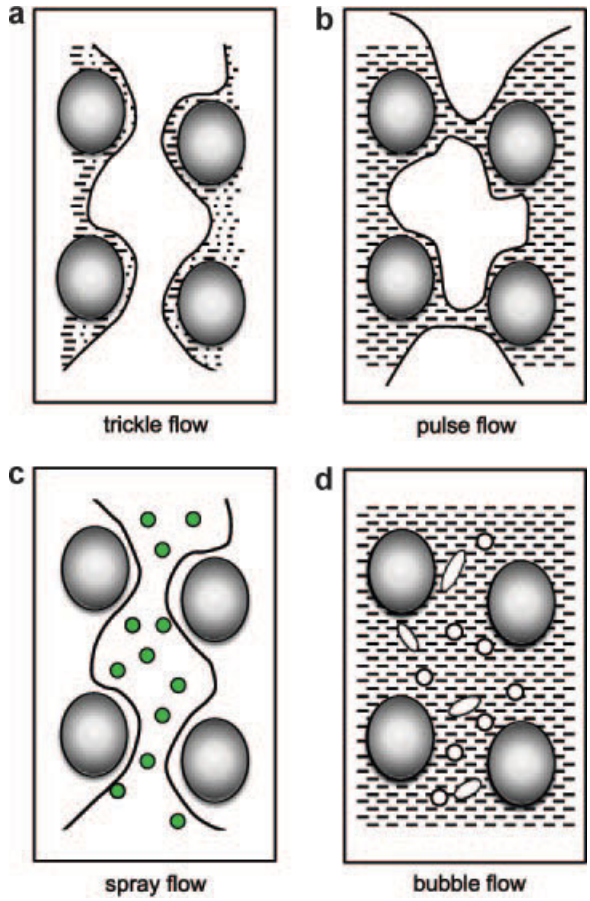

Figure 1. Schematic representation of the flow in trickle-bed reactors (Reinecke and Mewes, 1997): (a) trickle-flow regime, (b) pulse-flow regime, (c) spray-flow regime and (d) bubble-flow regime.

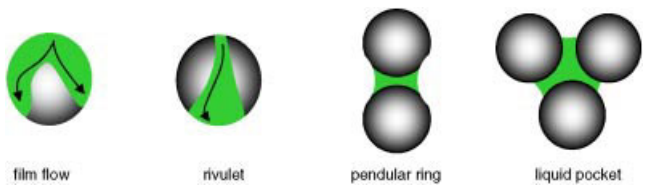

Figure 2. Schematic representation of liquid flow textures encountered in TBRs (Maiti et al., 2006).

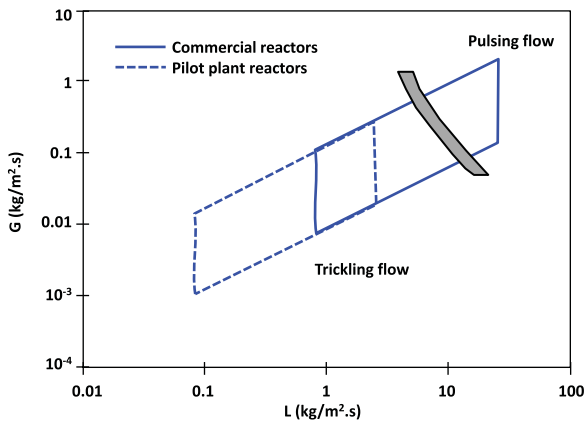

Figure 3. Representative flow conditions for petroleum processing in tickle-bed reactors (Satterfield, 1975; Nemec and Levec, 2005).

linear stability analysis (Attou and Ferschneider, 1999; Iliuta and Larachi, 2004c; Lopes and Quinta-Ferreira, 2010d).

MODELLING FRAMEWORK FOR MULTIPHASE FLOW IN TBRs

A trickle-bed multiphase flow can be simulated using standard methods from continuum mechanics whereby Navier–Stokes equations are solved for a realistic microscopically disordered geometry to yield ensemble (or volume)-averaged flow properties that reflect TBR local geometry and/or flow details. This is accomplished by viewing the multiphase system as a field made up of separate phases adhering to each other via bounded (stationary or moving) interfaces. The use of averaged transport equations allows numerical tractability (e.g. coarse meshing) and is often imposed as a surrogate approach to circumvent, provided pertinent closures are developed, the Achilles heel of a multi-boundary problem. However, these microscopic descriptions are invoked at the cost of averaging (jump conditions at interfaces) and lack formal descriptions of the newly generated additional terms. Closure models for such terms therefore become necessary. These closure models are system-dependent and are often formulated by recourse to approximate local flow field analysis, but also often to empiricism (Jakobsen, 2008).

Three typical modelling approaches pervade the literature on multiphase flow: the Euler–Lagrange, Euler–Euler and volume-of-fluid (VOF) approaches. (1) In the Euler–Langrange approach, the fluid phase is treated as a continuum by solving the Navier–Stokes equations in the same manner as for a single-phase system, while the dispersed phase is solved by tracking a large number of particles, bubbles or droplets through the calculated flow field using Newtonian equations of motion. A key assumption in this model is that the dispersed second phase occupies a low volume fraction. (2) In the Euler–Euler approach, the different phases are treated mathematically as interpenetrating continua. The volume fractions of each phase are assumed to be continuous functions of space and time and their sum is equal to unity. Conservation equations for each phase are derived to obtain a set of equations, which have similar structures for all phases. These equations require constitutive relations to achieve closure. (3) The VOF model is a surface-tracking technique applied to a fixed Eulerian mesh when the locus of the interface between two or more immiscible fluids is of interest. In the VOF model, a single set of momentum equations is shared by the fluids, and the volume fraction of each of the fluids in each computational cell is tracked throughout the domain. Typical applications of the VOF model include instances with steady-state or transient tracking of gas/liquid interfaces such as in free-surface flows or during the motion of large bubbles in a liquid (Li et al., 1999; Scardovelli and Zaleski, 1999; Fluent 6.3, 2006).

In the past two decades, two Eulerian-based multiphase modelling approaches (i.e. the Euler–Euler model and the VOF model) have been predominately practiced in the field of CFD simulation of TBRs (Jiang et al., 2002a,b; Gunjal et al., 2005a; Atta et al., 2007a; Janecki et al., 2008; Lappalainen et al., 2009a; Lopes and Quinta-Ferreira, 2007; Lopes and Quinta-Ferreira, 2010a,b), while the Euler–Lagrange approach remains scarce in the literature due to its limited suitability for cases characterised by a highly diluted phase. In the following sections, the general framework of continuity and momentum balance equations for these two modelling approaches will be presented, which could serve as a basis for further incorporation of appropriate closure models related to TBRs.

Eulerian VOF Multiphase Model

The various methods for interface simulation can be divided into two main classes: moving-grid or fixed-grid, depending on the nature of the grid used in the bulk of the phases. However, the oldest but still popular approach used to capture the fronts in multiphase flows relies directly on predefined, fixed grids that do not move with the interface. The VOF method (Hirt and Nichols, 1981), wherein a marker function is used, belongs to the fixed-grid category. The main hurdles to the use of VOF rest on preserving a sharp boundary between immiscible fluids and computations of surface tension (Brackbill et al., 1992; Tryggvason et al., 2001). An excellent review of the VOF method was given by Scardovelli and Zaleski (1999). Generally, the fixed-grid method becomes attractive because of its relatively simple description and ease of programming. Moreover, easier extension to three spatial dimensions is one of the principal advantages expected from this simplified formulation.

Actually, the VOF model is a surface-tracking technique using a fixed mesh system to resolve the sharp interface using the concept of a fractional VOF. It can be applicable for two or more immiscible fluids where the position of the interface between the fluids is of interest. A single set of momentum equations is shared by the fluids and the volume fraction of each fluid in each computational cell is tracked throughout the domain. The mass, momentum and energy conservation properties of the gas/liquid interface are modelled using continuum surface mechanisms. The physical processes across the sharp interface (such as surface tension and interphase mass transfer) are modelled utilising the concept of continuum surface force (CSF); (Brackbill et al., 1992; Fluent 6.3, 2006). Tracking of the interface between the phases is accomplished by the solution of continuity equation for the volume fraction of one (or more) of the phases. In the VOF model, the continuity equation for the q-th phase can be expressed in the following form:

$$\frac{\partial}{\partial t}(\alpha_q \rho_q) + \nabla(\alpha_q \rho_q u) = S_{\alpha_q} + \sum_{p=1}^{n} (\dot{m}_{pq} - \dot{m}_{qp}) \tag{1}$$

where $\dot{m}_{pq}$ is the mass transfer from phase q to phase p and $\dot{m}_{qp}$ is the mass transfer from phase p to phase q. S_{α_q} is used to compute the source term for each phase. The primary-phase volume fraction was computed based on the following constraint:

$$\sum_{q=1}^{n} \varepsilon_q = 1 \tag{2}$$

The VOF method belongs to the so-called *one* fluid family of methods, where a single set of conservation equations is solved. The momentum equation, which is dependent on the volume fractions of all phases through the mixture properties ρ_m and $\mu_{m,eff}$, is expressed by:

$$\frac{\partial(\rho_m u)}{\partial t} + \nabla(\rho_m u \otimes u) = -\nabla P + \nabla\left[\mu_{m,eff}\,(\nabla u + (\nabla u)^T)\right] + \rho_m g + F \tag{3}$$

This single-momentum equation is solved throughout the computational domain, and the resulting velocity field is shared among the phases. The VOF model includes the effects of surface tension along the interface between each pair of phases and the additional specification of the contact angles between the phases and the walls.

Surface tension acts to balance the radially inward intermolecular attractive force with the radially outward pressure gradient force across the surface. The most obvious associated difficulty relates to the singular term it gives rise to the Navier–Stokes equation (Scardovelli and Zaleski, 1999). This difficulty is manifest in several implementations as numerical instabilities, noise and in poor accuracy regarding capillary effects. Surface tension was thus ignored in many early implementations of the VOF method. Brackbill et al. (1992) pointed out that curvature of an interface modelled by a marker function can be computed by taking the divergence of a normal field in a region extended off the interface. This extension usually exists naturally, particularly if the marker function is smoothed slightly (Tryggvason et al., 2007). Once the normal field is found, the mean curvature is given by:

$$\kappa = \nabla \times n \tag{4}$$

This approach has become known as the CSF method (Brackbill et al., 1992). Using this model, adding surface tension to the VOF calculation results in a source term in the momentum equation. The surface tension is expressed in terms of the pressure jump across the surface. The force at the surface can be expressed as a volume force using the divergence theorem. It is this volume force that is the source term which is added to the momentum equation and has the following form:

$$F_{vol} = \sum_{\text{parts } ij, i<j} \sigma_{ij} \frac{\alpha_i \rho_i \kappa_j \nabla \alpha_j + \alpha_j \rho_j \kappa_i \nabla \alpha_i}{\frac{1}{2}(\rho_i + \rho_j)} \tag{5}$$

To specify the wall adhesion angle in conjunction with the surface tension model, the VOF model takes the model from Brackbill et al. (1992). Rather than imposing this boundary condition at the wall itself, the contact angle that the fluid is assumed to make with the wall is used to adjust the surface normal in cells near the wall. If θ_w is the contact angle at the wall, the surface normal at the live cell next to the wall is then given by:

$$\hat{n} = \hat{n}_w \cos\theta_w + \hat{t}_w \sin\theta_w \tag{6}$$

where $\hat{n}_w$ and $\hat{t}_w$ are the unit vectors normal and tangential to the wall, respectively. The combination of this contact angle with the regularly calculated surface normal one cell away from the wall determines the local curvature of the surface. This curvature is used to adjust the body force term in the surface tension calculation.

Eulerian Multifluid Multiphase Model

In the Eulerian multifluid approach, the gas and liquid phases are treated mathematically as interpenetrating continua. The derivation of the conservation equations for mass, momentum and energy for each of the individual phases is done by averaging the local instantaneous balances for each of the phases. The volume fractions are assumed to be continuous functions of space and time and their sum is equal to unity. The conservation equations for each phase have similar structures for all phases. Coupling of phases is taken into account through pressure and the so-called interphase mass, momentum and energy exchange coefficients. These coefficients are characteristic features of the model and play a key role. On the basis of the Eulerian modelling framework, the

averaged mass and momentum transport equations for each phase can therefore be written as follows:

Mass conservation equation:

$$\frac{\partial(\rho_k \varepsilon_k)}{\partial t} + \nabla(\rho_k \varepsilon_k u_k) = s_m \tag{7}$$

where the source term S_m contains the contribution added through phase changes or user-defined sources.

Momentum conservation equation:

$$\frac{\partial(\rho_k \varepsilon_k u_k)}{\partial t} + \nabla(\rho_k \varepsilon_k u_k \otimes u_k) = -\nabla(\varepsilon_k \tau_k) - \varepsilon_k \nabla P_k + \varepsilon_k \rho_k g + F_{I,k} \tag{8}$$

The respective terms on the right-hand side represent the stress, pressure gradient, gravitation and the interphase momentum exchange due to interfacial forces. The stress term of phase k is described as:

$$\tau_k = -\mu_{\text{eff},k}\left(\nabla u_k + (\nabla u_k)^T - \frac{2}{3} I(\nabla u_k)\right) \tag{9}$$

where $\mu_{eff,k}$ is the effective viscosity. The effective viscosity is composed of two contributions, the molecular viscosity and the turbulent viscosity:

$$\mu_{\text{eff},k} = \mu_{\text{lam}} + \mu_{\text{turb}} \tag{10}$$

To solve the whole system of governing equations, the interfacial momentum exchange term, $\mathbf{F}_{I,k}$, needs to be closed in terms of primary variables. In addition, turbulence has an influence on the effective viscosity, $\mu_{eff,k}$, therefore, a turbulence model has to be included for TBR for porous media, yielding additional closure equations. Furthermore, the closure relationship for the capillary pressure, P_c, which is represented by $P_c = P_G - P_L$ should be accounted for when the liquid saturations along the bed change significantly, and the capillary pressure gradient cannot then be neglected.

To properly model the gas–liquid flow distributions in trickle beds, it is essential to accomodate the complicating physics (related to trickling flow operation) into the multiphase flow model framework. In this regard, one should resolve the following critical issues (Jiang et al., 2001b): (i) how to implement the complex geometry of the packed bed in the flow equations (structure problem) and (ii) how to take into account the gas–liquid/solid interphase interactions (closure problem). In Computational Representation of Flow Geometries for Packed Beds of Spheres Section, the computational representation of flow geometry for packed beds of catalyst particles will be discussed first. The closure problems pertinent to interphase momentum exchange, interfacial capillary pressure, as well as turbulence in porous media, will then be addressed in Closure Methodolgies for CFD Modelling of TBRs Section.

COMPUTATIONAL REPRESENTATION OF FLOW GEOMETRIES FOR PACKED BEDS OF SPHERES

In a TBR, particles of a packing are randomly filled into the reactor, which results in structural non-ideality and inhomogeneities within the bed. Therefore, it is necessary to take into consideration the random nature of porous media (both the axial and radial distribution of the porosity of the packing) in developing CFD models for TBRs. Two different approaches of CFD modelling, the *effective porous medium approach* and the *discrete particle approach*, are found in the literature, and are discussed in turn in the following subsections.

"Effective Porous Medium" Approach and Porosity Distribution Representation

The effective-medium approximation is a method of treating a macroscopically inhomogeneous medium. In this approach, the bed is represented as an effective porous medium, with lumped parameters for dispersion and heat transfer (Ranade, 2002; Dixon et al., 2006). The velocity field can be obtained from a modified momentum balance or in the form of an Ergun-type equation. These approaches provide an averaged velocity field, usually in the form of a radially varying axial component of velocity, which is an improvement over the classical assumption of plug flow (constant unidirectional flow). Following introduction of the effective medium treatment of the porous medium or the random packings, the macroscopic modelling system can be cast into the Euler–Euler k-fluid framework whereby the presence of the particles is then modelled implicitly (with empirical correlations to describe the radial variation of porosity).

In a packed-bed reactor, the porosity varies sharply near the wall, resulting in near-wall velocity profile distortions. This can have a marked effect on the local flow distribution and wall heat transfer. Therefore, knowledge of the porosity distribution within a packed bed is important to any rigorous analysis of transport phenomena in the bed. There have been numerous research efforts during the past several decades to achieve a quantitative understanding of the porosity distribution in packed beds, and various researchers have proposed a number of empirical correlations to describe the radial variation of porosity. The correlations fall into two categories: oscillatory and exponential porosity correlations (du Toit, 2008; van Antwerpen et al., 2010). Table 2 summarises the relevant correlations for radial porosity distribution as well as their application/implementation in CFD simulation of TBRs in the literature.

In addition, some efforts have also been made to incorporate the global statistical nature of the porosity structure into CFD modelling (Jiang et al., 2002a; Gunjal et al., 2005a). Generally, cross-sectionally averaged porosity along the length of the bed is distributed randomly as well. To account for the globally random nature of cross-sectionally averaged porosity along the reactor length, Jiang et al. (2002a) developed a method to generate a random distribution of bed porosity using a porosity density function. The porosity distribution may then be represented by imposing random fluctuations over some correlations of axially averaged radial porosity. Boyer et al. (2005) attempted to measure the bed porosity at different bed heights and obtained a polynomial description of the cross-averaged bed porosity:

$$\varepsilon_0 = 0.421 - 0.124z + 0.047z^2 \tag{11}$$

where the axial coordinate, z, varies from 0 to 1.8 m.

The effect of different radial porosity models on liquid spreading in TBRs has been investigated through CFD simulations by Lappalainen et al. (2009a). The local packing structure and resulting porosity variation reflect the wall effect in the numerical model. It was shown by Lappalainen et al. (2009a) that the significance of wall channeling should be taken into account in CFD model development, especially for laboratory-scale TBRs with low D/d_p ratios. For industrial-scale reactors (high D/d_p ratios), the effect

Table 2. Summary of radial porosity distribution (RPD) models for packed beds in the literature

Refs.	Mathematical expressions of radial porosity distribution	Model characteristics	Application in TBRs (CFD)
Martin (1978)	$\varepsilon(x) = \begin{cases} \varepsilon_{\min} + (1-\varepsilon_{\min})x^2 & -1 \le x \le 0 \\ \varepsilon_b + (\varepsilon_{\min} - \varepsilon_b)e^{-x/4}\cos\left(\frac{\pi}{C}x\right) & x \ge 0 \end{cases}$ Where $x = 2\frac{R-r}{d_p} - 1$ $C = \begin{cases} 0.816 & (D/d_p) = \infty \\ 0.876 & (D/d_p) = 20.3 \end{cases}$ $\varepsilon_{\min} = 0.20 - 0.26$	Oscillatory correlation	
Cohen and Metzner (1981)	$\frac{1-\varepsilon(x)}{1-\varepsilon_b} = 4.5\left(x - \frac{7}{9}x^2\right)$ for $x \le 0.25$ $\frac{\varepsilon(x)-\varepsilon_b}{1-\varepsilon_b} = a_1 e^{-a_2 x}\cos[(a_3 x - a_4)\pi]$ for $x \in (0.25, 8)$ $\varepsilon(x) = \varepsilon_b$ for $x \ge 8$ With $x = \frac{R-r}{d_p}$ Constants: $a_1 = 0.3463, \quad a_2 = 0.4273, \quad a_3 = 2.4509, \quad a_4 = 2.2011$	Oscillatory correlation	Atta et al. (2007a) Lappalainen et al. (2009a)
Mueller (1991)	$\varepsilon(r) = \varepsilon_b + (1-\varepsilon_b)J_0(ar^*)\exp(-br^*)$ With $a = \begin{cases} 8.243 - \frac{12.98}{(D/d_p+3.156)} & \text{for } 2.61 \le D/d_p \le 13.0 \\ 7.383 - \frac{2.932}{(D/d_p-9.684)} & \text{for } D/d_p \ge 13.0 \end{cases}$ $b = 0.304 - \frac{0.724}{D/d_p},\ r^* = \frac{r}{d_p},\ \varepsilon_b = 0.379 + \frac{0.078}{(D/d_p-1.80)}$ J_0 is 0th-order Bessel function	Oscillatory correlation Zero-order first kind Bessel function	Lappalainen et al. (2009a) Gunjal et al. (2005a) Gunjal and Ranade (2007)
Mueller (1992)	$\varepsilon(r) = \varepsilon_b + (1-\varepsilon_b)J_0(ar^*)\exp(-br^*)$ With $a = \begin{cases} 7.45 - \frac{3.15}{D/d_p} & \text{for } 2.02 \le D/d_p \le 13.0 \\ 7.45 - \frac{11.25}{D/d_p} & \text{for } D/d_p \ge 13.0 \end{cases}$ $b = 0.315 - \frac{0.725}{D/d_p},\ r^* = \frac{r}{d_p},\ \varepsilon_b = 0.365 + \frac{0.220}{D/d_p}$ J_0 is 0th-order Bessel function	Oscillatory correlation Zero-order first kind Bessel function	
Bey and Eigenberger (1997)	$\varepsilon = \begin{cases} \varepsilon_{\min} + (1-\varepsilon_{\min})(r')^2 & r' < 0 \\ \varepsilon_0 + (\varepsilon_{\min} - \varepsilon_b)e^{-r'/c}\cos\left(\frac{\pi}{b}r'\right) & r' \ge 0 \end{cases}$ Where $r' = \frac{((D/2)-r)}{x_{\min}} - 1$ $x_{\min} = 0.5\left(D - \sqrt{(D-d_p)^2 - d_p^2}\right)$ $\bar{\varepsilon} = 0.375 + 0.34\frac{d_p}{D}$ (mean voidage) Constants: $\varepsilon_{\min} = 0.24,\ b = 0.876,\ c = 10$ Note: ε_0 is adjusted by fitting the integrated profile of $\varepsilon(r)$ to the value of $\bar{\varepsilon}$	Oscillatory correlation	Lappalainen et al. (2009a)
de Klerk (2003)	$\varepsilon(r) = \begin{cases} 2.14z^2 - 2.53z + 1 & \text{for } z \le 0.637 \\ \varepsilon_b + 0.29\exp(-0.6z)\cos(2.3\pi(z-0.16)) + 0.15\exp(-0.9z) & \text{for } z > 0.637 \end{cases}$ where $z = \frac{R-r}{d_p}$ $z = \frac{R-r}{d_p}$	Oscillatory correlation	Atta et al. (2010a)
Vortmeyer and Schuster (1983)	$\varepsilon = \varepsilon_b\left\{1 + C\exp\left(1 - 2\left(\frac{R-r}{d_p}\right)\right)\right\}$	Exponential correlation	
Sun et al. (2000)	$\varepsilon = 1 - (1-\varepsilon_b)\left\{1 - \exp\left(-2\left(\frac{R-r}{d_p}\right)^2\right)\right\}$	Exponential correlation	Atta et al. (2007a) Lappalainen et al. (2009a)

of near-wall channelling is less important and may be reasonably neglected in model implementation.

"Discrete Particle" Approach and Segmental Representation of Full Bed

The discrete particle approach (Dixon et al., 2006) is actually an interstitial flow modelling approach which accounts for the geometric complexity of the packing structure. Using this approach, fundamental understanding of the effects of bed geometry on transport phenomena in the reactor can be gained, though at the expense of cumbersome geometric modelling and grid generation, and computational power. So far, this approach has been restricted to small segments or periodic regions of the bed.

The reactants flowing through a packed-bed reactor can be both in the form of gas or liquid. In TBR applications, both gas and liquid phases are present as flowing phases. A great number of publications dealing with discrete particle CFD analysis of packed-bed reactors have been reported in the literature. Nonetheless, the majority of these efforts have been largely limited to *single-phase flow* through fixed beds (Logtenberg et al., 1999; McKenna and Spitz, 1999; Dixon and Nijemeisland, 2001; 2007; Nijemeisland and Dixon, 2001, 2004; Gunjal et al., 2005b; Guardo et al., 2006; Coussirat et al., 2007; Jafari et al., 2008; Motlagh and Hashemabadi, 2008; Xu and Jiang, 2008; Atmakidis and Kenig, 2009; Bai et al., 2009; Augier et al., 2010b; Baker and Tabor, 2010; Behnam et al., 2010; Dumas et al., 2010). An excellent review on discrete particle CFD analysis of single-phase flow through fixed beds has been provided by Dixon et al. (2006). However, relatively few studies have been conducted to date using a high-resolution CFD simulation approach for TBRs involving two moving phases. Nonetheless, research contributions, mainly from Professor Quinta-Ferreira's group (Portugal), are offered as progress in this direction.

A high-resolution CFD approach using discrete particles was proposed by Lopes and Quinta-Ferreira (Lopes et al., 2007; Lopes and Quinta-Ferreira, 2010a,b) to predict hydrodynamic parameters and reaction performance in TBRs. In their work, a TBR was designed using regularly shaped catalyst particles for the Euler–Euler simulation (Lopes et al., 2007; Lopes and Quinta-Ferreira, 2007, 2010a) and the Eulerian VOF simulation (Lopes and Quinta-Ferreira, 2010b). The gas and liquid phases flow through a catalytic bed comprising single-sized spherical catalyst particles (2-mm diameter) filling a cylindrical TBR unit (50-mm internal diameter $\times$ 1.0 m length). Given the high memory requirements, the computational mesh of the trickle bed was reduced in length so that the reactor could be filled with 10 layers in which around 200 spherical particles of 2-mm diameter were necessary for each axial layer. Numerical problems associated with mesh generation as reported in the literature (Nijemeisland and Dixon, 2001) were averted by not allowing the catalyst particles to touch each other and the distance gap was fixed at 2–3% of the sphere diameter. Different mesh sizes were evaluated for a grid-independent CFD solution of multiphase flow in the packed bed (Lopes and Quinta-Ferreira, 2010a,b). The CFD calculations were validated using experimental hydrodynamic data from the literature (Nemec and Levec, 2005b). Figure 4 provides a schematic representation of the packing geometry (Lopes and Quinta-Ferreira, 2010a) and the configuration of catalyst particles (Lopes and Quinta-Ferreira, 2009a) for the pilot-scale TBR adopted in their high-resolution CFD simulations.

Such high-resolution CFD approaches are very useful as learning tools to gain insights into the interplay between local flow structures, transport and reaction (Dixon et al., 2006). Furthermore, the understanding derived from high-solution CFD simulations could be rationalised into more computationally tractable "effective medium" simplified CFD models. By the way, studies of single-phase flow are themselves of particular interest since they are not only essential for single-phase applications, but also constitute the basis for studying two-phase flow through packed beds. Actually, the modelling methodologies and ideas of packing topology constructions that have been applied in fixed-bed CFD simulations with a single flowing phase could be adopted for use in CFD modelling of two-phase gas–liquid TBRs.

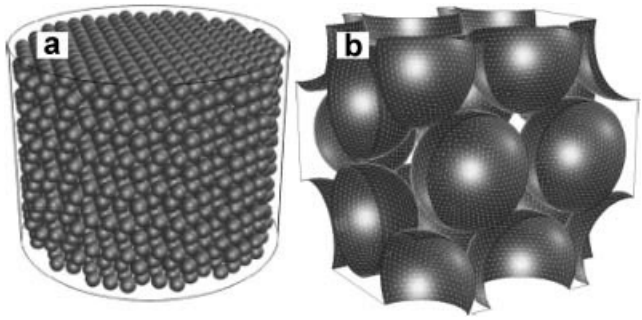

Figure 4. Schematic of the catalytic packing geometry: (a) the computational packing geometry of TBR (Lopes and Quinta-Ferreira, 2010a) and (b) the interstitial configuration of catalyst (Lopes and Quinta-Ferreira, 2009a).

CLOSURE METHODOLGIES FOR CFD MODELLING OF TBRs

The macroscopic multiphase models resulting from local averaging procedures must be supplemented with constitutive relationship, which is generally described as the closure problem. This refers to the fact that fluid–fluid and fluid–solid boundaries require closure relations that should be specified in order to properly deal with the phase interaction and the turbulence effects (if any) in the presence of porous media.

Interphase Interaction and Constitutive Equations for Momentum Exchange

Over the past several decades, considerable efforts have been invested in the study of the hydrodynamics of TBRs. As a result, along with a large body of empirical correlations available in the literature, some essential theoretical closure models linked with a fundamental physical basis or sound mechanistic concepts have been proposed in the literature as well. Among the theoretical approaches that provide closure in support of CFD simulation of TBRs, one can list the following: (i) the relative permeability model (Saez and Carbonell, 1985; Levec et al., 1986; Nemec and Levec, 2005a,b), (ii) slit model (Holub et al., 1992, 1993; Al-Dahhan and Dudukovic, 1994; Al-Dahhan et al., 1998; Iliuta and Larachi, 1999; Iliuta et al., 2000) and (iii) fundamental force balance model (Tung and Dhir, 1988; Attou et al., 1999; Narasimhan et al., 2002). Table 3 summarises these theoretical models for predicting the hydrodynamics of TBRs. In the sections that follow, the details of these theoretical models will be discussed further.

It is noted that, although a lot of research work has been conducted on the various hydrodynamic aspects of TBRs, most of the studies have been performed at atmospheric pressure, leading to correlations and models applicable at atmospheric conditions. Hydrodynamic studies performed in pressurised TBRs were summarised in the review of Al-Dahhan et al. (1997). They concluded

Table 3. Recent hydrodynamic models for the prediction of liquid holdup and pressure drop in trickle beds

Model type	Dimensionless model formulation	Refs.
I. Relative permeability model	$\psi_G = \left(\frac{\varepsilon_B}{\varepsilon_B-\varepsilon_L}\right)^{4.8}\left[\frac{E_1 Re_G}{Ga_G}+\frac{E_2 Re_G^2}{Ga_G}\right]$ $\psi_L = \left(\frac{\varepsilon_B-\varepsilon_L^0}{\varepsilon_L-\varepsilon_L^0}\right)^{2.43}\left[\frac{E_1 Re_L}{Ga_L}+\frac{E_2 Re_L^2}{Ga_L}\right]$	Saez and Carbonell (1985)
II-A. (Original) Single slit model	$\psi_G = \left(\frac{\varepsilon_B}{\varepsilon_B-\varepsilon_L}\right)^{3}\left[\frac{E_1 Re_G}{Ga_G}+\frac{E_2 Re_G^2}{Ga_G}\right]$ $\psi_L = \left(\frac{\varepsilon_B}{\varepsilon_L}\right)^{3}\left[\frac{E_1 Re_L}{Ga_L}+\frac{E_2 Re_L^2}{Ga_L}\right]$	Holub et al. (1992)
II-B. (Modified) Single slit model	$\psi_G = \left(\frac{\varepsilon_B}{\varepsilon_B-\varepsilon_L}\right)^{3}\left[\frac{E_1(Re_G-f_v(\varepsilon_B-\varepsilon_L)Re_i)}{Ga_G}+\frac{E_2(Re_G-f_v(\varepsilon_B-\varepsilon_L)Re_i)^2}{Ga_G}\right]$ $\psi_L = \left(\frac{\varepsilon_B}{\varepsilon_L}\right)^{3}\left[\frac{E_1 Re_L}{Ga_L}+\frac{E_2 Re_L^2}{Ga_L}\right]+f_s\frac{(\varepsilon_B-\varepsilon_L)}{\varepsilon_L}\left(1-\frac{\rho_G}{\rho_L}-\psi_L\right)$	Holub et al. (1993)
II-C. Double slit model	$\psi_G = \frac{\eta_e\varepsilon_B^3}{\left(\varepsilon_B-\frac{\varepsilon_L}{\eta_e}\right)^2(\varepsilon_B-\varepsilon_L)}\left[\frac{E_1\left(Re_G-f_v\left(\varepsilon_B-\frac{\varepsilon_L}{\eta_e}\right)Re_i\right)}{Ga_G}+\frac{E_2\left(Re_G-f_v\left(\varepsilon_B-\frac{\varepsilon_L}{\eta_e}\right)Re_i\right)^2}{Ga_G}\right]$ $+\frac{\varepsilon_B(1-\eta_e)}{(\varepsilon_B-\varepsilon_L)}\left(\frac{E_1 Re_G}{Ga_G}+\frac{E_2 Re_G^2}{Ga_G}\right)$ $\psi_L = \left(\frac{\varepsilon_B}{\varepsilon_L}\right)^{3}\left[\eta_e^2\frac{E_1 Re_L}{Ga_L}+\eta_e\frac{E_2 Re_L^2}{Ga_L}\right]+f_s\frac{(\eta_e\varepsilon_B-\varepsilon_L)}{\varepsilon_L}\left(1-\frac{\rho_G}{\rho_L}-\psi_L\right)$ $\eta_e = \frac{\phi^2}{2E_1}\left(\frac{\varepsilon_L}{\varepsilon_B}\right)^2\left(\psi_L-1+\frac{\rho_G}{\rho_L}\right)\frac{Ga_L}{Re_L}f_s+\left\{\begin{array}{l}\left[\frac{\phi^2}{2E_1}\left(\frac{\varepsilon_L}{\varepsilon_B}\right)^2\left(\psi_L-1+\frac{\rho_G}{\rho_L}\right)\frac{Ga_L}{Re_L}f_s\right]^2\\-\frac{\phi^2}{E_1}\left(\frac{\varepsilon_L}{\varepsilon_B}\right)^3\left(\psi_L-1+\frac{\rho_G}{\rho_L}\right)\frac{Ga_L}{Re_L}f_s\\+\frac{2\phi^2}{3E_1}\left(\frac{\varepsilon_L}{\varepsilon_B}\right)^3\psi_L\frac{Ga_L}{Re_L}\end{array}\right\}^{1/2}$	Iliuta et al. (2000)
III. Fundamental force balance model	$\psi_G = \left(\frac{1-\varepsilon_B+\varepsilon_L}{1-\varepsilon_L}\right)^{2/3}\left[\frac{E_1(1+\lambda)Re_G}{Ga_G}\left(\frac{\varepsilon_B}{\varepsilon_B-\varepsilon_L}\right)^3\left(\frac{1-\varepsilon_B+\varepsilon_L}{1-\varepsilon_B}\right)^2+\frac{E_2(1+\lambda^2)Re_G^2}{Ga_G}\right]$ $\psi_L = -\frac{\varepsilon_B-\varepsilon_L}{\varepsilon_L}\frac{\lambda\rho_G}{\rho_L}\left(\frac{1-\varepsilon_B+\varepsilon_L}{1-\varepsilon_B}\right)^{2/3}\left[\frac{E_1 Re_G}{Ga_G}\left(\frac{\varepsilon_B}{\varepsilon_B-\varepsilon_L}\right)^3\left(\frac{1-\varepsilon_B+\varepsilon_L}{1-\varepsilon_B}\right)^2+\frac{E_2\lambda Re_G^2}{Ga_G}\right]$ $+\frac{\varepsilon_B^4}{(\varepsilon_B-\varepsilon_L)^3\varepsilon_L}\left[\frac{E_1 Re_L}{Ga_L}+\frac{E_2 Re_L^2}{Ga_L}\right]$	Attou et al. (1999)

that the hydrodynamic parameters are affected considerably by gas density, and the relations established from atmospheric data are not valid at elevated pressures.

Relative permeability model

The relative permeability concept was first proposed by Saez and Carbonell (1985) for predicting the two-phase hydrodynamics (pressure drops and liquid holdups) of trickle flow in packed beds. The concept of relative permeability uses an expression for the drag force for single-phase flow, which is re-scaled to account for the second phase. This parameter, known as the *relative permeability*, is defined as the ratio of the drag force per unit volume under one-phase flow conditions to the drag force per unit volume under two-phase flow conditions at the same superficial velocity of a given phase, as expressed by:

$$k_\alpha = \frac{(F_\alpha/\varepsilon_\alpha)^0}{(F_\alpha/\varepsilon_\alpha)} \tag{12}$$

Using an Ergun-type equation for the single-phase pressure drop, the two-phase flow pressure drop can be written in the form:

$$\frac{F_\alpha}{\varepsilon_\alpha} = \frac{1}{k_\alpha(S_\alpha)}\left[\frac{E_1\,\mu_\alpha\,(1-\varepsilon_B)^2}{d_p^2\varepsilon_B^3}U_\alpha+\frac{E_2\rho_G(1-\varepsilon_B)}{d_p\varepsilon_B^3}U_\alpha^2\right] \tag{13}$$

where the constants E_1 and E_2 are the Blake–Kozeny–Carman and Burke–Plummer constants, respectively.

The relative permeability takes into account the blockage of flow in a pore as a result of the presence of a second phase. As a result, the relative permeability for a given phase is considered a function only of the fraction of the pore volume occupied by that phase. In the past two decades, determining the empirical expressions for the relative permeabilities (in terms of saturations of corresponding phases) has become a central topic and has attracted great interest. In addition, fitting the general Ergun equation to experimental pressure drop results of single-phase flow through packed beds in order to evaluate the constants E_1 and E_2 is of great importance, especially for beds made up of non-spherical particles.

Saez and Carbonell (1985) obtained optimal empirical expressions for the gas- and liquid-phase relative permeabilities based on holdup and pressure drop data taken from the literature. In the calculations, the constants E_1 and E_2 were set equal to 180 and 1.8, respectively, as recommended by Macdonald et al. (1979). These respective expressions were written as functions of the reduced liquid-phase saturation and the gas-phase saturation:

$$k_L = \delta_L^{2.43} \tag{14}$$

$$k_G = s_G^{4.8} \tag{15}$$

Using these expressions, the drag force expressions for two-phase flow in a trickle bed, which is directly related to CFD model

implementation, can then be obtained:

$$\frac{F_G}{\varepsilon_G} = \left(\frac{\varepsilon_B}{\varepsilon_B - \varepsilon_L}\right)^{4.8} \left[\frac{E_1\ \mu_G\ (1-\varepsilon_B)^2}{d_p^2 \varepsilon_B^3} U_G + \frac{E_2 \rho_G (1-\varepsilon_B)}{d_p \varepsilon_B^3} U_G^2\right] \quad (16)$$

$$\frac{F_L}{\varepsilon_L} = \left(\frac{\varepsilon_B - \varepsilon_L^0}{\varepsilon_L - \varepsilon_L^0}\right)^{2.43} \left[\frac{E_1\ \mu_L\ (1-\varepsilon_B)^2}{d_p^2 \varepsilon_B^3} U_L + \frac{E_2 \rho_L (1-\varepsilon_B)}{d_p \varepsilon_B^3} U_L^2\right] \quad (17)$$

Levec et al. (1986) showed that the relative permeability of the liquid phase was best represented by the following expression, depending on the mode of liquid flow rate (decreasing/increasing):

$$k_L = \begin{cases} \delta_L^{2.9} & (\delta_L \geq 0.2) \text{ (decreasing mode)} \\ 0.25\delta_L^{2.0} & (\delta_L < 0.2) \end{cases} \quad (18)$$

$$k_L = \delta_L^{2.0} \text{ (increasing mode)} \quad (19)$$

In addition, Levec et al. (1986) experimentally observed that the relative permeability of the gas phase might depend on its Reynolds number. This finding was later confirmed experimentally by Lakota et al. (2002), who suggested the following correlations for liquid- and gas-relative permeabilities:

$$k_L = \begin{cases} \delta_L^{2.92} & (\delta_L \geq 0.3) \text{ (liquid phase)} \\ 0.40\delta_L^{2.12} & (\delta_L < 0.3) \end{cases} \quad (20)$$

$$k_G = s_G^n,\ n = \chi + 0.478\, Re_G^{0.774} \text{ (gas phase)} \quad (21)$$

As shown in Equation (21), the gas-phase relative permeability is a function of the gas-phase saturation, the gas-phase Reynolds number and the particle shape.

In view of the industrial importance of high-pressure operation, Nemec et al. (2001) and Nemec and Levec (2005) attempted to measure pressure drops and liquid holdups in a variety of high-pressure, trickle-bed systems (in the range of 10–50 bars). The relation between the relative permeability of the liquid phase and the reduced liquid saturation proposed by Lakota et al. (2002) was adopted in their relative permeability models. Nemec et al. (2001) related the relative permeability of the gas phase to the gas-phase saturation by $k_G = 0.5\, s_G^{3.9}$, which is valid for $0 < s_G < 0.9$. The correlation provided a good fit; however, it does not comply with upper theoretical limit at $s_G = 1$ at which the value of k_G should reach 1.0. To overcome this drawback, Nemec and Levec (2005) later proposed a new two-region correlation for the gas-relative permeability, which reads:

$$k_G = \begin{cases} 0.40 s_G^{3.6} & (s_G \leq 0.64) \\ s_G^{5.5} & (s_G > 0.64) \end{cases} \quad (22)$$

Table 4 summarises the evolution of relative permeability models in the literature. The relative permeability approach, despite requiring a priori knowledge of the Ergun constants, is recognised to yield good estimations of liquid holdups and pressure drops. Moreover, the relative permeability functions essentially derived from one-dimensional flows are formally extendable to two- or three-dimensions to simulate non-uniform multiphase flows.

The implementation of relative permeability model in multidimensional CFD models has been attempted in the literature (Atta et al., 2007a, 2010a). The relative permeability model has proved to be well-balanced between a low level of detail and an adequate ability to capture the major hydrodynamic trends.

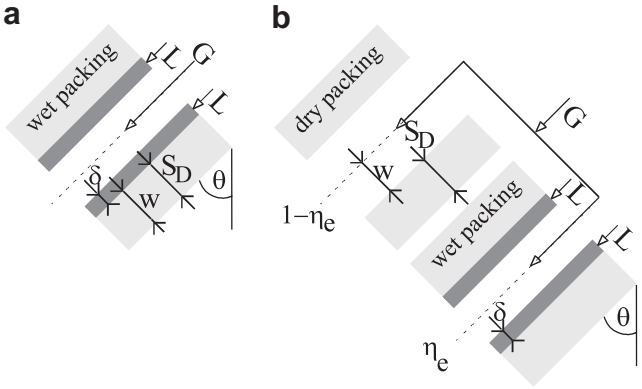

Figure 5. Geometry and phase distribution for classic slit models: (a) single slit and (b) double slit.

Slit flow approximation: single-slit models and double-slit models

Single-slit flow approximation. Holub et al. (1992, 1993) proposed a phenomenological model (so-called slit model) designed to map unidirectional two-phase flow at bed-scale into local flow at pellet scale by virtue of a representative inclined geometry (Figure 5). In a trickle-flow regime, the liquid flows over the catalyst bed as films or rivulets while the gas flows as a continuous phase through the remaining voids, so the liquid in the representative slit is assumed to be completely wetting the wall of the slit with a film of uniform thickness, while the gas flows in the central core. The two-phase momentum balance equations in the slit model are mapped to the actual bed-scale model, which yields drag force expressions in the form of a modified Ergun equation as follows:

$$\frac{F_G}{\varepsilon_G} = \frac{E_1\ \mu_G\ (1-\varepsilon_B)^2}{d_p^2 (\varepsilon_B - \varepsilon_L)^3} U_G + \frac{E_2 \rho_G (1-\varepsilon_B)}{d_p (\varepsilon_B - \varepsilon_L)^3} U_G^2 \quad (23)$$

$$\frac{F_L}{\varepsilon_L} = \frac{E_1\ \mu_L\ (1-\varepsilon_B)^2}{d_p^2 \varepsilon_L^3} U_L + \frac{E_2 \rho_L (1-\varepsilon_B)}{d_p \varepsilon_L^3} U_L^2 \quad (24)$$

Despite its simplicity, the model derives from local momentum and mass balances for the liquid and gas phases and leads to a coupling between liquid holdup and pressure drop similar to that in the relative permeability model. Holub et al. (1992, 1993) have demonstrated that the model is able to give reasonable predictions of pressure drop and liquid holdup based on data for atmospheric pressure.

Al-Dahhan and Dudukovic (1994) found that the experimental data in the high-interaction and high-pressure regimes could not be fit well using the single-slit model. The slit model was later extended by Al-Dahhan et al. (1998) to account for gas/liquid interfacial interactions, especially at elevated pressure and high gas superficial velocity. This work led to the development of a new set of empirical velocity and shear-slip factor functions, especially to fit high-pressure liquid holdup and pressure drop data.

Double-slit flow approximation. The above single-slit models are, in a strict sense, valid only for liquid throughputs sufficiently high to ensure complete wetting of the bed particles. Hence, these models are expected to deviate from experimental results when partial wetting prevails at very low liquid irrigation rates.

To take into account the partial wetting conditions, Iliuta and Larachi (1999) extended the single-slit model (Holub et al., 1993) using an assemblage of wet and dry slits. Such so-called

Table 4. Summary of relative permeability models for atmospheric and high-pressure TBRs in the literature

	Relative permeability		Ergun constants		
Refs.	Liquid phase	Gas phase	E_1	E_2	Remark on experimental conditions
Saez and Carbonell (1985)	$k_L = \delta_L^{2.43}$	$k_G = s_G^{4.8}$	$E_1 = 180$	$E_2 = 1.8$	Pressure drop and liquid holdup data taken from the literature Low-pressure data
Levec et al. (1986)	(i) Liquid flowrate decreasing mode: $k_L = \begin{cases} \delta_L^{2.9} & (\delta_L \geq 0.2) \\ 0.25\delta_L^{2.0} & (\delta_L < 0.2) \end{cases}$ (ii) Liquid flowrate increasing mode: $k_L = \delta_L^{2.0}$	$k_G = s_G^n$ ($n = 3.5$–7.5)	$E_1 = 180$	$E_2 = 1.8$	Atmospheric TBR $D = 17.2$ cm, $H = 130$ cm; $d_p = 0.3$ cm, 0.6 m Two-phase system: water + air Gas-phase relative permeability, n, is function of Re_G
Lakota et al. (2002)	$k_L = \begin{cases} \delta_L^{2.92} & (\delta_L \geq 0.3) \\ 0.40\delta_L^{2.12} & (\delta_L < 0.3) \end{cases}$	$k_G = s_G^n$ $n = \chi + 0.478\, Re_G^{0.774}$ $\chi = 4.37$ (spheres) $\chi = 3.31$ (extrudates)	Spherical particles: $E_1 = 150$ Nonspherical particles: $E_1 = 118$–381	Spherical particles: $E_2 = 1.75$ Nonspherical particles: $E_2 = 1.60$–6.65	Atmospheric TBR $D = 17.2$ cm, $H = 122$ cm Two-phase system: water + air Gas-phase relative permeability, η, is correlated with Re_G
Nemec et al. (2001)	$k_L = \begin{cases} \delta_L^{2.92} & (\delta_L \geq 0.3) \\ 0.40\delta_L^{2.12} & (\delta_L < 0.3) \end{cases}$	$k_G = 0.5 s_G^{3.9}$ valid within $0 < s_G < 0.9$	Spherical particles: $E_1 = 150$ Extrudates: $E_1 = 238$	Spherical particles: $E_2 = 1.75$ Extrudates: $E_2 = 2.41$	High-pressure TBR Pressure: 10–50 bars $D = 41$ mm, $H = 70$ cm Two-phase system: water + N_2
Nemec and Levec (2005b) Nemec and Levec (2005a)	$k_L = \begin{cases} \delta_L^{2.92} & (\delta_L \geq 0.3) \\ 0.40\delta_L^{2.12} & (\delta_L < 0.3) \end{cases}$	$k_G = \begin{cases} 0.40 s_G^{3.6} & (s_G \leq 0.64) \\ s_G^{5.5} & (s_G > 0.64) \end{cases}$	Spherical particles: $E_1 = 150$ Cylinders: $E_1 = \frac{150}{\phi_s^{3/2}}$ Polylobes: $E_1 = \frac{150}{\phi_s^{6/5}}$	Spherical particles: $E_2 = 1.75$ Cylinders: $E_2 = \frac{1.75}{\phi_s^{4/3}}$ Polylobes: $E_2 = \frac{1.75}{\phi_s^{2}}$	High-pressure TBR Pressure: 10–50 bars $D = 41$ mm, $H = 70$ cm $d_p = 1.0$–3.5 mm Two-phase system: water + N_2 New two-region correlation for gas-phase relative permeability

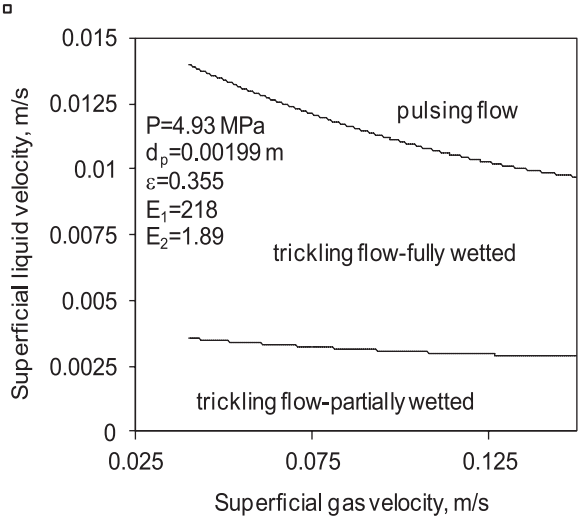

Figure 6. Transition between partially and fully wetted trickle flow regimes (Iliuta and Larachi, 1999)

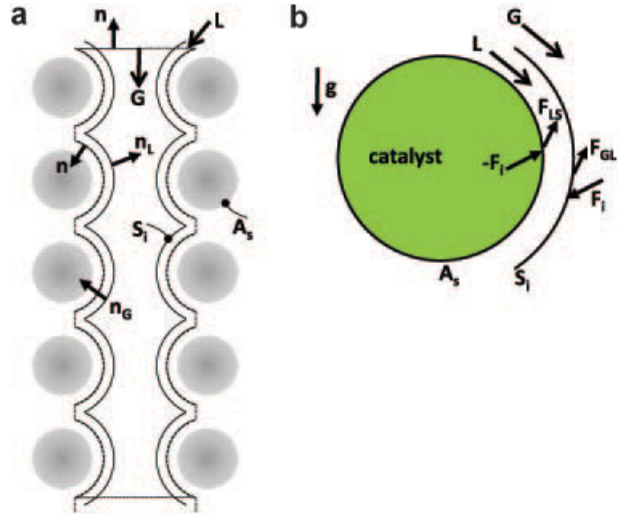

Figure 7. Schematic representation of co-current gas–liquid flow through the interstitial void space of the packed bed (Attou et al., 1999): (a) annular flow idealisation; (b) fundamental force components acting on the two-phase flow over catalyst particles.

"double slit" model is an extension of the single-slit model by virtue of the addition of a second adjoining completely dry slit. This allows for situations in which the particles are only partially covered by liquid. The wetting is associated with the ratio of wetted slits to total slits. Its estimation requires another constitutive relation relating wetting efficiency to holdup and pressure drop. This can be set by solving the liquid velocity profile in the wet slit in order to get an average velocity (Iliuta and Larachi, 1999; Iliuta et al., 2000). The mathematical derivation of the generalised model equations is detailed in Iliuta et al. (2000). The authors showed that the high-pressure and -temperature wetting efficiency, liquid holdup and pressure drop data for the trickle-flow regime reported in the literature were successfully represented by the double-slit model (Iliuta et al., 2000). One additional powerful feature of the model is that it can predict the changeover between partially wetted ($\eta_e < 1$) and the fully wetted pellet conditions ($\eta_e = 1$), as illustrated in Figure 6. This is a very interesting subdemarcation, following the global demarcation of conventional trickle-to-pulsing transition.

Fluid–fluid interfacial force model

In complementarity to the relative permeability and slit models, several investigators (Tung and Dhir, 1988; Attou et al., 1999; Narasimhan et al., 2002; Boyer et al., 2007) have attempted to develop physical models based on analysis of the fundamental force balance. In the literature, these models are called "fundamental force balance models" or "fluid–fluid interfacial force models" in which the drag force on each phase has contributions from the particle–fluid interactions as well as from fluid–fluid interactions.

Among others, the model by Attou et al. (1999) is one of the most established drag force models and has received popular attention as evidenced by its application in the CFD model implementation for TBR simulation. This model was based on a formulation deduced from the fundamental macroscopic balance laws as well as a physical description of the various interaction phenomena. In this model, the two-phase flow pattern was idealised to be an annular flow in which the gas and liquid phases are completely separated by a smooth and stable interface (Attou et al., 1999; Attou and Ferschneider, 2000). A physical sketch of two-phase trickle flow in an interstitial void volume between particles is represented in Figure 7a and the fundamental force components are shown in Figure 7b. The particle–liquid drag and the gas–liquid interactions, that is, the gas–liquid drag due to the relative motion between the fluids and the force by which the gas pushes the liquid against the solid particles, are derived from theoretical considerations in which an idealised flow pattern is assumed (Attou et al., 1999). Each component of the interaction term is described by the single-phase flow equation of Kozeny–Carman, involving both the viscous contribution and the fluid inertia contribution. The resultant of the forces exerted on the gas phase consists of two components. The first is the drag force exerted on the gas phase due to the slip motion between the two fluids. The second is the force by which the gas presses the liquid film against the fixed solid particles due to the tortuous pattern and the successive changes in the cross-sectional area of the interstitial flow path. The resultant of the forces exerted on the liquid phase involves two components: the drag force exerted on the liquid phase due to the shear stress in the vicinity of the packing surface and the gas–liquid drag force due to the slip between the fluids (Attou et al., 1999; Attou and Ferschneider, 2000). However, these drag force formulations involve some subtle treatments. For instance, the effective porosity and the effective particle diameter are used in the derivation of these interphase interaction terms as a correction to account for the presence of the liquid film. Moreover, for the liquid–solid interaction component, a correction factor is introduced to take into account the tortuous pattern of the liquid films at macroscopic level (Attou et al., 1999). The interphase gas–liquid, gas–solid and liquid–solid drag forces can be finally described as (Attou et al., 1999; Gunjal et al., 2005a):

$$F_{gl} = \varepsilon_G \left(\frac{180\ \mu_G\ (1-\varepsilon_G)^2}{\varepsilon_G^2 d_p^2} \left(\frac{\varepsilon_S}{1-\varepsilon_G} \right)^{2/3} + \frac{1.8 \rho_G |u_G - u_L| (1-\varepsilon_G)}{\varepsilon_G d_p} \left(\frac{\varepsilon_S}{1-\varepsilon_G} \right)^{1/3} \right) (u_G - u_L) \quad (25)$$

$$F_{gs} = \varepsilon_G \left(\frac{180\ \mu_G\ (1-\varepsilon_G)^2}{\varepsilon_G^2 d_p^2} \left(\frac{\varepsilon_S}{1-\varepsilon_G} \right)^{2/3} + \frac{1.8\rho_G |u_G| (1-\varepsilon_G)}{\varepsilon_G d_p} \left(\frac{\varepsilon_S}{1-\varepsilon_G} \right)^{1/3} \right) u_G \qquad (26)$$

$$F_{ls} = \varepsilon_L \left(\frac{180\ \mu_L\ (1-\varepsilon)^2}{\varepsilon_L^2 d_p^2} + \frac{1.8\rho_L\ |u_L|\ (1-\varepsilon)}{\varepsilon_L d_p} \right) u_L \qquad (27)$$

Reasonable agreement was achieved between predictions and literature experimental data in terms of both liquid saturation and pressure gradient over a wide range of operating conditions, in particular the influence of gas flow, that is, density or/and superficial gas velocity (Attou et al., 1999). To improve the overall prediction accuracy, Boyer et al. (2007) further modified the model of Attou et al. (1999) in order to optimise the closure law for two-phase flow tortuosity for a liquid film. In their work, a two-phase flow tortuosity term was generalised into the expression $(1-\alpha)^n$ where the exponent n was taken as $n=-1$ in the previous Attou et al. (1999) model. By fitting the expression of liquid–solid force on experimental values, the exponent n for tortuosity term was found to be $n=-0.54$ for aqueous fluids and $n=-0.02$ for organic fluids. The larger magnitude of exponent n for water/gas flows may be explained by greater liquid film curvature induced by the higher surface tension. With the new closure model, the prediction accuracy was shown to be significantly increased for both pressure drop and liquid saturation over a wide range of operating data.

Drag models of this kind have been tested by other investigators (Tung and Dhir, 1988; Narasimhan et al., 2002; Kundu et al., 2003) considering gas–liquid drag, gas–particle drag and liquid–particle interactions. Different from the model proposed by Tung and Dhir (1988), the concept of two-phase flow tortuosity was adopted in the pressure drop model by Narasimhan et al. (2002) and in the wetting efficiency model by Kundu et al. (2003), in which the liquid flow tortuosity was considered to be modified due to the gas flow inertia that induces liquid film curvature. It should be noted that, different from the model of Attou et al. (1999), the two-phase tortuosity correction was imposed on the gravitational term of the momentum balance equations in the work of Narasimhan et al. (2002) and Kundu et al. (2003). Evidently, from the standpoint of CFD model implementation, the interphase drag models having the tortuosity correction on the non-gravitational-term, such as the model of Attou et al. (1999), may be naturally compatible with the classical macroscopic momentum conservation framework.

Closure Relationship of Capillary Pressure Effect in TBRs

Capillary pressure can affect the flow distribution inside TBRs and is also related to the hysteresis phenomenon observed in the pressure drops and liquid holdups during co-current gas–liquid flow in packed beds (Jiang et al., 1999; Gunjal et al., 2005a; Lappalainen et al., 2009a). Therefore, incorporation of the capillary pressure effect into CFD models has received much attention in efforts to properly understand and analyse flow behaviour in TBRs. Several investigators in the literature have analysed capillary forces and proposed different correlations for capillary pressure. The capillary pressure models of Grosser et al. (1988) and Attou and Ferschneider (2000) are often used in CFD modelling of TBRs (Lappalainen et al., 2009b).

The equilibrium of forces at the interface can be represented using the pore-scale capillary pressure defined by the Young–Laplace equation:

$$P_c = 2\sigma \left(\frac{1}{d_1} + \frac{1}{d_2} \right) \qquad (28)$$

where $d_1 = 2r_1$ and $d_2 = 2r_2$ are the maximum and minimum diameters of the sphere with liquid film formed by the flowing liquid; r_1 and r_2 are the two principal radii of curvature of the gas/liquid interface at the pore-scale just before collapse.

Attou and Ferschneider (2000) proposed a correlation for capillary pressure based on geometric estimates of d_1 and d_2 and with empirical factor (F) to account for high-pressure operations, which has the following form:

$$P_c = 2\sigma \left(\frac{1-\varepsilon}{1-\varepsilon_G} \right)^{1/3} \left(\frac{1}{d_P} + \frac{1}{d_{min}} \right) F\left(\frac{\rho_G}{\rho_L} \right) \qquad (29)$$

where

$$d_{min} = \left(\frac{\sqrt{3}}{\pi} - \frac{1}{2} \right)^{1/2} d_P \qquad (30)$$

$$F\left(\frac{\rho_G}{\rho_L} \right) = 1 + 88.1 \left(\frac{\rho_G}{\rho_L} \right) \left(\text{for } \frac{\rho_G}{\rho_L} < 0.025 \right) \qquad (31)$$

The derivation of Equation (29) was based on the local linear momentum balance law applied to the gas/liquid interface, in which the effect of gas density was incorporated through $F(\rho_G/\rho_L)$ and was claimed to be suitable for systems at elevated pressures.

Grosser et al. (1988) used the relative permeability drag force expressions for two-phase flow (Saez and Carbonell, 1985) together with the Leverett correlation for the capillary pressure term:

$$P_c = \sigma \left(\frac{\varepsilon}{k} \right)^{0.5} J(\varepsilon_L) \qquad (32)$$

where

$$\left(\frac{\varepsilon}{k} \right)^{0.5} = \frac{(1-\varepsilon)}{\varepsilon d_e} E_1^{0.5} \qquad (33)$$

$$J(s_L) = 0.48 + 0.036 \ln \left(\frac{1-s_L}{s_L} \right) \qquad (34)$$

where σ is the surface tension; ε_L and s_L are liquid holdup and liquid saturation, respectively; k is the permeability of the porous medium, which is related to the Ergun constant and the equivalent particle diameter; J is a dimensionless function obtained from the experimental data taken on various sand samples with air and water (Leverett, 1941). The Leverett function depends only on liquid saturation and also exhibits hysteresis between liquid imbibition and drainage experiments. Jiang et al. (2002a) introduced the particle wetting efficiency, f, to the capillary pressure equation proposed by Grosser et al. (1988), leading to the following expression:

$$P_L = P_G - (1-f)\sigma \left(\frac{\varepsilon}{k} \right)^{0.5} J(\varepsilon_L) \qquad (35)$$

Equation (35) indicates that the macroscale capillary effect is negligible when the particles are completely wetted externally ($f = 1.0$), whereas this effect is most significant when the particle surfaces tend to be dominantly dry ($f \to 0$). The capillary pressure model proposed by Jiang et al. (2002a) was implemented by Boyer et al. (2005) and was shown to over-predict liquid spreading. To account for bed initial wetting conditions and the flow history dependence, Boyer et al. (2005) proposed a new model for capillary pressure, which takes the following forms for prewetted and non-prewetted beds, respectively:

$$P_L = \begin{cases} P_G - 2(1-f)^{-0.2}\sigma\left(\frac{\varepsilon}{k}\right)^{1/3}\left(\frac{1}{d_p}+\frac{1}{d_{min}}\right)F\left(\frac{\rho_g}{\rho_l}\right) & \text{(prewetted)} \\ P_G - 2(1-f)^{-0.6}\sigma\left(\frac{\varepsilon}{k}\right)^{1/3}\left(\frac{1}{d_p}+\frac{1}{d_{min}}\right)F\left(\frac{\rho_g}{\rho_l}\right) & \text{(non-prewetting)} \end{cases} \tag{36}$$

The capillary pressure models of both Grosser et al. (1988) and Attou and Ferschneider (2000) neglect the influence of the contact angle, which has been found important in liquid spreading over a solid surface. This is especially true in low liquid saturation conditions where liquid forms pendular rings at the particle contact points. A new analytical capillary pressure model was therefore developed by Lappalainen et al. (2009b) to describe the capillary pressure–saturation relationship for the pendular and funicular regions. The model was found to be suitable for predicting capillary pressure–liquid saturation relations for spherical particles. Lappalainen et al. (2009a) implemented this capillary pressure model into their CFD model by refitting it in polynomial expressions.

The aforementioned models are valid only for equilibrium conditions. From a physical standpoint, the arrangement of fluids in the pore space requires some relaxation time to attain a stable or equilibrium configuration during the displacement of one fluid by another through a porous medium. Actually, it has been experimentally observed that the capillary pressure–saturation curve under dynamic conditions is different from that under static conditions (Stauffer, 1978; Hassanizadeh et al., 2002; O'Carroll et al., 2005). Therefore, the incorporation of non-equilibrium or dynamic effects into continuum descriptions of multiphase flow has received growing research attention in the literature.

Based on thermodynamic arguments and volume-averaging of microscopic multiphase flow equations, Hassanizadeh and Gray (1993a,b) proposed that, in a two-fluid system, the dynamic capillary pressure P_c^{dyn} is related to the static capillary pressure P_c^{stat} as follows:

$$P_c^{dyn} = P_{nw} - P_w = P_c^{stat} - \tau_H(S_w)\frac{\partial S_w}{\partial t} \tag{37}$$

where P_{nw} and P_w are the phase pressures of non-wetting and wetting phases, respectively, and τ_H is a phenomenological coefficient that takes positive values and depends on the saturation, S_w. For a drainage process in which a non-wetting phase displaces the wetting one, the local time derivative of the wetting-phase saturation is negative ($((\partial S_w)/(\partial t)) < 0$) and, therefore, the dynamic capillary pressure is higher than the static one $\left(P_c^{dyn} > P_c^{stat}\right)$, in agreement with experimental observations (Hassanizadeh et al., 2002). The non-equilibrium effects are important where saturation changes are significant.

A different but related model was proposed by Barenblatt et al. (Barenblatt, 1971; Barenblatt and Vinnichenko, 1980). Using dimensional analysis and physical reasoning, Barenblatt proposed the following evolution (as opposed to an algebraic) relation:

$$\sigma_w = S_w - \tau_B(S_w)\frac{\partial S_w}{\partial t} \tag{38}$$

The Barenblatt model was originally proposed to account for non-equilibrium capillary pressure effects in two-phase flows in porous media. An important difference between the Hassanizadeh–Gray and the Barenblatt models is that the latter includes non-equilibrium effects in both capillary pressure and relative permeability. Extension of this model to the case of three-phase flow in porous media was recently attempted by Juanes (2009).

In general, capillary pressure bears a meaning at the pore-scale, despite the fact that it may lack clarity at the macro-scale. The standard approach is to assume that macro-scale capillary pressure is a function of saturation. Then, it is assumed that the pore-scale equilibrium also holds on the macro-scale; the difference between bulk non-wetting and wetting phase pressures is assumed to be equal to the macro-scale capillary pressure. This is an ad hoc approach which leads to hysteresis in capillary pressure, and to the fact that the standard model is only valid for equilibrium conditions, that is, for steady-state flow or the absence of flow (Niessner and Hassanizadeh, 2009). To remedy this situation, the concept of dynamic capillary pressure has been introduced for multiphase flow in porous media. To implement the dynamic capillary pressure model into CFD codes, additional non-equilibrium terms should be incorporated in the macroscopic momentum conservation equations.

Closure Relationship of Macroscopic Multiphase Turbulence in the Presence of Porous Packings

While both laminar and turbulent flows are important, modelling efforts reported for turbulent flows in porous media remain relatively scarce. Although it might be possible to describe some of these systems in a precise representation or a meaningful statistical approximation of the geometry, the computational effort required to solve the flow field in such geometries is prohibitive. These shortcomings motivate more research in the development of porous media approximations, representing the system composed of pores using a macroscopic homogeneous one with uniform properties (Teruel and Rizwan-uddina, 2009).

Engineering applications involving porous media flows rely on the ability to predict flow characteristics under different working conditions (Horton and Pokrajac, 2009). In porous materials, the dominant flow regime is laminar flow. However, turbulence may occur as suggested by the classification of the regime based on the pore Reynolds number (Re_p). The literature recognises distinct flow regimes (Dybbs and Edwards, 1984; Pedras and de Lemos, 2001a; de Lemos, 2006), namely: (a) Darcy or creeping flow regime ($Re_p < 1$); (b) Forchheimer flow regime ($1–10 < Re_p < 150$); (c) post-Forchheimer flow regime (unsteady laminar flow, $150 < Re_p < 300$) and (d) fully turbulent flow ($Re_p > 300$).

Generally, turbulent simulation of porous media encounters two challenges. The first problem consists of presenting a turbulence model that accurately mimicks the complex flow features in the pores. The second challenge is to develop a suitable macroscopic turbulence model, substituting the complex topology of the pore structures using the concept of space-time or time-space averaging (Kazerooni and Hannani, 2009). Numerical investigation of turbulent flow within the porous region can use either microscopic or macroscopic models. Microscopic models provide

detailed insights into the flow structure within simple geometries. Therefore, an efficient macroscopic turbulence model is required to investigate turbulence within porous media with complex geometrical characteristics (Chan et al., 2007).

The macroscopic turbulence model describes the characteristics of fluid flow within a porous medium by the volume-averaged variables. Additional source terms must be added to the right-hand sides of the classical k–ε model equations in order to account for the presence of porous media (Nakayama and Kuwahara, 2008). Turbulence modelling in porous media largely follows the modelling steps inherited from clear flows using the k–ε turbulence model. As a two-equation model, classical k–ε model actually consists of two transport equations which are introduced to calculate the turbulent kinetic energy and the turbulence dissipation. As evidenced in the literature, the k–ε turbulence model has commonly been adapted and modified to describe the macroscopic turbulence in porous media (Antohe and Lage, 1997; Nakayama and Kuwahara, 1999; Getachew et al., 2000; de Lemos, 2006). In the presence of porous media, the transport equation of the turbulent kinetic energy k may be written in the following form for multiphase flow:

$$\frac{\partial}{\partial t}(\varepsilon_\alpha \rho_\alpha k) + \frac{\partial}{\partial x_i}(\varepsilon_\alpha \rho_\alpha u_{\alpha,i} k) - \frac{\partial}{\partial x_i}\left(\varepsilon_\alpha \left(\mu_{\alpha,\mathrm{lam}} + \frac{\mu_{\alpha,\mathrm{turb}}}{\sigma_k}\right)\frac{\partial k}{\partial x_i}\right) = \varepsilon_\alpha (G_\alpha - \rho_\alpha \varepsilon) + S_{\alpha,k} \quad (39)$$

And the transport equation for the turbulent dissipation ε may be written as:

$$\frac{\partial}{\partial t}(\varepsilon_\alpha \rho_\alpha \varepsilon) + \frac{\partial}{\partial x_i}(\varepsilon_\alpha \rho_\alpha u_{\alpha,i} \varepsilon) - \frac{\partial}{\partial x_i}\left(\varepsilon_\alpha \left(\mu_{\alpha,\mathrm{lam}} + \frac{\mu_{\alpha,\mathrm{turb}}}{\sigma_\varepsilon}\right)\frac{\partial \varepsilon}{\partial x_i}\right) = \varepsilon_\alpha \frac{\varepsilon}{k}(C_{\varepsilon 1} G_\alpha - C_{\varepsilon 2} \rho_\alpha \varepsilon) + S_{\alpha,\varepsilon} \quad (40)$$

Here, $S_{\alpha,k}$ and $S_{\alpha,\varepsilon}$ are additional source terms due to the presence of porous media, that are not found in the conventional k–ε model. These additional source terms are characterised by the viscous and inertial drag forces resulting from the interaction between the solid and fluid phases. The extra source terms are commonly formulated by performing microscopic numerical experiments based on spatially periodic arrays (Pedras and de Lemos, 2001b,c; Chandesris et al., 2006; Teruel and Rizwan-uddina, 2009). de Lemos and Pedras (2001) attempted to establish a general classification of the published turbulence models for flow through porous media. In their work, a total of four major classes of turbulence models for porous matrixes were identified and their main characteristics were compared. Table 5 gives a summary of some representative source correlations proposed in the literature for modelling macroscopic turbulence for single-phase flow through permeable porous media (Guo et al., 2006; Nakayama and Kuwahara, 2008). However, research on developing source terms for macroscopic turbulence equations for two-phase flow through porous media has not been reported so far, and this area of research merits additional effort in the future.

It is noteworthy that a study of macroscopic turbulence for single-phase flow in porous media is, itself, of particular interest since it is not only essential for single-phase applications, but also constitutes a basis for the study of macroscopic turbulence for two-phase flow through porous media/packings. In general, macroscopic turbulence models for porous media flow can be developed to capture the phenomena of macroscopic turbulence by performing a space/time averaging, thereby leading to body forces in the k–ε turbulence model (de Lemos, 2006; Nakayama and Kuwahara, 2008; Teruel and Rizwan-uddina, 2009).

Table 5. Source terms in the turbulence equations for flow in porous media (packed spheres)

Refs.	s_k	s_ε	Remark
Nakayama and Kuwahara (1999)	$s_k = \rho\varepsilon_\infty$	$s_\varepsilon = \rho\frac{\varepsilon_\infty^2}{k_\infty}$	$k_\infty = 3.7\gamma^{3/2}(1-\gamma)\lvert u\rvert^2$ $\varepsilon_\infty = 39\gamma^2(1-\gamma)^{5/2}\frac{\lvert u\rvert^3}{d_\mathrm{p}}$
Pedras and de Lemos (2001a)	$s_k = c_k\rho\frac{k\gamma\lvert u\rvert}{\sqrt{K}}$	$s_\varepsilon = c_k\rho\frac{\varepsilon\gamma\lvert u\rvert}{\sqrt{K}}$	$c_k = 0.28$ $k = \frac{\gamma^2 d_\mathrm{p}^2}{150(1-\gamma)^2}$
Takeda (1994)	$s_k = c_k R_0\lvert u\rvert^2$	$s_\varepsilon = c_k R_0\frac{\varepsilon\lvert u\rvert^2}{k}$	$c_k = 0.0413$

CFD MODELLING AND SIMULATION OF TRICKLE-BED REACTION SYSTEMS

Hydrodynamics in TBRs can be described by means of global hydrodynamic parameters, such as pressure drop, liquid holdup, dispersion of fluid phases, liquid–solid wetting efficiency and flow regime. Therefore, a fundamental understanding and analysis of flow hydrodynamics and coupled-reaction conversions inside TBRs is a prerequisite for efficient design and scale-up of TBRs. The past decades have seen a number of works reported in the literature on the use of CFD for simulating TBRs (as summarised in Table 6). In the following section, the specific contributions of the CFD approach to predicting the non-reacting/reacting flow hydrodynamics and analysing possible process intensification in TBRs will be discussed.

CFD Simulation of Flow Hydrodynamics in TBRs

Prediction of pressure drop and liquid holdup

The research literature on hydrodynamics in terms of pressure drop and liquid holdup has been an important topic in the CFD study of TBRs.

Jiang et al. (2002a,b) developed a k-fluid CFD model to predict the overall liquid saturation and pressure gradient. The results from CFD model were tested against the theoretical predictions from two bed-scale hydrodynamic models, namely, the single-slit model (Holub et al., 1992) and the original relative permeability model (Saez and Carbonell, 1985). It was shown by directly benchmarking the literature experimental data (Szady and Sundaresan, 1991) that the k-fluid CFD model and the model of Saez and Carbonell offered more reasonable predictions for the pressure gradient and better predictions for liquid saturation.

Gunjal et al. (2005a) proposed an Euler–Euler CFD model to predict hydrodynamic parameters in TBRs. Using this model, parametric analysis of the hysteresis phenomena in pressure drop and liquid holdup was performed at various operating conditions. The CFD model predictions were compared with three different data sets in the literature (Specchia and Baldi, 1977; Rao et al., 1983; Szady and Sundaresan, 1991). The model predictions generally showed good agreement with the experimental data on pressure drop and liquid saturation.

Atta et al. (2007a) proposed a two-phase Eulerian CFD model coupled with the original drag-closure-based relative permeability

Table 6. An "overview" summary of the simulation details of the literature multidimensional CFD work on TBRs

Refs.	Modelling approach	Turbulence model	Drag force model	Reaction system considered	Geometry	Operating details	Numerical details
Ramajo et al. (2010)	Eulerian–Eulerian two-fluid model	Standard k–ε turbulence model	Drag function: CD = 0.44 (fully turbulent regime)	No reaction	TBR reactor: $D = 0.56$ m, $H = 6.5$ m (H_catalyst = 4.7 m)	Working fluids: hydrogen–liquid (C4)	Grid generation software: ICEM 11.0
				Hydrodynamics only	Perforated-plate of the tray	$m_L = 3.46$ kg/s, $m_G = 2.3 \times 10^{-3}$ kg/s	Number of cells: 1845 274 (tetrahedral)
					7 gas chimney: $D = 37$ mm 68 holes for liquid flow ($D = 10$ mm) tray: $D = 0.56$ m, thickness = 8 mm		Time steps range: 0.001–0.01 s Time integration: first-order backward Euler scheme
							Convergence criterion: $<1 \times 10^{-6}$ CFD package: CFX 11.0
Bazmi et al. (2011)	Euler–Euler approach	Not included	Gas–liquid, gas–solid, and liquid–solid momentum exchanges (Attou and Ferschneider, 1999)	No reaction	Packed with industrial trilobe catalyst $D = 14$ cm, $H = 100$ cm, $d_p = 1$ mm × 4.2 mm (trilobe)	Working fluids: nitrogen–water	3D simulation
			Radial porosity distribution (trilobe catalyst: (Bazmi et al., 2011)	Hydrodynamics only		$U_L = 0.21$ cm/s, 0.32 cm/s	Number of cells: ~200,000 cells
						$U_G = 0.01$–0.06 m/s	Time step: 10^{-3} s
Strasser (2010)	Euler–Euler approach	Shear stress transport (SST) k–ω two-equation	Ergun-like drag force expression for gas–solid momentum exchange Implemented as isotropic porous media momentum sinks (with estimated isotropic permeability)	Hydrogenation of unsaturated hydrocarbons	Undisclosed (proprietary geometry)	Undisclosed (proprietary conditions)	2D (axi-symmetric)/3D simulations Time discretisation: first-order scheme Newton–Raphson linearisation Coupled ILU algebraic multigrid technique Coarse mesh: ~2000 hexahedral cells Fine mesh:(factor of >5 of coarse mesh) CFD package: ANSYS CFX 11/12

(*Continued*)

Table 6. (*Continued*)

Refs.	Modelling approach	Turbulence model	Drag force model	Reaction system considered	Geometry	Operating details	Numerical details
Augier et al. (2010a)	Volume-of-fluid (VOF)	Not included	Brackbill et al. (1992) model: surface tension and wall adhesion	No reaction Hydrodynamics only	Pile-forming particles: $d = 2.0$ mm	Working fluids: air + liquid (water or ethanol) Solid phase: polypropylene (or alumina) Liquid was fed smoothly at the top of the first particle (0.3 mm dia. portion) Contact angle: 20°, 30°, 53°, 89° Atmospheric pressure Room temperature	2D/3D simulations Number of cells: 50,000 cells (2D) $\sim 10^6$ cells (3D) Interface resolution (CICSAM algorithm) Explicit fixed time-step method: 10^{-5} CFD package: FLUENT 6.3
Lopes and Quinta-Ferreira (2010e)	Volume-of-fluid (VOF)	Mixture k–ε turbulence model	Brackbill et al. (1992) model: surface tension and wall adhesion	CWAO of phenolic waste waters	Laboratory-scale TBR unit (50 mm i.d. × 1.0 m length)	$Q_L = 1.0$–5.0 L/h $G = 0.1$–0.7 kg/m^2/s $L = 1$–15 kg/m^2 s $P = 30$ bar $T = 160$–200°C	3D simulation Residual values: $<10^{-3}$ At least second-order accurate in space CFD tool: FLUENT 6
Lopes and Quinta-Ferreira (2010d)	Euler–Euler approach	Mixture k–ε turbulence model	Gas–liquid, gas–solid, and liquid–solid momentum exchanges (Attou and Ferschneider, 2000)	No reaction Hydrodynamics only (periodic operation of TBRs with induced pulses by modulatinginlet liquid velocity)	Cylindrical vessel (50 mm i.d. × 1.0 m length) Packed with spherical catalyst (2 mm diameter)	$G = 0.10$–0.70kg/m^2/s $L = 0.05$–15 kg/m^2 s $P = 10$–30 bar $T = 290$–500 K	3D simulation Unstructured finite volume method Meshed in tetrahedral cells Second-order upwind scheme Discretisation for spatial derivatives Convergence: scaled residues $<10^{-6}$ CFD tool: FLUENT

(*Continued*)

Table 6. (*Continued*)

Refs.	Modelling approach	Turbulence model	Drag force model	Reaction system considered	Geometry	Operating details	Numerical details
Lopes and Quinta-Ferreira (2010c)	Euler–Euler approach	Standard k–ε dispersed turbulence model	Gas–liquid, gas–solid, and liquid–solid momentum exchanges (Attou and Ferschneider, 2000)	CWAO of phenolic solutions	Laboratory-scale TBR unit (50 mm i.d. × 1.0 m length)	$G = 0.10$–0.70 kg/m^2/s	3D simulation
					Packed with cylindrical catalyst	$L = 1.0$–10.0 kg/m^2/s $P = 30$ bar $T = 160$–200°C	Time step: 10^{-7}–10^{-5} s $Y+$ criterion: <200 Momentum: MUSCL CFD tool: FLUENT
Lopes and Quinta-Ferreira (2010b)	Volume-of-fluid (VOF)	Mixture k–ε turbulence model	Brackbill et al. (1992) model: surface tension and wall adhesion	CWAO of phenolic waste waters	Laboratory-scale TBR unit (50 mm i.d. × 1.0 m length)	$G = 0.5$ kg/m^2 s $L = 5.0$ kg/m^2/s $P = 30$ bar $T = 200$, 160°C	3D simulation Time step: 10^{-7}–10^{-4} s or 10^{-3} s Residual values: $<10^{-3}$ $Y+$ criterion: <200 At least second-order accurate in space CFD tool: FLUENT
Lopes and Quinta-Ferreira (2010a)	Euler–Euler approach + volume-of-fluid (VOF)	Standard k–ε dispersed turbulence model	Euler–Euler approach: gas–liquid, gas–solid, and liquid–solid momentum exchanges (Attou and Ferschneider, 2000) VOF approach: Brackbill et al. (1992) model: surface tension and wall adhesion	CWAO of phenolic waste waters	Cylindrical vessel (50 mm i.d. × 1.0 m length) Packed with spherical catalyst (2 mm diameter)	$G = 0.5$ kg/ m^2/s $L = 5.0$ kg/m^2 s $P = 30$ bar $T = 200^\circ$C	3D simulation Time step:10^{-7} s (initially) At least second-order accurate in space CFD tool: FLUENT

(*Continued*)

Table 6. (*Continued*)

Refs.	Modelling approach	Turbulence model	Drag force model	Reaction system considered	Geometry	Operating details	Numerical details
Atta et al. (2010b)	Euler–Euler two-phase approach	Standard k–ε turbulence model (per phase)	Relative permeability model (Saez and Carbonell, 1985)	No reaction	$D = 57$ mm	Liquid modulation: base-impulse method	2D simulation (axisymmetric domain)
	Gas phase (primary phase)		Radial porosity distribution (de Klerk, 2003)	Hydrodynamics only (periodic operation related)	$H = 1.6$ m	Superficial velocities: $U_G = 0.062$, 0.250 m/s, $U_{L,base} = 1.4 \times 10^{-3}$ m/s, $U_{L,impulse} = 2.8 \times 10^{-3}$ m/s	Discretisation
	Liquid phase (secondary phase)		Capillary pressure force: neglected		$d_p = 3$ mm	Periodic parameters: cycle period = 10 s, 60 s, split ratio = 0.5	Momentum: MUSCL
					$E_b = 0.395$		Time step: 10^{-4}
							CFD tool: FLUENT
Atta et al. (2010a)	Euler–Euler two-phase approach	Not included	Relative permeability model (Saez and Carbonell, 1985; Nemec and Levec, 2005b)	No reaction	Case I: $d_p = 1.14$ mm, $E_b = 0.392$, $d_p = 1.52$ mm, $E_b = 0.412$	Case I: $P = 0.3$–5.0 MPa	2D simulation (axisymmetric domain)
	Gas phase (primary phase)		Radial porosity distribution (de Klerk, 2003)	Hydrodynamics only	Case II: $d_p = 3$ mm, $E_b = 0.395$	Case II: $P = 0.5$ MPa	CFD tool: FLUENT
	Liquid phase (secondary phase)		Capillary pressure force: neglected		Case III: $d_p = 2$ mm, $E_b = 0.38$	Case III: $P = 2.1$ MPa	
Lopes and Quinta-Ferreira (2009d)	Euler–Euler approach	k–ε turbulence models (SKE, RKE, RNG)	Gas–liquid, gas–solid, and liquid–solid momentum exchanges (Attou and Ferschneider, 2000)	No reaction	Pilot TBR unit (50 mm i.d. × 1.0 m length)	$G = 0.1$–0.7 kg/ m^2/s	Computational mesh: 13 layers (around 200 nonoverlappingspherical particles)
		k–ε turbulence model (mixture)		Hydrodynamics only	$D_p = 2$ mm	$L = 1$–15 kg/m^2/s	
		k–ε turbulence model (dispersed)				$P = 30$ bar	Number of cells: 2×10^5–10^6
		k–ε turbulence model (per phase)				$T = 25^\circ$C, 200°C	Discretisation:
		RSM turbulence model					Volume fraction: FOU, QUICK
							Momentum: FOU, SOU, PL, QUICK, MUSCL
							k, ε: FOU, SOU, PL, QUICK, MUSCL
							Time step: 10^{-5}–10^{-2}
							Convergence criteria: 10^{-5}–10^{-2}

(*Continued*)

Table 6. (*Continued*)

Refs.	Modelling approach	Turbulence model	Drag force model	Reaction system considered	Geometry	Operating details	Numerical details
Lopes and Quinta-Ferreira (2009c)	Volume-of-fluid (VOF)	Mixture k–ε turbulence model	Brackbill et al. (1992) model: surface tension and wall adhesion	No reaction	Pilot TBR unit (50 mm i.d. × 1.0 m length)	$G = 0.1$–$0.7\ kg/m^2/s$	Computational mesh: 10 layers (around 200 nonoverlapping-spherical particles)
				Hydrodynamics only	$D_p = 2\ mm$	$L = 1$–$15\ kg/m^2\ s$	
						$P = 30\ bar$	Distance gap: 2–3% particle diameter
						$T = 25°C$	Number of cells: 2×10^5–10^6 Time step: 10^{-7}–10^{-2} Convergence criteria: 10^{-6}–10^{-3} Discretisation method: QUICK, Geo-Reconstruct, CICSAM and HRIC Under-relaxation factors 0.4 (pressure), 0.6 (velocity) $Y+$ criterion: <200
Lopes and Quinta-Ferreira (2009b)	Euler–Euler approach	Standard k–ε dispersed model	Gas–liquid, gas–solid, and liquid–solid momentum exchanges (Attou and Ferschneider, 2000)	No reaction	Pilot TBR unit (50 mm i.d. × 1.0 m length)	$G = 0.1$–$0.7\ kg/m^2/s$	Computational mesh: 13 layers (around 200 nonoverlapping-spherical particles)
				Hydrodynamics only	$D_p = 2\ mm$	$L = 1, 5, 10, 15\ kg/m^2/s$	
					Distributors: D_1: single-point entry (2 mm diameter), D_2: 60 capillary tubes (0.12 mm internal diameter), D_3: perfectly uniform distributor	$P = 1\ bar, 30\ bar$	Number of cells: 2×10^5–10^6
						$T = 25°C$	Discretisation Volume fraction: QUICK Momentum: MUSCL k, ε: QUICK Time step: 10^{-5}–10^{-2} Convergence criteria: 10^{-5}–10^{-2}

(*Continued*)

Table 6. (*Continued*)

Refs.	Modelling approach	Turbulence model	Drag force model	Reaction system considered	Geometry	Operating details	Numerical details
Lopes and Quinta-Ferreira (2009a)	Volume-of-fluid (VOF)	Standard k–ε model (SKE) Realisable k–ε model (RKE) RNG turbulence model RSM turbulence model	Brackbill et al. (1992) model: surface tension and wall adhesion	No reaction Hydrodynamics only	Pilot TBR unit (50 mm i.d. × 1.0 m length) $D_p = 2$ mm	$G = 0.1$, 0.3, 0.5, 0.7 kg/m^2/s $L = 1$, 5, 10, 15 kg/m^2/s $P = 30$ bar $T = 25$°C	Grid generation Prismatic cells (on tube) Structured tetrahedral (on wall spheres) Structured tetrahedral cells (in between) Number of cells: 2×10^5–10^6 Time step: 10^{-5}–10^{-2}
Lappalainen et al. (2009a)	Euler–Euler approach	Not included	Phase interaction force model (Lappalainen et al., 2009a) Wetting efficiency model (Lappalainen et al., 2009a) Capillary pressure model (Lappalainen et al., 2009b)	No reaction Hydrodynamics only	Case I: 114 mm (i.d.) × 0.55 m (length) (cylindrical column) Case II: 400 mm (i.d.) × 1.8 m (length) (cylindrical column) Case III: 800 mm × 600 mm × 200 mm (rectangular column)	Case I: $U_L = 0.25$ cm/s, $U_G = 1.0$ m/s Case II: $U_L = 0.03$ cm/s, $U_G = 9.95$ m/s Case III: $U_L = 0.1$ cm/s, $U_G = 4.27$ m/s	Cell spacing: 5 mm (cases I, II, 2D-axi) 10 mm (vertil) + 6 mm (Horizon) (Case III, 3D) Discretisation Volume fraction: first-order scheme Momentum: second-order scheme Time step: 10^{-2}–0.1
Lopes and Quinta-Ferreira (2008)	Euler–Euler approach	Standard k–ε model (SKE)	Gas–liquid, gas–solid, and liquid–solid momentum exchanges (Attou and Ferschneider, 2000)	No reaction Hydrodynamics only	Pilot TBR unit (50 mm i.d. × 1.0 m length) $D_p = 1$, 2, 3, and 4 mm	$G = 0.1$–0.7 kg/m^2/s $L = 1$, 5, 10, 15 kg/m^2/s $P = 30$ bar $T = 25$°C	Computational mesh: 10 layers (around 200 nonoverlapping-spherical particles) Under-relaxation factors 0.4 (pressure), 0.6 (velocity) $Y+$ criterion: <200 Time step: 10^{-3} Grid convergence criterion 1% relative error

(*Continued*)

Table 6. (*Continued*)

Refs.	Modelling approach	Turbulence model	Drag force model	Reaction system considered	Geometry	Operating details	Numerical details
Janecki et al. (2008)	Euler–Euler (three-fluids) approach	Not included	Phase interaction force model (Attou and Ferschneider, 1999)	No reaction	Laboratory-scale TBR unit (57 mmi.d. × 1.4 m length)	Liquid modulation: base-impulse method	2D simulation (axi-symmetry)
	Gas phase (primary phase)		Radial porosity distribution (Mueller, 1992)	Hydrodynamics only	$D_p = 3$ mm	Superficial velocity ranges $U_G = 0.08$–0.28 m/s	Spatial discretisation
	Liquid phase (secondary phase)		Axial porosity distribution: normal distribution (given mean value and standard deviation)			$U_L = 5.0E{-}3$–8.2E−3 m/s	22 Cells (radial direction)
	Solid phase (secondary phase)		Zero capillary pressure was assumed			Periodic parameters: ($t_b/t_{ip} = 2/1$, 3/1, 3/2, 20/3)	275 Cells (axial direction)
	The velocity of solid phase was assumed to be 0						Number of cells: 6050 cells Time step: 10^{-2} CFD tool: FLUENT 6.1.22
Atta et al. (2007a)	Euler–Euler two-phase approach	Not included (assumed to be insignificant)	Relative permeability model (Saez and Carbonell, 1985)	No reaction	Case 1: $D/H/d_p = 165$ mm/1.49 m/3 mm	$U_G = 0.13$–0.95 m/s	2D simulation (axisymmetric domain)
	Gas phase (primary phase)		Radial porosity distribution: uniform and constant	Hydrodynamics only	Case 2: $D/H/d_p = 80$ mm/1.05 m/2.7 mm	$U_L = (0.4$–$9.2) \times 10^{-3}$ m/s atmospheric pressure	Discretisation scheme: first-order upwind
	Liquid phase (secondary phase)		Capillary pressure force: neglected		Case 3: $D/H/d_p = 92.4$ mm/1.835 m/6.27 mm Case 4: $D/H/d_p = 165$ mm/1.49 m/3 mm Case 5: $D/H/d_p = 114$ mm/1.0 m/6 mm		Under-relaxation factors 0.3 (pressure), 0.7 (velocity) 0.2 (volume fraction), 1.0 (body force) Time step: 5×10^{-3} Convergence criterion: 10^{-5}

(*Continued*)

Table 6. (*Continued*)

Refs.	Modelling approach	Turbulence model	Drag force model	Reaction system considered	Geometry	Operating details	Numerical details
Atta et al. (2007b)	Euler–Euler two-phase approach	Not included (assumed to be insignificant)	Relative permeability model (Saez and Carbonell, 1985)	No reaction	Dimension of TBR unit	$U_G = 0.02$–0.154 m/s	Time step: three orders of magnitude
			Radial porosity distribution	Hydrodynamics only	Bigger column: 300 mmi.d. × 1.3 m length	$U_L = 0.001$–0.006 m/s	Smaller than the respective mean residence time
			Small column (Cohen and Metzner, 1981)		Small column: 114 mmi.d. × 0.7 m length		
			Big column (Cohen and Metzner, 1981)		$D_p = 2$ mm		Convergence criterion: mass residual $<10^{-4}$
			Capillary pressure force: neglected		Distributors (bigger column, Marcandelli et al., 2000): D_1: 25 10 mm ID orifices (Multi-orifice), D_2: two 25 mm ID orifices (Bi-orifice), D_3: one 25 mm ID orifice(Mono-orifice)		3D simulation
					Distributors (small column, Herskowitz and Smith, 1978): D_1: point-source feed		CFD tool: FLUENT 6.2
Lopes et al. (2007)	Euler–Euler two-fluid model	Multiphase k–ε turbulence model	Interphase momentum exchanges (Attou and Ferschneider, 1999)	CWAO of vanillic acid	Pilot TBR unit (50 mm i.d. × 1.0 m length)	$G = 0.1$–0.7 kg/m^2/s	Grid generation
				Catalyst: manganese cerium oxide (Mn-Ce-O)		$L = 0.05$–15 kg/m^2/s	Tetrahedral (around/over particles)
						$P = 10$–30 bar	Hexahedral (elsewherete)
						$T = 200$–220°C	Number of cells: ~800 000
							Discretisation
							Momentum: second upwind scheme
							k, ε: QUICK

(*Continued*)

Table 6. (*Continued*)

Refs.	Modelling approach	Turbulence model	Drag force model	Reaction system considered	Geometry	Operating details	Numerical details
Lopes and Quinta-Ferreira (2007)	Euler–Euler two-fluid model	Multiphase k–ε turbulence model	Interphase momentum exchanges (Attou and Ferschneider, 1999)	CWAO of phenolic acids	Pilot TBR unit (50 mm i.d. × 1.0 m length)	$G = 0.1$–$0.7\ kg/m^2/s$	Grid generation
					$D_p = 2$ mm	$L = 0.05$–$15\ kg/m^2/s$ $P = 10$–30 bar $T = 290$–500 K	Tetrahedral (around/over particles) Hexahedral (elsewherete) Cell sknewness: <0.6 Reactor wall and catalyst surfaces (nonslip boundaries with standard wall functions) First-order upwind scheme discretisation for spatial derivatives Grid convergence criterion <5% Change in pressure drop <1% Change in liquid volume fraction Convergence criteria: scaled residuals $<10^{-3}$
Gunjal et al. (2007)	Euler–Euler (three-fluids) approach	Not included	Phase interaction force model (Attou and Ferschneider, 1999)	Major hydroprocessing reactions	Lab. scale reactor: $D/H/d_p = 19$ mm/0.5 m/2.4 mm	LHSV $= 1.5\ h^{-1}$	2D simulation (axisymmetric domain)
	Gas phase (primary phase)		Radial porosity distribution (Mueller, 1991)	Hydro-desulfurisation	Commericalscale reactor: $D/H/d_p = 1900$ mm/8.0 m/2.4 mm	$P = 20$–80 MPa	Grid convergence criterion
	Liquid phase (secondary phase)		Axial porosity distribution: assuming axially averaged porosity varies about 5% of the mean value	Hydro-dearomatisation		$T = 593$–653 K	<5% change in pressure drop
	Solid phase (secondary phase) The velocity of solid phase was assumed to be 0 cells		Capillary pressure effect: neglected			Initial H_2S conc.: 1.0–2.5%	<0.75% change in liquid volume fraction Number of cells: ~16 000 Discretisation scheme: QUICK Time step: 5×10^{-3}

(*Continued*)

Table 6. (*Continued*)

Refs.	Modelling approach	Turbulence model	Drag force model	Reaction system considered	Geometry	Operating details	Numerical details
Boyer et al. (2005)	Euler–Euler *k*-fluid approach	Not included	Fluid–particle momentum exchange (single-slit model, Holub et al., 1992)	No reaction	Dimension of TBR unit: $D/H/d_p = 400$ mm/ 1.8 m/1.99 mm	$L = 128\ h^{-1}$	2D simulation (axisymmetric domain)
			Gas–liquid momentum exchange (Attou et al., 1999)	Hydrodynamics only	Distributor single-source liquid inlet configuration	$G = 45\ m^3/h$ (cases I and III)	Grid sizes
			Axial porosity distribution $\varepsilon(z) = 0.421 - 0.124z + 0.047z^2$			$G = 90\ m^3/h$ (case II)	1 cm (axial), 0.4 cm (radial)
			Capillary pressure correlation considered Attou and Ferschneider (2000) or Grosser et al. (1988)			Non-prewetting (cases I and II)	Initial liquid hold
			Wetting efficiency model (El-Hisnawi, 1981)			Prewetting (case III)	0.0 (Non-prewetted), 0.05 (prewetted)
							CFD package: CFDLIB
Souadnia et al. (2005)	Euler–Euler *k*-fluid approach	Not included	Relative permeability model (Saez and Carbonell, 1985)	No reaction	Dimension of TBR unit: $D/H/d_p = 500$ mm/ 1.6 m/5.0 mm	$G = 0.61\ kg/m^2/s$	CFD tool: in-house package
			Radial porosity distribution: uniform and constant	Hydrodynamics only		$L = 8.06\ kg/m^2/s$	1D simulation
			Capillary pressure is neglected				Number of cells: 100
							Numerical approach Finite-volume method (FVM) Crank–Nicholson scheme (discretisation) Second-order Godunov's method (extrapolation) Initial liquid saturation: 0.15 (uniform) Time step: 1×10^{-3}

(*Continued*)

Table 6. (*Continued*)

Refs.	Modelling approach	Turbulence model	Drag force model	Reaction system considered	Geometry	Operating details	Numerical details
Jiang et al. (2005)	Euler–Euler (three-fluids) approach	Not included	Fluid–particle momentum exchange (single-slit model, Holub et al., 1992)	Reaction: an irreversible solid catalysed reaction between gaseous reactant A and liquid reactant B of the general form	$D = 100$ mm	$U_G = 0.06$ m/s	2D simulation (axisymmetric domain)
	Mixing cell network model		Gas–liquid momentum exchange (Attou et al., 1999) Axial porosity distribution: pseudo-Gaussian distribution Capillary pressure correlation considered Attou and Ferschneider (2000) or Grosser et al. (1988) Wetting efficiency model (El-Hisnawi, 1981)		$H = 0.5$ m $d_p = 3$ mm	$U_L = 3 \times 10^{-3}$ m/s	CFD package: CFDLIB
Ortiz-Arroyo and Larachi (2005)	Lagrange–Euler–Euler approach	Not included	Fluid–particle momentum exchange (single-slit model, Holub et al., 1992)	No reaction	Kerosene–air-catalyst system (+kaolinites)	$G = 0.09$–0.43 kg/m^2/s	CFD package: CFDLIB
			Gas–liquid momentum exchange: (neglected)	Hydrodynamics only (filtration hydrodynamics: two-phase gas–liquid flow seeded with fines)	$D = 38$ mm $H = 0.9$ m Stationary packing: $d_p = 4$ mm (spherical catalyst) $d_p = 1.29$ mm (trilobes catalyst) Flowing fines: $D_{fine} = 0.7 \times 10^{-6}$ m (kaolinite)	$L = 0.9$–3.6 kg/m^2/s Atmospheric pressure	

(*Continued*)

Table 6. (*Continued*)

Refs.	Modelling approach	Turbulence model	Drag force model	Reaction system considered	Geometry	Operating details	Numerical details
Gunjal et al. (2005a)	Euler–Euler (three-fluids) approach	Not included	Phase interaction force model (Attou et al., 1999)	No reaction	Case 1: $D/H/d_p = 165$ mm/ 1.49 m/3 mm	$U_G = 0.2$–5.5 m/s	2D simulation (axisymmetric domain)
	Gas phase (primary phase)		Radial porosity distribution (Mueller, 1991)	Hydrodynamics only	Case 2: $D/H/d_p = 80$ mm/ 1.05 m/2.7 mm	$U_L = (0.2$–$2.8) \times 10^{-3}$ m/s	Number of cells: 25 000
	Liquid phase (secondary phase)		Axial porosity distribution: random fluctuations (following Gaussian distribution)		Case 3: $D/H/d_p = 92.4$ mm/ 1.835 m/6 mm	Atmospheric pressure	Grid division: 500 cells (axial)
	Solid phase (secondary phase)		Capillary pressure model (Attou and Ferschneider, 2000)				50 Cells (radial)
	The velocity of solid phase was assumed to be 0 cells						Grid convergence criterion <5% change in pressure drop <0.75% change in liquid volume fraction Time step: 5×10^{-3}
Gunjal et al. (2005b)	Volume-of-fluid (VOF)	Not included	Brackbill et al. (1992) model: surface tension and wall adhesion	No reaction	Droplet diameters: $d_p = 4.2$ mm/2.5 mm/ 2.75 mm	Impact velocities: $V = 0.22$, 0.3, 0.45, 1.0, 4.0 m/s	2D axisymmetric simulation domain (if impact velocities <1 m/s)
				Hydrodynamics only	Typical 2D domain: 6 mm × 7 mm (axisymmetric domain)	$Re = 550$–$10\,300$	
						We, $a = 1.5$–$10\,000$	3D simulation domain (if impact velocities >1 m/s)
							Grid division: 10, 13.3, 20, 40 (cells/mm) Time step: 1×10^{-6}–5×10^{-6} s Result record: 1×10^{-3} or 2.5×10^{-3} s CFD tool: FLUENT 6.0

(*Continued*)

Table 6. (*Continued*)

Refs.	Modelling approach	Turbulence model	Drag force model	Reaction system considered	Geometry	Operating details	Numerical details
Gunjal et al. (2003a)	Euler–Euler (three-fluids) approach	Not included	Phase interaction force model (Attou and Ferschneider, 2000)	No reaction	$D = 100$ mm	$U_G = 0.0$–0.44 m/s	2D simulation (axisymmetric domain)
	Gas phase (primary phase)			Hydrodynamics only (liquid distribution and RTD)	$H = 1.05$ m	$U_L = (3.0$–$10.0) \times 10^{-3}$ m/s	Grid division
	Liquid phase (secondary phase)		Radial porosity distribution (Mueller, 1991)		$d_p = 3$ mm/6 mm	Atmospheric pressure	2D sim.: 150 cells (axial), 20 cells (radial)
	Solid phase (secondary phase)				$E_b = 0.37/0.356$		3D sim.: 100 cells (axial), 20 cells (others)
	The velocity of solid phase was assumed to be 0 cells		Axial porosity distribution				Time step: 1×10^{-2}
			Random fluctuations (following Gaussian distribution)				CFD tool: FLUENT 4.5
			Capillary pressure model (Attou and Ferschneider, 2000)				
Gunjal et al. (2003b)	Volume-of-fluid (VOF)	Not included	Brackbill et al. (1992) model: surface tension and wall adhesion	No reaction	Droplet diameter: $d_p = 4.2$ mm	Drop impact velocities: $V = \sim 0.2$ m/s	Grid spacing: 0.2 mm
				Hydrodynamics only	2D Domain: 20 mm × 15 mm (axisymmetric domain)	Contact angle: 45°	CFD tool: FLUENT 6.0

(*Continued*)

Table 6. (*Continued*)

Refs.	Modelling approach	Turbulence model	Drag force model	Reaction system considered	Geometry	Operating details	Numerical details
Ortiz-Arroyo et al. (2002)	Euler–Euler *k*-fluid approach	Not included	Fluid–particle interaction model: Blake–Kozeny–Carman drag (modified)	No reaction	Kerosene–air–glass sphere (+carbon black)	Liquid phase: $Re_L = 0.1$, 0.5, 1.0	2D axisymmetric simulation domain
			Axial porosity distribution: random fluctuations (normal Gaussian distribution)	Hydrodynamics only (filtration hydrodynamics: single-phase liquid flow seeded with fines)	$D = 25.4$ mm	Fines loading: 100–200 mg/L	Number of cells: ~3000
					$H = 0.30$ m	Atmospheric pressure	Initial state: steady-state clean liquid flow
					$E_b = 0.37$	Room temperature	Grid independence criterion
					Stationary packing: $d_p = 1.0$ mm (glass sphere)		MARE <0.5% (pressure drop)
					Flowing fines: $D_{fine} = (5–8) \times 10^{-6}$ m (carbon black)		MARE <0.5% (specific deposit profile)
							CFD package: CFDLIB
Jiang et al. (2002a,b)	Eulerian *k*-fluid approach	Not included	Fluid–particle momentum exchange (I. single-slit model, Holub et al. (1992) with $E_1 = 215$, $E_2 = 1.4$) (II. Saez and Carbonell model, 1985)	No reaction	Working fluids: air + water	The experimental operating conditions from Szady and Sundaresan (1991)	2D axisymmetric simulation domain
			Gas–liquid momentum exchange (Attou et al., 1999)	Hydrodynamics only	Case I: 2D cylindrical bed:		Grid division
			Axial porosity distribution: (pseudo-Gaussian distribution)		$D = 0.152$ m		2D axisymmetric simulation:
&		Radial porosity distribution: Mueller's correlation (1991)			$H = 1.50$ m	1.0 cm (axial)	
			Capillary pressure correlation considered: Attou and Ferschneider (2000) or Grosser et al. (1988)		$d_p = 3.0$ mm		Two-region (radial)
					$E_b = 0.37$		2D rectangular simulation
			wetting efficiency model: El-Hisnawi (1981)		Case II: 2D rectangular bed		33 Cells (vertical)
					Width = 7.2 cm		8 Cells (horizontal)
					Height = 29.7 cm		CFD package: CFDLIB
					$E_b = 0.406$		

(*Continued*)

Table 6. (*Continued*)

Refs.	Modelling approach	Turbulence model	Drag force model	Reaction system considered	Geometry	Operating details	Numerical details
Harter et al. (2001)	Volume-of-fluid (VOF)	Standard k–ε model (SKE)	Brackbill et al. (1992) model: surface tension and wall adhesion	No reaction	Working fluids: water + N_2	$G = 0.06$–0.52 kg/m^2/s	Time step: 10^{-7}–10^{-3} s
				Hydrodynamics only	Mock-up unit (1/5 industrial size) with collecting system	$L = 0.35$–14.0 kg/m^2/s	CFD package: Fluent 5.4
					$D = 600$ mm $H = 5$ m	$P = 1.0$–4.0 bar	
Jiang et al. (2001a)	Eulerian k-fluid approach	Not included	Fluid–particle momentum exchange (single-slit model, Holub et al., 1992) (with $E_1 = 180$, $E_2 = 1.8$)	No reaction	Case I: cylindrical bed	$U_G = 6.0$ cm/s	2D axisymmetric/rectangular simulation domain
			Gas–liquid momentum exchange (Attou et al., 1999)	Hydrodynamics only	$D = 2.4$ cm	$U_L = 0.4$ cm/s	Grid division (2D rectangular bed)
			Axial porosity distribution: (pseudo-Gaussian distribution)		$H = 22.5$ cm	Periodic liquid inflow	33 cells (vertical)
			Radial porosity distribution: Mueller's correlation (1991)		$d_p = 1.5$ mm	Cycle time: 60–15 s (ON) + 45 s (OFF)	8 Cells (horizontal)
			Capillary pressure correlation considered Grosser et al. (1988) model modified by Jiang et al.				
			Wetting efficiency model: Al-Dahhan and Dudukovic (1995)				
					Case II: 2D rectangular bed Width = 7.2 cm Height = 29.7 cm		CFD package: CFDLIB

(*Continued*)

Table 6. (*Continued*)

Refs.	Modelling approach	Turbulence model	Drag force model	Reaction system considered	Geometry	Operating details	Numerical details
Jiang et al. (2001b)	Eulerian *k*-fluid approach	Not included	Fluid–particle momentum exchange (single-slit model, Holub et al., 1992) (with $E_1 = 180$, $E_2 = 1.8$)	No reaction	2D rectangular bed	$U_G = 6.0$ cm/s	2D rectangular simulation domain
			Gas–liquid momentum exchange (Attou et al., 1999)	Hydrodynamics only	Width = 10.0 cm	$U_L = 0.3$ cm/s	Grid division: 50 cells (vertical)
			Porosity distribution: (pseudo-Gaussian distribution)		Height = 50.0 cm		10 cells (horizontal)
			Capillary pressure correlation considered Grosser et al. (1988) model modified by Jiang et al. (1999)		$d_p = 3.0$ mm		CFD package: CFDLIB
			Wetting efficiency model: Al-Dahhan and Dudukovic (1995)		$E_b = 0.399/0.404$		
Propp et al. (2000)	Euler–Euler approach	Not included	Relative permeability model (Saez and Carbonell, 1985)	No reaction	—	—	2D rectangular/cylindrical domain
				Hydrodynamics only			Finite volume discretisation

(*Continued*)

Table 6. An "overview" summary of the simulation details of the literature multidimensional CFD work on TBRs

Refs.	Modelling approach	Turbulence model	Drag force model	Reaction system considered	Geometry	Operating details	Numerical details
Jiang et al. (1999)	Eulerian *k*-fluid approach	Not included	Fluid–particle momentum exchange (Holub et al., 1992)	No reaction	"2D"model reactor	$U_G = 0.05$ m/s	2D rectangular simulation domain
			Porosity distribution: (pseudo-random distribution)	Hydrodynamics only	Width = 7.2 cm (8 cells)	$U_L = 0.00148$ m/s	CFD package: CFDLIB
			Capillary pressure correlation considered Grosser et al. (1988)		Height = 28.8 cm (32 cells)	Atmospheric pressure	
			Wetting efficiency model: introduced		Thickness = 0.9 cm (1 cell)	Prewetted and non-prewetting packing	
					$d_p = 3.0$ mm (glass beads)	Single-point source liquid inlet	
					$E_b = 0.415$		
Anderson and Sapre (1991)	Euler–Euler approach	Not included	Relative permeability model (Saez and Carbonell, 1985)	No reaction	"2D"model reactor	$G = 0.14$ kg/m^2 s (air)	2D rectangular simulation domain
				Hydrodynamics only	Width = 1.2 m	$L = 2.2$ kg/m^2 s (water)	Grid size: 10×15 or 19×29
					Height = 1.6 m		Finite difference discretisation
					Thickness = 0.025 m		
					$d_p = 3.0$ mm (glass beads)		
					System: air–water–glass beads		

model by Saez and Carbonell (1985). Comparative studies of the hydrodynamic parameters (i.e. pressure drop and liquid holdup) and experimental data from the literature (Specchia and Baldi, 1977; Rao et al., 1983; Szady and Sundaresan, 1991) were conducted under cold-flow conditions. To test the applicability of the proposed CFD model in high-pressure TBR scenarios, Atta et al. (2010a) evaluated different combinations of relative permeability correlations to predict the pressure drop and liquid holdup. The CFD model predictions were compared with high-pressure experimental data collected from different sources. The authors concluded that the CFD methodology based on the porous-media concept was less computationally intensive, yet functioned well in predicting two-phase hydrodynamics for high-pressure TBRs.

Gas–liquid flow maldistribution

One of the major challenges in the design and operation of TBRs is the prevention of liquid flow maldistribution (Stanek et al., 1981; Sundaresan, 1994; Maiti and Nigam, 2007), which results in incomplete wetting of parts of the bed. As a consequence the catalyst bed is under-utilised and reactor performance and productivity suffer, particularly for liquid limited reactions at low liquid velocities. The macro-level flow distribution is mainly affected by inlet liquid distribution, particle shape and size, fluid velocity and packing method. Due to its multidimensional nature, multiphase CFD simulation of TBRs, linked with appropriate constitutive equations, has unique capabilities for capturing flow distribution in non-uniform gas and liquid flow conditions where plug flow cannot be assumed. A number of CFD investigations addressing flow maldistribution phenomena in TBRs have been reported in the literature in recent years.

Jiang et al. (2001a) used the Eulerian *k*-fluid CFD model to test the effect of forced periodic operation on liquid maldistribution. A two-dimensional rectangular reactor (29.7 cm $\times$ 7.2 cm) was considered and the liquid flow was injected at two central cells at the top (0.1 cm/s) and gas was fed into the rest of the cells (10.0 cm/s). It was demonstrated that unsteady-state operation ensures better uniformity in liquid distribution at all locations than that observed in steady-state operation. Boyer et al. (2005) studied liquid spreading from a single point source in a trickle bed using gamma-ray tomography and CFD simulation. The simulation results showed that Euler–Euler simulation can semiquantitatively predict the liquid spreading from a point source and that the capillary pressure term has a significant effect on predictions of the radial spreading of the liquid flow. A modified capillary pressure expression accounting for initial bed wetting was suggested to qualitatively predict the behaviour of liquid spread from a single-source liquid inlet. Atta et al. (2007b) developed a three-dimensional two-phase Eulerian CFD model to understand and predict liquid maldistribution in TBRs under cold-flow conditions. In this model, the inter-phase coupling terms were implemented using a relative permeability concept (Saez and Carbonell, 1985). The model performed well in the case of a multi-orifice liquid distributor. However, the simulation results for a single-orifice liquid distributor showed significant spreading only in cases where the ratio of the column diameter to the particle diameter was very low ($\sim$12) and a radial porosity profile was applied. Lopes and Quinta-Ferreira (2009b) developed an Eulerian multiphase model to predict the liquid holdup and pressure drop under conditions of imposed liquid maldistribution at the bed top. Three types of liquid distributors (single-point distributor, 60-hole distributor and uniform distributor) were considered in the CFD simulations. The simulation results indicated that the distributor geometry has a major effect on hydrodynamics in lower-interaction regimes, while the liquid flow rate controls the radial distribution of multiphase flow in higher-interaction regimes. Lappalainen et al. (2009a) developed a CFD model by fully taking into account three different mechanisms (i.e. mechanical dispersion, capillary dispersion and overloading) contributing to liquid spreading. The CFD model was validated against the literature experimental data with liquid phase fed from single-point sources. It was shown that liquid spreading is dominated by capillary dispersion for small particles and by mechanical dispersion for large particles.

Fine filtration two-phase flow in TBRs

When liquids containing low concentrations of fine solid impurities are treated in packed-bed reactors, clogging develops and severely restricts the flow. This phenomenon, called deep-bed filtration, constitutes a serious concern for the hydrotreating or hydrocracking of bituminous sands in packed-bed reactors, in which non-filterable fines, such as native clay or incipient coke cause reactor dysfunction by clogging. The complex multiphase hydrodynamics, along with the effects of fines aggregation/collection, alter the physicochemical mechanisms inside TBRs, making the process fundamentals difficult to grasp. The contribution from the research group of Laval University highlighted the possibilities of multiphase CFD simulations for flows relevant to petroleum refining involving filtration mechanisms.

Ortiz-Arroyo et al. (2002) proposed a CFD framework to provide a qualitative/quantitative assessment of the impact of fines buildup during *single-phase flow* hydrodynamics. Efforts were made to formulate appropriate drag closures and an effective-specific surface area model for the unsteady-state simulation under filtration conditions. The authors benchmarked the computational results with experimental observations from Narayan et al. (1997). As a further extension, Ortiz-Arroyo and Larachi (2005) developed a Lagrange–Euler–Euler CFD approach to represent *two-phase flow* in TBRs undergoing deposition of colloidal/non-colloidal fines. New equations for collection efficiencies and filtration coefficients were established for monolayer and multilayer collection mechanisms. The simulations were put to the test using the experimental pressure drop data and observations by Gray et al. (2002), who studied experimentally the plugging of a cold-flow trickle-bed unit during the flow of kerosene–clay suspensions through trickle beds containing spherical and trilobe catalyst. The comparison between the CFD simulations and the experimental data is demonstrated in Figure 8.

Iliuta et al. (2003) developed a one-dimensional two-fluid model to describe two-phase flow and space-time evolution of the deposition of fines in TBRs, with the assumption that plugging develops through deep-bed filtration mechanisms. The model incorporates physical effects of porosity and effective-specific surface area changes due to the fines capture by the catalyst particles, inertial effects in the gas and the suspension, and coupling effects between the filtration parameters and the interfacial momentum exchange force terms. Both mono- and multiple-layer deposition mechanisms during the ripening stages were accounted for by including the appropriate filter coefficient formulation. The approach was validated using the experiments and observations of Gray et al. (2002). To assess how clean beds evolve from an initial trickle-flow regime to a pulse-flow regime as a result of

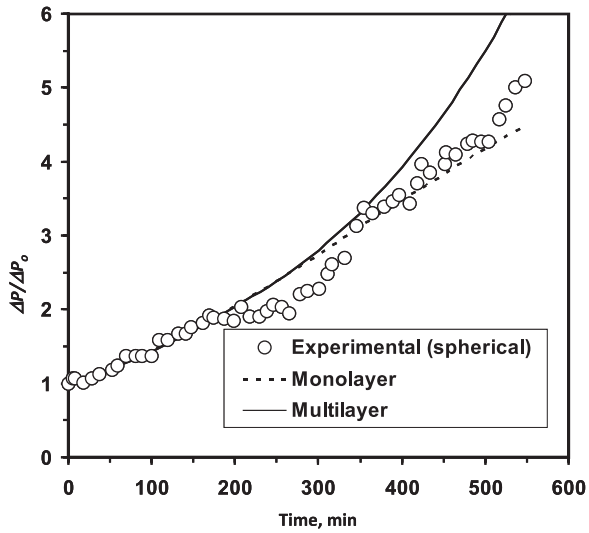

Figure 8. Comparison of experimental data with CFD simulations (Ortiz-Arroyo and Larachi, 2005).

flow obstruction induced by fines deposition, Iliuta and Larachi (2004c) developed a macroscopic two-fluid modelling framework which is coupled with a fines deposition model and a linear stability analysis of two-phase flow. The transition between trickle- and pulse-flow regimes is described from the stability analysis of the solution of the transient two-fluid model around an equilibrium state of trickle flow. It is shown that, for larger fines, the transition to pulse flow occurs rapidly in the entrance region of the bed, with a relatively slow progression along the bed. For fines diameters in the micrometer range, plugging is more uniformly distributed along the bed and the transition between trickle- and pulse-flow regimes rapidly fills up the entire packed bed. Liquid and gas superficial velocities at the transition decrease linearly with the local volume-averaged-specific deposit.

If liquid flow shock or periodic operation is implemented, the *detachment* of deposited fines or the *inhibition* of fines deposition over some regions of the collector can be expected to alleviate the plugging. Current physical models linking gas–liquid flow to the filtration process in trickle beds have neglected the possible *detachment* of fine particles and the potential beneficial impact of induced pulsing to reduce the plugging in trickle beds. Iliuta and Larachi (2005a,b) attempted to develop a dynamic multiphase flow deep-bed filtration model to describe two-phase flow and the space-time evolution of both *deposition* and *detachment* of fine particles in TBRs. The release of the fine particles from the collector surface was assumed to be induced by colloidal forces in the case of Brownian particles or by hydrodynamic forces in the case of non-Brownian particles. Simulations were conducted at room temperature under cold-flow plugging conditions (Iliuta and Larachi, 2005a) and high-pressure/temperature hot-flow plugging conditions (Iliuta and Larachi, 2005b). The effects of periodic operation of a TBR on the release of fine particles was investigated more specifically for stretching the life cycle of trickle-bed hydrotreaters. One of the important aspects not addressed in the literature is the *aggregation* of fines and the *detachment* of fine particles/aggregates during plugging with Brownian particles. To address this issue, Iliuta and Larachi (2006a) attempted to develop an Euler–Euler fluid dynamic model, which accounts for the filtration equations for the Brownian particles/aggregates as well as the discrete population balance equations for the agglomeration of particles. The model is proposed for the description of two-phase flow and deposition/aggregation/release of Brownian fine solids in high-pressure/temperature TBRs. The simulation results showed that most of the colloidal aggregates were formed from small primary Brownian particles. The number of large non-Brownian aggregates prone to detach due to hydrodynamic forces is very low. Without exception, the modelling work on fines deposition in trickle-bed systems in the literature has confined itself to inertial non-reactive conditions. To assess the effect of fine particle deposition under chemical reaction conditions, Iliuta et al. (2006a) attempted to develop a dynamic multiphase deep-bed filtration model that was coupled with heat and species balance equations in liquid, gas and solid (catalyst plus solid deposit) phases. Hydrodesulfurisation of dibenzothiophene (in the presence of sulfided Co-Mo/Al_2O_3 catalyst) was investigated as a case study. An important finding was that the fine particle deposition process does not appreciably change TBR performance. The unique undesirable consequences of fine-particle deposition are bed plugging and increased resistance to two-phase flow.

Bio-trickling bed two-phase flow

Biological pollutant degradation treatment, which occurs at normal temperature and pressure, represents a potentially energy-efficient technology, as opposed to traditional energy-demanding physical and chemical abatement processes (e.g. catalytic oxidation, incineration, absorption or regenerative adsorption). Trickle-bed bioreactors, in which the biocatalysts are immobilised in a stationary matrix of porous solids to achieve a desired bio-reaction/conversion, have become increasingly important in waste gas and wastewater treatment. A major drawback limiting the use of trickle-bed bioreactors for biological wastewater treatment is the biological clogging phenomenon induced by the formation of excessive biomass, leading to progressive obstruction of the bed, increased pressure drop and flow channelling. Clogging is a complex phenomenon determined by such diverse factors as the biological and physical characteristics of the compounds involved and the structural characteristics of the packing material. Therefore, it is vital to gain fundamental knowledge by tackling the complex hydrodynamic, physical and microbiological phenomena involved in the clogging of trickle beds due to the formation of excessive amounts of biomass and the retention of suspended fine particles.

Over the past decade, several investigators have attempted to describe the transient behaviour of biomass accumulation in gas-phase bioreactors for waste gas treatment. However, the importance of the coupling between hydrodynamics, clogging, mass transport and bioreaction in terms of pressure buildup and transient operation at the bioreactor scale has not been addressed comprehensively. In fact, physical models linking the two-phase flow to the space-time evolution of biological clogging are virtually non-existent at present. Given that one of the most acute engineering challenges in biofilm reactors is related to the control of biofilm thickness and structure, there is a need for new types of models to address this coupling (between hydrodynamics, bioreactions and clogging) for trickle-bed bioreactors.

Iliuta and Larachi (2004a) developed a one-dimensional two-fluid model to describe the space-time evolution of biological clogging in trickle-bed bioreactors for wastewater treatment. The two-phase hydrodynamic model is coupled with the simultaneous transport and consumption of phenol and oxygen within the biofilm, and with the simultaneous diffusion of both phenol and oxygen and adsorption of phenol within the activated carbon particles. Biodegradation of phenol using *Pseudomonas putida* as the

predominant species immobilised on activated carbon was chosen as a case study to illustrate the influence of biomass accumulation on bioreactor hydrodynamics. The simulation results showed that as time passes the clogging front progressively fills up the column. However, biomass accumulation (clogging) is mostly confined to the entrance region due to the higher rate of cell growth there. There is a noticeable decrease in the local porosity in the entrance section of the bed. It was also shown that lower bed porosity or particle diameter induces a thinner biofilm but leads to a greater rise in the pressure drop. Later, a predictive dynamic model was proposed by Iliuta et al. (2005) to link two-phase hydrodynamics to the space-time distribution of bioclogging and biokinetics in trickle-bed bioreactors for waste gas treatment. Toluene degradation using biodegrading microbes immobilised on diatomaceous earth biological support media was investigated as a case study. The simulation results showed that biomass formation adversely affects pressure drop, which first increases slowly, and then almost exponentially, with void loss at the expense of biomass accumulation. With increasing substrate feed concentration, both cell growth rate and biomass accumulation increase, yielding thicker biofilms and larger pressure drops. A reduction in the total dry biomass in the biofilm causes an increase in the biofilm thickness that translates into larger pressure drops. Biomass loss is an important controlling factor as it contributes to the mitigation of biological clogging.

One of the important features associated with biological clogging in trickle-bed bioreactors is the *aggregation* of cells and the *detachment* of cells and aggregates from pore bodies within the porous bed. However, current theoretical models describing the transient behaviour of biomass accumulation and the biological clogging in trickle-bed bioreactors for waste gas and wastewater treatment neglect cell aggregation and aggregate detachment. Iliuta and Larachi (2006b) attempted to develop a two-fluid dynamic model accounting for momentum equations, species balance equations, the biomass dynamics equation, filtration equations for the cells and the aggregates, as well as discrete population balance equations for cell agglomeration. Biodegradation of phenol by *Pseudomonas putida* immobilised on activated carbon was analysed. The simulation results showed that, in the first period of biofilm growth, only a small number of cells and aggregates detach from the surface, indicating that the process is dominated by growth, attachment and aggregation. A lower fractal dimension implies that larger numbers of non-Brownian aggregates are hydrodynamically non-detachable. Higher values of the hydrodynamic detachment rate coefficient are consistent with the delayed buildup of pressure drop.

Wastewaters may well contain significant amounts of colloidal and particulate matter in addition to soluble substances. In combination with biological clogging, progressive physical plugging phenomena induced by the retention of these inert suspended fine particles can also exacerbate the narrowing of the free space available for two-phase flow. The concurrent overgrowth of attached biomass and deep-bed filtration of suspended fine particles lead to the progressive diminution of porosity and obstruction of the bed. To quantify and understand the space-time evolution of simultaneous *biological clogging* and *physical plugging*, Iliuta and Larachi (2005c) proposed a general two-fluid model based on the volume-average mass and momentum balance equations for the gas and liquid phases and the continuity equation for the solid phase, the species balance equation for the fine particles, as well as simultaneous transport and consumption of substrate and oxygen within the biofilm and solid particles. The hypothesis of the model is that physical plugging occurs via mono-layer deep-bed filtration mechanisms and that biological clogging is induced by the formation of excessive biomass. The model incorporates physical effects of porosity and effective-specific surface area changes due to the capture of fine particles and biomass accumulation, the effects of biomass loss (via biomass decay and physical shearing), inertial effects of the phases and coupling effects between the filtration parameters and the interfacial momentum exchange force terms. Through this work, a new generalised two-fluid transient model has been developed that describes simultaneous *biological clogging* and *physical plugging*. Phenol biodegradation using *Pseudomonas putida* as the predominant species immobilised on activated carbon was analysed as a case study. The simulation results showed that the deposition of larger fine particles promotes more confined physical plugging in the entrance region. However, for smaller fines (Brownian particles), the extent of fines deposition is more homogeneous and physical plugging is distributed more uniformly along the bed. With increasing phenol concentration at the inlet, both the cell growth rate and the biomass accumulation increase, yielding greater biofilm thickness and thereby resulting in the bed porosity decreases (biological plugging) and two-phase pressure drop increases. Higher fines concentrations give rise to higher filtration rates and consequently increased deposition. As a result, the bed porosity decreases (physical plugging) and the two-phase pressure drop increases.

Trickle-flow magnetohydrodynamics

The ability to influence two-phase flows through porous media and intensify the catalytic process through the use of external magnetic fields is of considerable interest in the operation of TBRs, especially in mini- or micro-sized reactors. The application of inhomogenous magnetic fields in trickle-bed oxidation catalysis, in which the paramagnetic properties of oxygen gas may be propitious to macrogravity operation, could enhance liquid holdup and wetting efficiency. External inhomogeneous magnetic fields exert a body force (magnetisation force) on electrically non-conducting and magnetically permeable fluids. The force acts on both paramagnetic and diamagnetic fluids and can be used to compensate for or to amplify the gravitational body force, unlike the Lorentz braking force that manifests itself only for electrically conducting liquids, such as liquid metals. Evidently, it is of great importance to understand the complex magnetohydrodynamics (MHD) under two-phase flow conditions to ensure proper design and to predict the associated process performance.

Iliuta and Larachi (2003a, 2004b) developed an isothermal one-dimensional two-fluid MHD model to describe gas–liquid downflow under a spatially uniform magnetic field. The slit model approximation was used for the drag force closures in the momentum equations. Four gas–liquid combinations (paramagnetic gas-diamagnetic liquid, paramagnetic gas and liquid, diamagnetic gas and liquid, diamagnetic gas-paramagnetic liquid) were analysed and the advantages of process intensification via external inhomogeneous magnetic fields were rationalised in terms of catalytic reactions (Table 7). As shown in this table, an increase of BdB/dz amplifies the effect of gravity, thereby reducing pressure drop (except in diamagnetic gas and liquid systems). For negative BdB/dz, the upward liquid or gas magnetisation forces induce sub-gravity conditions and an augmentation of two-phase pressure drop (except in diamagnetic gas and liquid systems). Paramagnetic gas-diamagnetic liquid systems deserve particular attention. Elevated magnetic fields improve the liquid holdup and thus the wetting efficiency of catalyst particles. For limited liquid-reactant reactions (such as in catalytic oxidation reactions), both

improvements contribute to increase the chemical conversion of the catalytic reaction, while, simultaneously, the two-phase pressure drop is reduced considerably.

Iliuta and Larachi (2003b) proposed a macroscopic one-dimensional two-fluid MHD model based on the volume-averaged mass, charge and momentum balance equations and the Maxwell equations coupled via the Lorentz force and Ohm's law to predict two-phase pressure drop and total liquid holdup in trickle beds in the presence of a homogeneous transverse magnetic field. The liquid–solid drag force expression was adapted to take into account the influence of the magnetic field on the laminar term and the damping of turbulence/inertia in the liquid phase. Furthermore, model asymptotic formulations have been adapted from the general MHD model for electrically conducting fluids flowing downward with stagnant gas or in single-phase upflow. The model has been validated using literature experimental data in single-phase flow at high temperature and with various magnetic flux densities. The simulation results indicated that both liquid holdup and two-phase pressure drop are functions of magnetic flux density. The two-phase pressure drop and the liquid holdup markedly increase with increasing magnetic flux density due to an increase in liquid shear stress at the liquid/solid interface and the increased importance of the Lorentz force.

Iliuta and Larachi (2003c) developed a comprehensive modelling framework to illustrate how external inhomogeneous magnetic fields may potentially influence the hydrodynamics and the reaction performance in TBRs. The model accounts for the mass and momentum balance equations as well as the volume-averaged species balance equations under a spatially uniform magnetic field gradient. The catalytic wet-air oxidation of phenol in the presence of a CuO/ZnO/CoO catalyst was considered as a case study. The simulation results indicated that reactions limited by liquid reactant (such as the catalytic wet oxidation of phenol) are better performed under external inhomogeneous magnetic fields. Also, with increased magnetic field gradient, the two-phase pressure drop may be drastically reduced (except at low pressures and high liquid velocities).

Linear stability analysis of trickling-to-pulsing transition

Grosser et al. (1988) developed a macroscopic one-dimensional hydrodynamic model for analysing the stability of two-phase flow in trickle beds. This approach is based on the volume-averaged equations of motion of the two phases. The loss of stability of steady-state solutions or non-existence of any solution for the steady-state equations of motion has been identified as the onset of pulsing. The relative permeability drag force expressions for two-phase flow (Saez and Carbonell, 1985), together with the Leverett correlation for the capillary pressure term, were used to obtain reasonable agreement on the effects of gas and liquid flow rates on the trickling-to-pulsing transition. The study of Grosser et al. (1988) was restricted to a linear stability analysis of the uniform state, and no attempt was made to follow the solution structure, which evolves after the loss of stability. In an attempt to understand the onset and evolution of fully developed pulsing flow in trickle beds, Dankworth et al. (1990) used the Grosser et al. (1988) model to predict how the velocity of the liquid pulses moving through the bed depends on gas-phase velocity, and found very reasonable agreement with the experimental observations of Rao and Drinkenberg (1983). Later, further analysis using two-dimensional perturbations was provided by Dankworth and Sundaresan (1992). In their work,

Table 7. Rationalisation of simulations for potential process intensification routes

	Paramagnetic gas + diamagnetic liquid		Paramagnetic gas + paramagnetic liquid		Diamagnetic gas + paramagnetic liquid		Diamagnetic gas + diamagnetic liquid	
	$\Delta P/\Delta P_0^*$	$\varepsilon_L/\varepsilon_{l,0}$	$\Delta P/\Delta P_0$	$\varepsilon_L/\varepsilon_{l,0}$	$\Delta P/\Delta P_0$	$\varepsilon_L/\varepsilon_{l,0}$	$\Delta P/\Delta P_0$	$\varepsilon_L/\varepsilon_{l,0}$
(BdB/dz > 0) ↑	→	↑	→	→	→	→	↑	↑
(BdB/dz < 0) ↓	←	→	←	←	←	←	→	→
	$F_{M,g}$ is controlling		High pressure: $F_{M,l} = F_{M,g}$; low pressure: $F_{M,l} > F_{M,g}$		$F_{M,l}$ is controlling		$F_{M,l}$ is controlling	

Floquet theory was applied to analyse the linear stability of these time-periodic solutions. A two-dimensional linear stability analysis around the uniform "trickling" flow solution suggests that lateral perturbations have a stabilising effect. The results showed remarkable differences between the stability of fully developed waves and the corresponding uniform flow solutions when subjected to the same perturbations. The analysis also showed that two-dimensional flow patterns are likely to evolve from the early stages of pulse growth, and not from breakup of fully developed one-dimensional waves. Attou and Ferschneider (1999) studied the transition from trickling to pulsing flow using the fluid–fluid interfacial drag force expressions (Attou et al., 1999), together with a capillary pressure expression derived by approximating the curvature of the gas/liquid interface during trickling flow around a single particle. Attou and Ferschneider (1999) found that this linear stability analysis model also agreed well with the Grosser et al. (1988) model and with experimental data.

Iliuta and Larachi (2004c) explored the progressive onset of pulse flow along a packed bed under fines filtration conditions. Space-time evolution and two-phase flow of the deposition of fines in TBRs under trickle-flow regime was described using a one-dimensional two-fluid model taking into account the mass and momentum balance equations and species balance equation for the fines. The transition between trickle- and pulse-flow regimes was described from the stability analysis of the solution of the transient two-fluid model around an equilibrium state of trickle flow. It was shown that for larger fines, the transition to pulse flow occurs rapidly in the entrance region of the bed, with a relatively slow progression along the bed. For fines diameters in the micrometer range, plugging is more uniformly distributed along the bed and the transition between trickle- and pulse-flow regimes rapidly fills up the packed bed. Liquid and gas superficial velocities at the transition decrease linearly with the local volume-averaged specific deposit. Using a stability analysis, Iliuta et al. (2006b) modelled the onset of pulsing in trickle beds for two-phase flow with non-Newtonian liquid. The model was developed for the versatile Herschel–Bulkley constitutive rheological equation from which special solutions for plastic Bingham fluids, power–law shear-thinning and thickening fluids, as well as Newtonian fluids were derived. The simulation results indicated that increasing the temperature or pressure promotes pulse flow at higher superficial liquid and gas velocities. The model was found to be capable of predicting very well the trickle-to-pulse flow transition of air + CMS systems at high temperature and pressure. Munteanu and Larachi (2009) performed a linear stability analysis of trickle-to-pulse-transition under external inhomogeneous magnetic fields. The Grosser et al. (1988) transition model was adapted in their work and the magnetic field effect was included via the gravitational amplification factor term. Model predictions were in qualitative accord with experimental findings. The quantitative differences between experiments and model predictions were attributed to non-uniform magnetic field effects. The simulation results showed that the gravitational force on the liquid phase (instead of the gas phase) plays a key role in the return to pulse flow from trickle flow.

Lopes and Quinta-Ferreira (2010d) recently developed an Euler–Euler multidimensional CFD framework coupled with the linear stability analysis of two-phase flow hydrodynamics in TBRs. The relevant parameters that can affect the hydrodynamic transition from the gas-continuous flow regime to the pulsing flow regime were identified under high-pressure conditions. Several parameters were examined to characterise the pulsing flow, which specifically include the velocity of pulses traveling along the bed, the frequency of pulsations and their structure, the length of the pulses and the length of the liquid-rich zone.

CFD Simulation of Hydrodynamics and Reaction Coupling in TBRs

Incorporation of mass transfer and chemical reaction effects into CFD simulations of trickle beds has achieved limited success to date because of numerical limitations stemming from coupling of additional conservation equations of species and energy (Michele, 2002). Therefore, CFD approaches that include these effects have not been adequately investigated so far.

Gunjal and Ranade (2007) developed a two-dimensional Eulerian three-fluid CFD model to simulate hydrodynamics and reaction performance in hydrotreating reactors. The major hydroprocessing reactions—hydrodesulfurisation and hydrodearomatisation reactions—were considered and the model of Attou and Ferschneider (1999) was used as drag force closure to account for interphase momentum interactions. The simulation results showed that the predicted performance of the commercial reactor was always better than the laboratory-scale reactor. The scale of the reactor has a minimal effect at high operating temperatures and pressures, however, it is important at low temperatures and high liquid flow rates, which are of interest to the commercial hydroprocessing community. Lopes and Quinta-Ferreira (Lopes and Quinta-Ferreira, 2007; Lopes et al., 2007) developed an Euler–Euler two-fluid hydrodynamic model coupled with the energy and species equation. The CFD simulations were performed in unsteady-state for the catalytic wet-air oxidation of the vanillic acids (Lopes et al., 2007) and phenolic acids (Lopes and Quinta-Ferreira, 2007). The CFD simulations of both studies showed that the conversion of total organic carbon (TOC) depends heavily on the bed temperature, while the operating pressure has a minor influence on final conversion (Lopes and Quinta-Ferreira, 2007; Lopes et al., 2007). In these studies, the numerical simulations were validated against hydrodynamic data, but not reaction data. Aiming to validate the Eulerian CFD model by confronting reacting parameters, Lopes and Quinta-Ferreira (2010a) carried out experiments on catalytic wet-air oxidation of phenolic acids in a pilot plant TBR. The experimental results were used to validate the CFD model computations under reacting flow conditions. It was shown that, compared to the case of lower operating temperature, the CFD model gave better predictions of TOC removal efficiency at elevated operating temperatures. Along with their Euler–Euler CFD models, Lopes and Quinta-Ferreira (2010b) also attempted to develop a VOF model which was used to analyse the reaction behaviour of catalytic wet-air oxidation of a phenolic solution in TBR. It was shown that the VOF model over-predicted both the experimental TOC removal and the measured temperature elevation, compared to the experimental data measured at two different operating conditions. The simulation indicated that backmixing effects were more pronounced at lower temperatures and poor radial mixing was noted, mainly at the hot spot locations. The radial profile TOC suggested that the lower pollutant concentrations were achieved at the center of the TBR while the maximum values were achieved at the wall. An interesting comparison of the VOF approach and the Euler–Euler approach was also made by Lopes and Quinta-Ferreira (2010b). The catalytic wet-air oxidation of phenolic acids in a TBR was simulated as a case study. Based on hydrodynamic validation in terms of pressure drop and liquid holdup, the Euler–Euler model was shown to offer better predictions than the VOF model. Both CFD models

were used to investigate the transient performance of TBRs under reaction conditions. It was shown that the highest TOC conversion and temperature at the hot spot as well as the poorest radial mixing were obtained using the VOF model, while the Euler–Euler model predicted the existence of hot spot formation (in the first half of TBR) as well.

Khadilkar et al. (2005) developed a one-dimensional reactor that was coupled with a pellet-scale transport and reaction model. In this work, hydrogenation of α-methylstyrene (gas-limited reaction) was considered as a model reaction system. The gas–liquid drag force was described by the model of Attou and Ferschneider (1999) and the fluid–solid drag forces were described by the model of Holub et al. (1993). Simulation runs were first carried out to simulate the reaction behaviour under steady-state conditions. This was followed by simulation of forced non-steady operation with periodic modulation of liquid flow. Model simulations showed that periodic liquid flow modulation can alter the supply of liquid and gaseous reactants to the catalyst and result in reactor performance enhancement above that achieved in steady-state operation.

Iliuta and Larachi (2003c) developed a one-dimensional two-fluid model to investigate the influence of external inhomogeneous magnetic fields on the hydrodynamics and reaction performance in TBRs. The catalytic wet-air oxidation of phenol in the presence of a catalyst consisting of a CuO/ZnO/CoO mixture was considered as a case study. It was shown that external inhomogeneous magnetic fields can enhance the performance of liquid reactant-limited reactions (such as the catalytic wet oxidation of phenol). Iliuta and Larachi (2005c) developed a general one-dimensional CFD model to describe the space-time evolution of simultaneous *biological clogging* and *physical plugging*, which involves simultaneous transport and consumption of substrate and oxygen within the biofilm and solid particles. This model was applied to analyse phenol biodegradation by *Pseudomonas putida* immobilised on activated carbon.

CFD Simulation of Periodic Operations for Process Intensification of TBRs

Periodic operation of TBRs implies the repercussions from both the multidimensional spatial and transient effects of the flow behaviours of the phases. In these circumstances, CFD modelling and simulation based on first principles could be viewed as a very powerful tool to gain insight into the underlying physics as well as to track the hydrodynamic evolution at both global and local scales during the operation cycles.

Jiang et al. (2002b) adopted the Eulerian *k*-fluid CFD model (CFDLIB) to model macroscale multiphase flow in packed beds in which the geometric complexity of the bed structure is resolved through statistical implementation of sectional porosities. Periodic simulations were carried out with a liquid flow ON time of 15 s and a total cycle time of 60 s (45 s liquid OFF). It was shown that unsteady-state operation offers better uniformity of liquid distribution at all locations over that observed in steady-state operation (in particular, in the bottom zone). Iliuta and Larachi (2005a) developed a one-dimensional dynamic multiphase flow model for describing the space-time evolution of both the deposition and release of fine particles in TBRs. The effect of periodic operation of a TBR on the release of fine particles was studied with a view to stretching the life cycle of trickle-bed hydrotreaters. In the case of non-Brownian particles, periodic operation was shown to reduce the specific solids deposition and plugging in the reactor. Periodic operation is not a viable solution for the attenuation of plugging attributed to Brownian fine particles in TBRs. Gunjal et al. (2005a) simulated flow in trickle beds operated with liquid-induced pulsing, maintaining constant time-averaged flow rates. The frequency of liquid-induced pulsing was set from experimental measurements of natural pulsing. Simulations with induced periodic flow indicated that, within the range investigated, induced pulsing has a negligible effect on the predicted pressure drop. Khadilkar et al. (2005) developed a one-dimensional bed- and pellet-scale reactive CFD model to simulate forced unsteady-state operation in TBRs. Simulation results showed that periodic liquid flow modulation can improve the supply of liquid and gaseous reactants to the catalyst and result in reactor performance enhancement above that achieved in steady-state operation. The effects of key modulation parameters (such as total cycle period, cycle split and liquid mass velocity) were simulated and the resulting model predictions were found to be in agreement with experimentally observed trends in the literature. Janecki et al. (2008) performed CFD simulations of the hydrodynamic behaviour in a periodically operated TBR. Both slow and fast modes of liquid feeding were analysed by means of the base-impulse method. The CFD simulation results showed reasonable compatibility with the experimental data from the viewpoint of qualitative trend response to changes in the operational parameters and the quantitative predictions. Atta et al. (2010b) proposed a two-phase Eulerian CFD framework based on the porous medium concept to elucidate the behaviour and the effects of a *solitary* liquid-rich square-wave on the continuous mode of periodic operation. These authors singled out a solitary liquid-rich square wave and studied its propagation inside the bed. The numerical predictions were in qualitative agreement with experimental results and the suggested CFD model showed sound capability to predict the hydrodynamics of a cyclic TBR. Lopes and Quinta-Ferreira (2010d) simulated periodic operation in trickle beds with induced pulses by manipulating the inlet liquid velocity. The relevant parameters that affect the hydrodynamic transition from trickling flow to pulsing flow were identified by means of a CFD model based on an Eulerian framework. Several parameters that characterise the pulsing flow (namely, the velocity of pulses traveling along the bed, the frequency of pulsations and their structure, the length of the pulses and the length of the liquid-rich zone) were examined at high pressure.

SUMMARY AND CONCLUSIONS

The analysis of fluid flow, transport processes and their couplings with physical processes and chemical reactions in TBRs has been reviewed in the framework of CFD modelling and simulation. It is a fact that the sheer complexity of TBR hydrodynamics has inhibited the development of CFD design procedures based on first principles (from solving the complete velocity field). This embarrased situation has been mitigated over the past several decades, however, by the explosive growth in computing power, which has stimulated the development of chemical and physical models and enabled multiphase CFD simulations of TBRs as part of a rapidly expanding field of research.

Resorting to the effective medium approach, the whole TBR system can be cast into the Euler–Euler modelling framework. There is no need to deal with the intricacies of precise particle boundaries and the detailed resolution of geometrical topology of the packings can be avoided. CFD models of this kind can handle the simulation of flow dynamics in a full-bed manner. On the other hand, the discrete particles approach, which does not require simplified treatment of the geometrical topology of the

packing structures, has recently received growing interest. A high grid resolution makes it possible to obtain accurate flow profiles and offers a more fundamental understanding of the transport and reaction phenomena in the reactors. Due to its excessive demands for computing power, the discrete particle approach is currently restricted to small segments (or periodic regions) of the bed, and, hence, is impractical for routine design of TBRs. In light of these considerations, the Euler–Euler CFD models seem to be a rational choice for flow simulation of large-scale TBRs, given that appropriate closures can be formulated for gas–liquid and fluid–particle interactions.

The ability of a multiphase CFD model to predict multiphase flows depends to a large degree on the development of suitable models to account for the complex interactions between the individual fluids. Formulation of these interfacial closure relationships remains the cornerstone of the Eulerian–Eulerian interpenetrating continua approach for predicting the complex flow behaviours within TBR systems. Over the last two decades, considerable progress has been made on the development of drag force expressions for two-phase gas–liquid flow in packed beds. The relative permeability approach, the slit flow approximation and the fluid–fluid interfacial drag force model have been proposed. Various investigators have attempted to implement all of these models in CFD codes for multidimensional TBR simulations. The superiority of CFD approaches over phenomenological hydrodynamic models can be attributed to the ability of the former to provide not only the global hydrodynamic quantities, for example, liquid holdup and pressure drop, but also the spatial distributions of these properties in multidimensional packed beds. The results in the literature showed that CFD tools are able to predict reasonably well the hydrodynamic and reaction parameters of multiphase reactors operating in the trickle-flow regime.

Despite great progress on computational TBR models, there are still challenges ahead. Therefore, we conclude the present review by discussing some possible directions for future research. Much work remains to be done:

(1) The essential step in CFD model development is the formulation of closure relations or closure laws determining interfacial momentum interactions. Despite a formidable amount of work related to the study of trickle-bed hydrodynamics, no consensus has emerged as to whether general approaches yielding pressure drop and liquid holdup with acceptable accuracy can be recommended. Therefore, the development of closure laws for phenomena occurring in the vicinity of interfaces should be considered in more detail. In particular, there is a compelling need for the precise identification of interfaces which may offer some essential information for constructing effective constitutive relationships of the inter-phase momentum exchanges.

(2) Turbulence modelling of multiphase flow through porous media deserves much more attention in the future. Development of physically realistic turbulence models suitable for modelling and simulation of two-phase flow in porous media (packings) is challenging. The ability of the models to resolve time scales associated with flow unsteadiness requires special consideration. Turbulence models for two-phase flow in porous media, as well as improvements to handle unsteady flows, require more careful investigation.

(3) There are numerical problems associated with unsteady (or forced periodic flow) multiphase flow simulation. Regarding the efficiency and accuracy, a number of additional problems must be taken into consideration numerically when the multiphase modelling is conducted based on unsteady Navier–Stokes equations. Actually, the wave dissipation and dispersion characteristics of steady-state numerical scheme are not suitable for unsteady flow simulations. In addition, the enormous computational requirements in terms of both CPU time and memory have to be mitigated by the development of efficient parallel algorithms.

(4) Intensive efforts should be focused on carefully designed experiments under realistic conditions to enable better understanding of coupled flow and reaction phenomena for model validation, in parallel with improvements in modelling approaches. In this regard, recent advances in imaging techniques and non-invasive monitoring of multiphase opaque flows will hopefully serve to facilitate experimental validation of CFD models.

REFERENCES

Al-Dahhan, M. H. and M. P. Dudukovic, "Pressure Drop and Liquid Holdup in High Pressure Trickle-Bed Reactors," Chem. Eng. Sci. **49**(24B), 5681–5698 (1994).

Al-Dahhan, M. H. and M. P. Dudukovic, "Catalyst Wetting Efficiency in Trickle-Bed Reactors at High-Pressure," Chem. Eng. Sci. **50**(15), 2377–2389 (1995).

Al-Dahhan, M. H., M. R. Khadilkar, Y. Wu and M. P. Dudukovic, "Prediction of Pressure Drop and Liquid Holdup in High-Pressure Trickle-Bed Reactors," Ind. Eng. Chem. Res. **37**(3), 793–798 (1998).

Al-Dahhan, M. H., F. Larachi, M. P. Dudukovic and A. Laurent, "High-Pressure Trickle-Bed Reactors: A Review," Ind. Eng. Chem. Res. **36**(8), 3292–3314 (1997).

Anadon, L. D., A. J. Sederman and L. F. Gladden, "Mechanism of the Trickle-to-Pulse Flow Transition in Fixed-Bed Reactors," AIChE J. **52**(4), 1522–1532 (2006).

Anderson, D. H. and A. V. Sapre, "Trickle-Bed Reactor Flow Simulation," AIChE J. **37**(3), 377–382 (1991).

Antohe, B. V. and J. L. Lage, "A General Two-Equation Macroscopic Turbulence Model for Incompressible Flow in Porous Media," Int. J. Heat Mass Transf. **13**, 3013–3024 (1997).

Atmakidis, T. and E. Y. Kenig, "CFD-Based Analysis of the Wall Effect on the Pressure Drop in Packed Beds With Moderate Tube/Particle Diameter Ratios in the Laminar Flow Regime," Chem. Eng. J. **155**(1–2), 404–410 (2009).

Atta, A., M. Hamidipour, S. Roy, K. D. P. Nigam and F. Larachi, "Propagation of Slow/Fast-Mode Solitary Liquid Waves in Trickle Beds Via Electrical Capacitance Tomography and Computational Fluid Dynamics," Chem. Eng. Sci. **65**(3), 1144–1150 (2010b).

Atta, A., S. Roy and K. D. P. Nigam, "Prediction of Pressure Drop and Liquid Holdup in Trickle Bed Reactor Using Relative Permeability Concept in CFD," Chem. Eng. Sci. **62**(21), 5870–5879 (2007a).

Atta, A., S. Roy and K. D. P. Nigam, "Investigation of Liquid Maldistribution in Trickle-Bed Reactors Using Porous Media Concept in CFD," Chem. Eng. Sci. **62**(24), 7033–7044 (2007b).

Atta, A., S. Roy and K. D. P. Nigam, "A Two-Phase Eulerian Approach Using Relative Permeability Concept for Modelling of Hydrodynamics in Trickle-Bed Reactors at Elevated Pressure," Chem. Eng. Res. Design **88**(3A), 369–378 (2010a).

Attou, A. and C. Boyer, "Hydrodynamics of Gas–Liquid–Solid Trickle-Bed Reactors: A Critical Review," Oil Gas Sci. Technol. **54**(1), 29–66 (1999).

Attou, A., C. Boyer and G. Ferschneider, "Modelling of the Hydrodynamics of the Cocurrent Gas–Liquid Trickle Flow Through a Trickle-Bed Reactor," Chem. Eng. Sci. **54**(6), 785–802 (1999).

Attou, A. and G. Ferschneider, "A Two-Fluid Model for Flow Regime Transition in Gas–Liquid Trickle-Bed Reactors," Chem. Eng. Sci. **54**(21), 5031–5037 (1999).

Attou, A. and G. Ferschneider, "A Two-Fluid Hydrodynamic Model for the Transition Between Trickle and Pulse Flow in a Cocurrent Gas–Liquid Packed-Bed Reactor," Chem. Eng. Sci. **55**(3), 491–511 (2000).

Augier, F., F. Idoux and J. Y. Delenne, "Numerical Simulations of Transfer and Transport Properties Inside Packed Beds of Spherical Particles," Chem. Eng. Sci. **65**(3), 1055–1064 (2010a).

Augier, F., A. Koudil, A. Royon-Lebeaud, L. Muszynski and Q. Yanouri, "Numerical Approach to Predict Wetting and Catalyst Efficiencies Inside Trickle Bed Reactors," Chem. Eng. Sci. **65**, 255–260 (2010b).

Bai, H., J. Theuerkauf, P. A. Gillis and P. M. Witt, "A Coupled DEM and CFD Simulation of Flow Field and Pressure Drop in Fixed Bed Reactor With Randomly Packed Catalyst Particles," Ind. Eng. Chem. Res. **48**(8), 4060–4074 (2009).

Baker, M. J. and G. R. Tabor, "Computational Analysis of Transitional Air Flow Through Packed Columns of Spheres Using the Finite Volume Technique," Comp. Chem. Eng. **34**(6), 878–885 (2010).

Baldi, G., "Design and Scale-Up of Trickle-Bed Reactors: Solid–Liquid Contacting Effectiveness," in "Multiphase Chemical Reactors," Vol. **52**, A. E. Rodrigues, J. M. Calo and N. H. Sweed, Eds., NATO Advanced Study Institite Series E, Sitjhoff & Noordhoff Aalphen aan den Rijn, The Netherlands (1981a), pp. 323.

Baldi, G., "Heat Transfer in Gas–Liquid–Solid Reactors," in "Multiphase Chemical Reactors," Vol. **52**, A. E. Rodrigues, J. M. Calo and N. H. Sweed, Eds., NATO Advanced Study Institute Series E, Sitjhoff & Noordhoff Aalphen aan den Rijn, The Netherlands (1981b), pp. 307.

Baldi, G., "Hydrodynamics of Multiphase Reactors," in "Multiphase Chemical Reactors," Vol. **52**, A. E. Rodrigues, J. M. Calo and N. H. Sweed, Eds., NATO Advanced Study Institute Series E, Sitjhoff & Noordhoff Aalphen aan den Rijn, The Netherlands (1981c), pp. 271.

Bansal, A., R. K. Wanchoo and S. K. Sharma, "Flow Regime Transition in a Trickle Bed Reactor," Chem. Eng. Commun. **192**(8), 1046–1066 (2005).

Barenblatt, G. I., "Filtration of Two Nonmixing Fluids in a Homogeneous Porous Medium," Sov. Acad. Izv. Mech. Gas Fluids **5**, 857–864 (1971).

Barenblatt, G. I. and A. P. Vinnichenko, "Non-Equilibrium Seepage of Immiscible Fluids," Adv. Mech. **3**(3), 35–50 (1980).

Bazmi, M., S. H. Hashemabadi and M. Bayat, "CFD Simulation and Experimental Study for Two-Phase Flow Through the Trickle Bed Reactors, Sock and Dense Loaded by Trilobe Catalysts," Int. Commun. Heat Mass Transf. **38**(3), 391–397 (2011).

Behnam, M., A. G. Dixon, M. Nijemeisland and E. H. Stitt, "Catalyst Deactivation in 3D CFD Resolved Particle Simulations of Propane Dehydrogenation," Ind. Eng. Chem. Res. **49**(21), 10641–10650 (2010).

Bey, O. and G. Eigenberger, "Fluid Flow Through Catalyst Filled Tubes," Chem. Eng. Sci. **52**(8), 1365–1376 (1997).

Blok, J. R., J. Varkevisser and A. A. H. Drinkenburg, "Transition to Pulsing Flow, Holdup and Pressure Drop in Packed Columns With Cocurrent Gas–Liquid Downflow," Chem. Eng. Sci. **38**, 687–699 (1983).

Boyer, C., A. Koudil, P. Chen and M. P. Dudukovic, "Study of Liquid Spreading From a Point Source in a Trickle Bed Via Gamma-Ray Tomography and CFD Simulation," Chem. Eng. Sci. **60**(22), 6279–6288 (2005).

Boyer, C., C. Volpi and G. Ferschneider, "Hydrodynamics of Trickle Bed Reactors at High Pressure: Two-Phase Flow Model for Pressure Drop and Liquid Holdup, Formulation and Experimental Validation," Chem. Eng. Sci. **62**(24), 7026–7032 (2007).

Brackbill, J. U., D. B. Kothe and C. Zemach, "A Continuum Method for Modelling Surface Tension," J. Comput. Phys. **100**(2), 335–354 (1992).

Carbonell, R. G., "Multiphase Flow Models in Packed Beds," Oil Gas Sci. Technol. **55**(4), 417–425 (2000).

Chan, H. C., W. C. Huang, J. M. Leu and C. J. Lai, "Macroscopic Modelling of Turbulent Flow Over a Porous Medium," Int. J. Heat Fluid Flow **28**(5), 1157–1166 (2007).

Chandesris, M., G. Serre and P. Sagaut, "A Macroscopic Turbulence Model for Flow in Porous Media Suited for Channel, Pipe and Rod Bundle Flows," Int. J. Heat Mass Transf. **49**, 2739–2750 (2006).

Charpentier, J. C., "Recent Progress in Two-Phase Gas–Liquid Mass Transfer in Packed Beds," Chem. Eng. J. **11**, 161–181 (1976).

Charpentier, J. C., "Gas–Liquid Reactors," in "Chemical Reaction Engineering Reviews," D. Luss and V. W. Weekman, Eds., ACS Symposium Series 72, American Chemical Society, Washington, DC, USA (1978), pp. 223.

Charpentier, J. C., "Hydrodynamics of Two-Phase Flow Through Porous Media," in "Chemical Engineering of Gas–Liquid–Solid Catalyst Reactions," G. A. L'Homme, Ed., CEBEDOC, Liege, Belgium (1979), pp. 78.

Charpentier, J. C., "Mass Transfer in Fixed Bed Reactors," in "Multiphase Chemical Reactors—Theory, Design, Scale-Up," A. Gianetto and P. L. Silveston, Eds., Hemisphere Publ. Co., Washington (1986), pp. 289.

Charpentier, J. C., C. Prost and P. Le Goff, "Ecoulement Ruisselant de Liquide Dans Une Colonne à Garnissage," Gén. Chim. **100**, 653–665 (1968a).

Charpentier, J. C., C. Prost, W. van Swaaij and P. Le Goff, "Etude de la Rétention de Liquide Dans Une Colonne à Garnissage Arrosé à co-Courant et à Contre-Courant de gaz et de Liquide," Gén. Chim. **99**, 803–826 (1968b).

Cohen, Y. and A. B. Metzner, "Wall Effects in Laminar-Flow of Fluids Through Packed-Beds," AIChE J. **27**(5), 705–715 (1981).

Coussirat, M., A. Guardo, B. Mateos and E. Egusquiza, "Performance of Stress-Transport Models in the Prediction of Particle-to-Fluid Heat Transfer in Packed Beds," Chem. Eng. Sci. **62**, 6897–6907 (2007).

Crine, M. and G. L'Homme, "Recent Trends in the Modelling of Catalytic Trickle-Bed Reactors," in "Mass Transfer With Chemical Reaction in Multiphase Systems: Three-Phase

Systems," Vol. **II**, E. Alper, Ed., Martinus Nijhoff Publ., The Hague, The Netherlands (1983), pp. 99.
Dankworth, D. C. and S. Sundaresan, "Stability of Periodic Travelling Waves in Trickle Beds," Chemical Engineering Science **47**(13/14), 3257–3264 (1992).
Dankworth, D. C., I. G. Kevrekidis and S. Sundaresan, "Dynamics of Pulsing Flow in Trickle Beds," AIChE J. **36**(4), 605–621 (1990).
de Klerk, A., "Voidage Variation in Packed Beds at Small Column to Particle Diameter Ratio," AICHE J. **49**(8), 2022–2029 (2003).
de Lemos, M. J. S., "Turbulence in Porous Media: Modelling and Applications," Elsevier Ltd., London, UK (2006).
de Lemos, M. J. S. and M. H. J. Pedras, "Recent Mathematical Models for Turbulent Flow in Saturated Rigid Porous Media," J. Fluids Eng. **123**, 935–940 (2001).
de Santos, J. M., T. R. Melli and L. E. Scriven, "Mechanics of Gas–Liquid Flow in Packed-Bed Contactors," Annu. Rev. Fluid Mech. **23**, 233–260 (1991).
Dixon, A. G. and M. Nijemeisland, "CFD as a Design Tool for Fixed-bed Reactors," Ind. Eng. Chem. Res. **40**(23), 5246–5254 (2001).
Dixon, A. G., M. Nijemeisland and E. H. Stitt, "Packed Tubular Reactor Modelling and Catalyst Design Using Computational Fluid Dynamics," Adv. Chem. Eng. **31**, 307–389 (2006).
Dixon, A. G., M. E. Taskin, E. H. Stitt and M. Nijemeisland, "3D CFD Simulations of Steam Reforming With Resolved Intraparticle Reaction and Gradients," Chem. Eng. Sci. **62**(18–20), 4963–4966 (2007).
Dudukovic, M. P. and P. L. Mills, "Contacting and Hydrodynamics in Trickle-Bed Reactors," in "Encyclopedia of Fluid Mechanics: Gas–Liquid Flows," Vol. **3**, N. P. Cheremisinoff, Ed., Gulf Publ. Corp., Houston, TX, USA (1986), pp. 969.
Dudukovic, M. P., F. Larachi and P. L. Mills, "Multiphase Reactors—Revisited," Chem. Eng. Sci. **54**, 1975–1995 (1999).
Dumas, T., F. Lesage and M. A. Latifi, "Modelling and Measurements of the Velocity Gradient and Local Flow Direction at the Pore Scale of a Packed Bed," Chem. Eng. Res. Design **88**(3A), 379–384 (2010).
du Toit, C. G., "Radial Variation in Porosity in Annular Packed Beds," Nucl. Eng. Design **238**(11), 3073–3079 (2008).
Dybbs, A. and R. V. Edwards, "A New look at Porous Media Fluid Mechanics – Darcy to Turbulent," in "Fundamentals of Transport Phenomena in Porous Media," J. Bear and M. Corapcioglu, Eds., Martins Nijhoff, Dordrecht (1984), pp. 199–256.
El-Hisnawi, A. A., "Tracer Reaction Studies in Trickle-Bed Reactors," PhD Thesis, Washington University, St. F Louis, USA (1981).
Fluent 6.3, "Fluent 6.3 User's Guide," Fluent Inc., Lebanon, USA (2006).
Getachew, D., W. J. Minkowycz and J. L. Lage, "A Modified Form of the k–ε Model for Turbulent Flows of an Incompressible Fluid in Porous Media," Int. J. Heat Mass Transf. **43**, 2909–2915 (2000).
Gianetto, A., G. Baldi, V. Specchia and S. Sicardi, "Hydrodynamics and Solid–Liquid Contacting Effectiveness in Trickle-Bed Reactors," AIChE J. **24**(6), 1087–1104 (1978).
Gianetto, A. and F. Berruti, "Modelling of Trickle-Bed Reactors," in "Chemical Reactor Design and Technology," H. I. De Lasa, Ed., Nijhoff, The Hague, The Netherlands (1986), pp. 631.
Gianetto, A. and V. Specchia, "Trickle-Bed Reactors—State of Art and Perspectives," Chem. Eng. Sci. **47**(13–14), 3197–3213 (1992).
Gladden, L. F., L. D. Anadon, M. H. M. Lim, A. J. Sederman and E. H. Stitt, "Insights into the Mechanism of the Trickle-to-Pulse Transition in Trickle-Bed Reactors," Ind. Eng. Chem. Res. **44**(16), 6320–6331 (2005).
Goto, S., J. Levec and J. M. Smith, "Trickle-Bed Oxidation Reactors," Catal. Rev. Sci. Eng. **15**(2), 187–247 (1977).
Gray, M. R., N. Srinivasan and J. H. Masliyah, "Pressure Buildup in Gas–Liquid Flow Through Packed Beds Due to Deposition of Fine Particles," Can. J. Chem. Eng. **80**(3), 346–354 (2002).
Grosser, K., R. G. Carbonell and S. Sundaresan, "Onset of Pulsing in 2-Phase Cocurrent Downflow Through a Packed-Bed," AIChE J. **34**(11), 1850–1860 (1988).
Guardo, A., M. Coussirat, M. A. Larrayoza, F. Recasensa and E. Egusquizab, "Influence of the Turbulence Model in CFD Modelling of Wall-to-Fluid Heat Transfer in Packed Beds," Chem. Eng. Sci. **60**(6), 1733–1742 (2006).
Gunjal, P. R., M. N. Kashid, V. V. Ranade and R. V. Chaudhari, "Hydrodynamics of Trickle-Bed Reactors: Experiments and CFD Modelling," Ind. Eng. Chem. Res. **44**(16), 6278–6294 (2005a).
Gunjal, P. R. and V. V. Ranade, "Modelling of Laboratory and Commercial Scale Hydro-Processing Reactors Using CFD," Chem. Eng. Sci. **62**(18–20), 5512–5526 (2007).
Gunjal, P. R., V. V. Ranade and R. V. Chaudhari, "Liquid Distribution and RTD in Trickle Bed Reactors: Experiments and CFD Simulations," Can. J. Chem. Eng. **81**(3–4), 821–830 (2003a).
Gunjal, P. R., V. V. Ranade and R. V. Chaudhari, "Experimental and Computational Study of Liquid Drop Over Flat and Spherical Surfaces," Catal. Today **79**(1–4), 267–273 (2003b).
Gunjal, P. R., V. V. Ranade and R. V. Chaudhari, "Computational Study of a Single-Phase Flow in Packed Beds of Spheres," AIChE J. **51**(2), 365–378 (2005b).
Guo, B. Y., A. B. Yu, B. Wright and P. Zulli, "Simulation of Turbulent Flow in a Packed Bed," Chem. Eng. Technol. **29**(5), 596–603 (2006).
Hanika, J. and V. Stanek, "Operation and Design of Trickle-Bed Reactors," in "Handbook of Heat and Mass Transfer: Mass Transfer and Reactor Design," Vol. **2**, N. P. Cheremisinoff, Ed., Gulf Publ. Corp., Houston, TX, USA (1986), pp. 1029.
Harter, I., C. Boyer, L. Raynal, G. Ferschneider and T. Gauthier, "Flow Distribution Studies Applied to Deep Hydro-Desulfurisation," Ind. Eng. Chem. Res. **40**(23), 5262–5267 (2001).
Hartley, D. E. and W. Murgatroyd, "Criteria for the Break-Up of Thin Liquid Layers Flowing Isothermally Over Solid Surfaces," Int. J. Heat Mass Transf. **7**, 1003–1015 (1964).
Hassanizadeh, S. M., M. A. Celia and H. K. Dahle, "Dynamic Effects in the Capillary Pressure–Saturation Relationship and Its Impact on Unsaturated Flow," Vadose Zone J. **1**(1), 38–57 (2002).
Hassanizadeh, S. M. and W. G. Gray, "Thermodynamic Basis of Capillary Pressure in Porous Media," Water Resour. Res. **29**(10), 3389–3405 (1993a).
Hassanizadeh, S. M. and W. G. Gray, "Toward an Improved Description of the Physics of Two-Phase Flow," Adv. Water Resour. **16**(1), 53–67 (1993b).
Herskowitz, M. and J. M. Smith, "Liquid Distribution in Trickle Bed Reactors," A.I.Ch.E.J. **24**, 439–450 (1978).

Herskowitz, M. and J. M. Smith, "Trickle-Bed Reactors—A Review," AIChE J. **29**(1), 1–18 (1983).
Hirt, C. and B. Nichols, "Volume of Fluid (VOF) Method for the Dynamics of Free Boundaries," J. Comp. Phys. **39**, 201–225 (1981).
Hofmann, H. P., "Multiphase Catalytic Packed-Bed Reactors," Catal. Rev. Sci. Eng. **17**(1), 71–117 (1978).
Holub, R. A., M. P. Dudukovic and P. A. Ramachandran, "A Phenomenological Model for Pressure-Drop, Liquid Holdup, and Flow Regime Transition in Gas–Liquid Trickle Flow," Chem. Eng. Sci. **47**(9–11), 2343–2348 (1992).
Holub, R. A., M. P. Dudukovic and P. A. Ramachandran, "Pressure-Drop, Liquid Holdup, and Flow Regime Transition in Trickle Flow," AIChE J. **39**(2), 302–321 (1993).
Horton, N. A. and D. Pokrajac, "Onset of Turbulence in a Regular Porous Medium: An Experimental Study," Phys. Fluids **21**, 045104 (2009).
Iliuta, I., B. Aydin and F. Larachi, "Onset of Pulsing in Trickle Beds With Non-Newtonian Liquids at Elevated Temperature and Pressure—Modelling and Experimental Verification," Chem. Eng. Sci. **61**(2), 526–537 (2006b).
Iliuta, I. and F. Larachi, "The Generalised Slit Model: Pressure Gradient, Liquid Holdup & Wetting Efficiency in Gas–Liquid Trickle Flow," Chem. Eng. Sci. **54**, 5039–5045 (1999).
Iliuta, I. and F. Larachi, "Theory of Trickle-Bed Magnetohydrodynamics Under Magnetic-Field Gradients," AIChE J. **49**(6), 1525–1532 (2003a).
Iliuta, I. and F. Larachi, "Magnetohydrodynamics of Trickle Bed Reactors: Mechanistic Model, Experimental Validation and Simulations," Chem. Eng. Sci. **58**(2), 297–307 (2003b).
Iliuta, I. and F. Larachi, "Two-Phase Flow in Porous Media Under Spatially Uniform Magnetic-Field Gradients: Novel Way to Process Intensification," Can. J. Chem. Eng. **81**(3–4), 776–783 (2003c).
Iliuta, I. and F. Larachi, "Biomass Accumulation and Clogging in Trickle-Bed Bioreactors," AIChE J. **50**(10), 2541–2551 (2004a).
Iliuta, I. and F. Larachi, "Modelling and Simulation of Trickle-Bed Magnetohydrodynamics in Inhomogeneous Magnetic Fields," Chem. Eng. Process. **43**(11), 1417–1427 (2004b).
Iliuta, I. and F. Larachi, "Onset of Pulsing in Gas–Liquid Trickle Bed Filtration," Chem. Eng. Sci. **59**(6), 1199–1211 (2004c).
Iliuta, I. and F. Larachi, "Stretching Operational Life of Trickle-Bed Filters by Liquid-Induced Pulse Flow," AIChE J. **51**(7), 2034–2047 (2005a).
Iliuta, I. and F. Larachi, "Mitigating Fines Plugging in High Pressure/Temperature Hydrotreaters Using an Induced-Pulsing Trickle-Bed Filtration Approach," Chem. Eng. Sci. **60**(22), 6217–6225 (2005b).
Iliuta, I. and F. Larachi, "Modelling Simultaneous Biological Clogging and Physical Plugging in Trickle-Bed Bioreactors for Wastewater Treatment," Chem. Eng. Sci. **60**(5), 1477–1489 (2005c).
Iliuta, I. and F. Larachi, "Modelling the Hydrodynamics of Gas–Liquid Packed Beds Via Slit Models: A Review," Int. J. Chem. Reactor Eng. **3**, R4 (2005d).
Iliuta, I. and F. Larachi, "Deposition and Aggregation of Brownian Particles in Trickle-Bed Reactors," AIChE J. **52**(12), 4167–4180 (2006a).
Iliuta, I. and F. Larachi, "Dynamics of Cells Attachment, Aggregation, Growth and Detachment in Trickle-Bed Bioreactors," Chem. Eng. Sci. **61**(15), 4893–4908 (2006b).
Iliuta, I., F. Larachi and M. H. Al-Dahhan, "Double-Slit Model for Partially Wetted Trickle Flow Hydrodynamics," AIChE J. **46**(3), 597–609 (2000).
Iliuta, I., F. Larachi and B. P. A. Grandjean, "Fines Deposition Dynamics in Gas–Liquid Trickle-Flow Reactors," AIChE J. **49**(2), 485–495 (2003).
Iliuta, I., F. Larachi, B. A. Grandjean and G. Wild, "Gas–Liquid Interfacial Mass Transfer in Trickle-Bed Reactors: State-of-the-Art Correlations," Chem. Eng. Sci. **54**, 5633–5645 (1999a).
Iliuta, I., M. C. Iliuta and F. Larachi, "Hydrodynamics Modelling of Bioclogging in Waste Gas Treating Trickle-Bed Bioreactors," Ind. Eng. Chem. Res. **44**(14), 5044–5052 (2005).
Iliuta, I., A. Ortiz-Arroyo, F. Larachi, B. P. A. Grandjean and G. Wild, "Hydrodynamics and Mass Transfer in Trickle-Bed Reactors: An Overview," Chem. Eng. Sci. **54**, 5329–5337 (1999b).
Iliuta, I., Z. Ring and F. Larachi, "Simulating Simultaneous Fines Deposition Under Catalytic Hydrodesulfurisation in Hydrotreating Trickle Beds—Does Bed Plugging Affect HDS Performance?" Chem. Eng. Sci. **61**(4), 1321–1333 (2006a).
Jafari, A., P. Zamankhan, S. M. Mousavi and K. Pietarinen, "Modelling and CFD Simulation of Flow Behaviour and Dispersivity Through Randomly Packed Bed Reactors," Chem. Eng. J. **144**(3), 476–482 (2008).
Jakobsen, H. A., "Chemical Reactor Modelling: Multiphase Reactive Flows," Springer-Verlag, Berlin, Germany (2008).
Janecki, D., A. Burghardt and G. Bartelmus, "Computational Simulations of the Hydrodynamic Parameters of a Trickle-Bed Reactor Operating at Periodically Changing Feeding the Bed With Liquid," Chem. Process. Eng. **29**(3), 583–596 (2008).
Jiang, Y., M. H. Al-Dahhan and M. P. Dudukovic, "Statistical Characterisation of Macroscale Multiphase Flow Textures in Trickle Beds," Chem. Eng. Sci. **56**(4), 1647–1656 (2001b).
Jiang, Y., J. Guo and M. H. Al-Dahhan, "Multiphase Flow Packed-Bed Reactor Modelling: Combining CFD and Cell Network Model," Ind. Eng. Chem. Res. **44**(14), 4940–4948 (2005).
Jiang, Y., M. R. Khadilkar, M. H. Al-Dahhan and M. P. Dudukovic, "Two-Phase Flow Distribution in 2D Trickle-Bed Reactors," Chem. Eng. Sci. **54**(13–14), 2409–2419 (1999).
Jiang, Y., M. R. Khadilkar, M. H. Al-Dahhan and M. P. Dudukovic, "CFD Modelling of Multiphase Flow Distribution in Catalytic Packed Bed Reactors: Scale Down Issues," Catal. Today **66**(2–4), 209–218 (2001a).
Jiang, Y., M. R. Khadilkar, M. H. Al-Dahhan and A. P. Dudukovic, "CFD of Multiphase Flow in Packed-Bed Reactors: I. k-Fluid Modelling Issue," AICHE J. **48**(4), 701–715 (2002a).
Jiang, Y., M. R. Khadilkar, M. H. Al-Dahhan and A. P. Dudukovic, "CFD of Multiphase Flow in Packed-Bed Reactors: II. Results and Applications," AICHE J. **48**(4), 716–730 (2002b).
Juanes, R., "Nonequilibrium Effects in Models of Three-Phase Flow in Porous Media," Adv. Water Resour. **31**, 661–673 (2009).
Kazerooni, R. B. and S. K. Hannani, "Simulation of Turbulent Flow Through Porous Media Employing a v2f Model," Trans. B Mech. Eng. **16**(2), 159–167 (2009).
Khadilkar, M. R., M. H. Al-Dahhan and M. P. Dudukovic, "Multicomponent Flow-Transport-Reaction Modelling of Trickle Bed Reactors: Application to Unsteady State Liquid

Flow Modulation," Ind. Eng. Chem. Res. **44**(16), 6354–6370 (2005).
Kundu, A., K. D. P. Nigam and R. P. Verma, "Catalyst Wetting Characteristics in Trickle-Bed Reactors," AIChE J. **49**(9), 2253–2263 (2003).
Lakota, A., J. Levec and R. G. Carbonell, "Hydrodynamics of Trickling Flow in Packed Beds: Relative Permeability Concept," AIChE J. **48**(4), 731–738 (2002).
Lappalainen, K., M. Manninen and V. Alopaeus, "CFD Modelling of Radial Spreading of Flow in Trickle-Bed Reactors Due to Mechanical and Capillary Dispersion," Chem. Eng. Sci. **64**(2), 207–218 (2009a).
Lappalainen, K., M. Manninen, V. Alopaeus, J. Aittamaa and J. Dodds, "An Analytical Model for Capillary Pressure–Saturation Relation For Gas–Liquid System in a Packed-Bed of Spherical Particles," Transp. Porous Media **77**, 17–40 (2009b).
Lemcoff, N. O., A. L. Cukierman and O. M. Martinez, "Effectiveness Factor of Partially Wetted Catalyst Particles—Evaluation and Application to the Modelling of Trickle Bed Reactors," Catal. Rev. Sci. Eng. **30**(3), 393–456 (1988).
Levec, J., A. E. Saez and R. G. Carbonell, "The Hydrodynamics of Trickling Flow in Packed-Beds. 2. Experimental-Observations," AIChE J. **32**(3), 369–380 (1986).
Leverett, M. C., "Capillary Behaviour in Porous Solids," Trans. AIME **142**, 159–169 (1941).
Li, Y., J. P. Zhang and L. S. Fan, "Numerical Simulation of Gas–Liquid–Solid Fluidisation Systems Using a Combined CFD-VOF-DPM Method: Bubble Wake Behaviour," Chem. Eng. Sci. **54**(21), 5101–5107 (1999).
Logtenberg, S. A., M. Nijemeisland and A. G. Dixon, "Computational Fluid Dynamics Simulations of Fluid Flow and Heat Transfer at the Wall-Particle Contact Points in a Fixed-Bed Reactor," Chem. Eng. Sci. **54**(13–14), 2433–2439 (1999).
Lopes, R. J. G. and R. M. Quinta-Ferreira, "Trickle-Bed CFD Studies in the Catalytic Wet Oxidation of Phenolic Acids," Chem. Eng. Sci. **62**(24), 7045–7052 (2007).
Lopes, R. J. G. and R. M. Quinta-Ferreira, "Three-Dimensional Numerical Simulation of Pressure Drop and Liquid Holdup for High-Pressure Trickle-Bed Reactor," Chem. Eng. J. **145**(1), 112–120 (2008).
Lopes, R. J. G. and R. M. Quinta-Ferreira, "Numerical Simulation of Trickle-Bed Reactor Hydrodynamics With RANS-Based Models Using a Volume of Fluid Technique," Ind. Eng. Chem. Res. **48**, 1740–1748 (2009a).
Lopes, R. J. G. and R. M. Quinta-Ferreira, "CFD Modelling of Multiphase Flow Distribution in Trickle Beds," Chem. Eng. J. **147**(2–3), 342–355 (2009b).
Lopes, R. J. G. and R. M. Quinta-Ferreira, "Volume-of-Fluid-Based Model for Multiphase Flow in High-Pressure Trickle-Bed Reactor: Optimisation of Numerical Parameters," AIChE J. **55**(11), 2920–2933 (2009c).
Lopes, R. J. G. and R. M. Quinta-Ferreira, "Turbulence Modelling of Multiphase Flow in High-Pressure Trickle-Bed Reactors," Chem. Eng. Sci. **64**(8), 1806–1819 (2009d).
Lopes, R. J. G. and R. M. Quinta-Ferreira, "Assessment of CFD Euler–Euler Method for Trickle-Bed Reactor Modelling in the Catalytic Wet Oxidation of Phenolic Wastewaters," Chem. Eng. J. **160**(1), 293–301 (2010a).
Lopes, R. J. G. and R. M. Quinta-Ferreira, "Assessment of CFD-VOF Method for Trickle-Bed Reactor Modelling in the Catalytic Wet Oxidation of Phenolic Wastewaters," Ind. Eng. Chem. Res. **49**(6), 2638–2648 (2010b).
Lopes, R. J. G. and R. M. Quinta-Ferreira, "Evaluation of Multiphase CFD Models in Gas–Liquid Packed-Bed Reactors for Water Pollution Abatement," Chem. Eng. Sci. **65**(1), 291–297 (2010c).
Lopes, R. J. G. and R. M. Quinta-Ferreira, "Hydrodynamic Simulation of Pulsing-Flow Regime in High-Pressure Trickle-Bed Reactors," Ind. Eng. Chem. Res. **49**(3), 1105–1112 (2010d).
Lopes, R. J. G. and R. M. Quinta-Ferreira, "Numerical Studies of Catalyst Wetting and Total Organic Carbon Reaction on Environmentally Based Trickle-Bed Reactors," Ind. Eng. Chem. Res. **49**(21), 10730–10743 (2010e).
Lopes, R. J. G., A. M. T. Silva and R. M. Quinta-Ferreira, "Kinetic Modelling and Trickle-Bed CFD Studies in the Catalytic Wet Oxidation of Vanillic Acid," Ind. Eng. Chem. Res. **46**(25), 8380–8387 (2007).
Macdonald, I. F., M. S. El-Sayed, K. Mow and F. A. L. Dullien, "Flow Through Porous Media—The Ergun Equation Revisited," Ind. Eng. Chem. Fundam. **18**(3), 199–208 (1979).
Maiti, R., R. Khanna and K. D. P. Nigam, "Hysteresis in Trickle-Bed Reactors: A Review," Ind. Eng. Chem. Res. **45**(15), 5185–5198 (2006).
Maiti, R. N. and K. D. P. Nigam, "Gas–Liquid Distributors for Trickle-Bed Reactors: A Review," Ind. Eng. Chem. Res. **46**(19), 6164–6182 (2007).
Maiti, R. N., P. K. Sen and K. D. P. Nigam, "Trickle-Bed Reactors: Liquid Distribution and Flow Texture," Rev. Chem. Eng. **20**(1–2), 57–109 (2004).
Marcandelli, C., A. S. Lamine, J. R. Bernard and G. Wild, "Liquid Distribution in Trickle Bed Reactor," Oil & Gas Science and Technology Rev—IFP **55**, 407–415 (2000).
Martin, H., "Low Peclet Number Particle-to-Fluid Heat and Mass-Transfer in Packed-Beds," Chem. Eng. Sci. **33**, 913–919 (1978).
Mary, G., J. Chaouki and F. Luck, "Trickle-Bed Laboratory Reactors for Kinetic Studies," Int. J. Chem. Reactor Eng. **7**, R2 (2009).
McKenna, T. F. and R. Spitz, "Heat Transfer From Catalysts With Computational Fluid Dynamics," AIChE J. **45**(11), 2392–2410 (1999).
Mederos, F. S., J. Ancheyta and J. Chen, "Review on Criteria to Ensure Ideal Behaviours in Trickle-Bed Reactors," Appl. Catal. A Gen. **355**(1–2), 1–19 (2009a).
Mederos, F. S., I. Elizalde and J. Ancheyta, "Steady-State and Dynamic Reactor Models for Hydrotreatment of Oil Fractions: A Review," Catal. Rev. Sci. Eng. **51**(4), 485–607 (2009b).
Meyers, R. A., "Handbook of Petroleum Refining Processes," 2nd ed., McGraw-Hill, New York, USA (1996).
Michele, V., "CFD Modelling and Measurement of Liquid Flow Structure and Phase Holdup in Two- and Three-Phase Bubble Columns," PhD Thesis, Braunschweig University of Technology, Germany (2002).
Mills, P. L. and M. P. Dudukovic, "A Comparison of Current Models for Isothermal Trickle-Bed Reactors: Application of a Model Reaction System," ACS Symp. Ser. **234**, 37–59 (1984).
Motlagh, A. H. A. and S. H. Hashemabadi, "CFD Based Evaluation of Heat Transfer Coefficient From Cylindrical Particles," Int. Commun. Heat Mass Transf. **35**, 674–680 (2008).

Mueller, G. E., "Prediction of Radial Porosity Distributions in Randomly Packed Fixed-Beds of Uniformly Sized Spheres in Cylindrical Containers," Chem. Eng. Sci. **46**(2), 706–708 (1991).
Mueller, G. E., "Radial Void Fraction Distributions in Randomly Packed Fixed-Beds of Uniformly Sized Spheres in Cylindrical Containers," Powder Technol. **72**(3), 269–275 (1992).
Munteanu, M. C. and F. Larachi, "Flow Regimes in Trickle Beds Using Magnetic Emulation of Micro/Macrogravity," Chem. Eng. Sci. **64**(2), 391–402 (2009).
Nakayama, A. and F. Kuwahara, "A Macroscopic Turbulence Model for Flow in a Porous Medium," J. Fluids Eng. **121**(2), 427–433 (1999).
Nakayama, A. and F. Kuwahara, "A General Macroscopic Turbulence Model for Flows in Packed Beds, Channels, Pipes, and Rod Bundles," J. Fluids Eng. **130**(101205), 1–7 (2008).
Narasimhan, C. S. L., R. P. Verma, A. Kundu and K. D. P. Nigam, "Modelling Hydrodynamics of Trickle-Bed Reactors at High Pressure," AIChE J. **48**(11), 2459–2474 (2002).
Narayan, R., J. R. Coury, J. H. Masliyah and M. R. Gray, "Particle Capture and Plugging in Packed-Bed Reactors," Ind. Eng. Chem. Res. **36**(11), 4620–4627 (1997).
Nemec, D., G. Bercic and J. Levec, "The Hydrodynamics of Trickling Flow in Packed Beds Operating at High Pressures. The Relative Permeability Concept," Chem. Eng. Sci. **56**(21–22), 5955–5962 (2001).
Nemec, D. and J. Levec, "Flow Through Packed Bed Reactors: 1. Single-Phase Flow," Chem. Eng. Sci. **60**(24), 6947–6957 (2005a).
Nemec, D. and J. Levec, "Flow Through Packed Bed Reactors: 2. Two-Phase Concurrent Downflow," Chem. Eng. Sci. **60**(24), 6958–6970 (2005b).
Ng, K. M., "A Model for Flow Regime Transitions in Cocurrent Downflow Trickle-Bed Reactors," AIChE J. **32**, 115–122 (1986).
Ng, K. M. and C. F. Chu, "Trickle-Bed Reactors," Chem. Eng. Prog. **83**(11), 55–63 (1987).
Niessner, J. and S. Hassanizadeh, "Non-Equilibrium Interphase Heat and Mass Transfer During Two-Phase Flow in Porous Media—Theoretical Considerations and Modeling," Adv. Water Resour. **32**(12), 1756–1766 (2009).
Nigam, K. D. P. and F. Larachi, "Process Intensification in Trickle-Bed Reactors," Chem. Eng. Sci. **60**(22), 5880–5894 (2005).
Nijemeisland, M. and A. G. Dixon, "Comparison of CFD Simulations to Experiment for Convective Heat Transfer in a Gas–Solid Fixed Bed," Chem. Eng. J. **82**, 231–246 (2001).
Nijemeisland, M. and A. G. Dixon, "CFD Study of Fluid Flow and Wall Heat Transfer in a Fixed Bed of Spheres," AIChE J. **50**(5), 906–921 (2004).
O'Carroll, D. M., T. J. Phelan and L. M. Abriola, "Exploring Dynamic Effects in Capillary Pressure in Multistep Outflow Experiments," Water Resour. Res. **41**(11), W11419 (2005).
Ortiz-Arroyo, A. and F. Larachi, "Lagrange–Euler–Euler CFD Approach for Modelling Deep-Bed Filtration in Trickle Flow Reactors," Sep. Purif. Technol. **41**(2), 155–172 (2005).
Ortiz-Arroyo, A., F. Larachi, B. P. A. Grandjean and S. Roy, "CFD Modelling and Simulation of Clogging in Packed Beds With Nonaqueous Media," AIChE J. **48**(8), 1596–1609 (2002).
Østergaard, K., "Gas–Liquid–Particle Operations in Chemical Reaction Engineering," in "Advances in Chemical Engineering," Vol. 7, T. B. Drew, G. R. Cokelet, J. W. Hoopes and T. Vermeulen, Eds., Academic Press, New York (1968), pp. 71.
Pedras, M. H. J. and M. J. S. de Lemos, "Macroscopic Turbulence Modelling for Incompressible Flow Through Undeformable Porous Media," Int. J. Heat Mass Transf. **44**(6), 1081–1093 (2001a).
Pedras, M. H. J. and M. J. S. de Lemos, "Simulation of Turbulent Flow in Porous Media Using a Spatially Periodic Array and a Low Re Two-Equation Closure," Numer. Heat Transf. A **39**(1), 35–59 (2001b).
Pedras, M. H. J. and M. J. S. de Lemos, "On the Mathematical Description and Simulation of Turbulent Flow in a Porous Medium Formed by an Array of Elliptic Rods," J. Fluids Eng. **123**(4), 941–947 (2001c).
Propp, R. M., P. Colella, W. Y. Crutchfield and M. S. Day, "A Numerical Model for Trickle Bed Reactors," J. Comp. Phys. **165**(2), 311–333 (2000).
Ramachandran, P. A., M. P. Dudukovic and P. L. Mills, "Recent Advances in the Analysis and Design of Trickle-Bed Reactors," Sadhana Acad. Proc. Eng. Sci. **10**, 269–298 (1987).
Ramajo, D. E., S. M. Damian, M. Ravicule, M. M. Monsalvo, M. Storti and N. Nigro, "Flow Study and Wetting Efficiency of a Perforated-Plate Tray Distributor in a Trickle Bed Reactor," Int. J. Chem. Reactor Eng. **8**, A137 (2010).
Ranade, V. V., "Computational Flow Modelling for Chemical Reactor Engineering," Academic Press, USA (2002).
Ranade, V. V., R. Chaudhari and P. R. Gunjal, "Trickle Bed Reactors: Reactor Engineering & Applications," Elsevier, UK (2011).
Rao, V. G. and A. A. H. Drinkenberg, "Pressure Drop and Hydrodynamic Properties of Pulses in Two-Phase Gas-Liquid Downflow Through Packed Columns," Can. Chem. Eng. J. **62**, 158 (1983).
Rao, V. G., M. S. Ananth and Y. B. G. Varma, "Hydrodynamics of Two Phase Cocurrent Downflow Through Packed Beds," AIChE J. **29**(3), 467–473 (1983).
Ravindra, P. V., D. P. Rao and M. S. Rao, "Liquid Flow Texture in Trickle-Bed Reactors: An Experimental Study," Ind. Eng. Chem. Res. **36**, 5133–5145 (1997).
Reinecke, N. and D. Mewes, "Investigation of the Two Phase Flow in Trickle-Bed Reactors Using Capacitance Tomography," Chem. Eng. Sci. **52**(13), 2111–2127 (1997).
Saez, A. E. and R. G. Carbonell, "Hydrodynamic Parameters for Gas–Liquid Cocurrent Flow in Packed-Beds," AIChE J. **31**(1), 52–62 (1985).
Saroha, A. K. and K. D. P. Nigam, "Trickle Bed Reactors," Rev. Chem. Eng. **12**(3–4), 207–347 (1996).
Satterfield, C. N., "Trickle-Bed Reactors," AIChE J. **21**(2), 209–228 (1975).
Scardovelli, R. and S. Zaleski, "Direct Numerical Simulation of Free-Surface and Interfacial Flow," Annu. Rev. Fluid Mech. **31**, 567–603 (1999).
Sederman, A. J. and L. F. Gladden, "Magnetic Resonance Imaging as a Quantitative Probe of Gas–Liquid Distribution and Wetting Efficiency in Trickle-Bed Reactors," Chem. Eng. Sci. **56**, 2615–2628 (2001).
Sicardi, S. and H. Hofmann, "Influence of Gas Velocity and Packing Geometry on Pulsing Inception in Trickle-Bed Reactors," Chem. Eng. J. **20**, 231–253 (1980).
Sie, S. T., "Scale Effects in Laboratory and Pilot-Plant Reactors for Trickle Flow Processes," Rev. Inst. Fr. Petrole **6**(4), 501–515 (1999).

Sie, S. T. and R. Krishna, "Process Development and Scale Up: III. Scale-Up and Scale-Down of Trickle Bed Processes," Rev. Chem. Eng. **14**(3), 203–252 (1998).
Souadnia, A., F. Soltana, F. Lesage and M. A. Latifi, "Some Computational Aspects in the Simulation of Hydrodynamics in a Trickle-Bed Reactor," Chem. Eng. Process. **44**(8), 847–854 (2005).
Specchia, V. and G. Baldi, "Pressure Drop and Liquid Hold Up for Two Phase Cocurrent Flow in Packed Bed," Chem. Eng. Sci. **32**, 515–523 (1977).
Stanek, V., J. Hanika, V. Hlavacek and O. Trnka, "The Effect of Liquid Flow Distribution on the Behaviour of a Trickle Bed Reactor," Chem. Eng. Sci. **36**(6), 1045–1067 (1981).
Stauffer, F., "Time Dependence of the Relations Between Capillary Pressure, Water Content and Conductivity During Drainage of Porous Media," *in* IAHR Symposium on Scale Effects in Porous Media, Thessaloniki, Greece (1978).
Strasser, W., "CFD Study of an Evaporative Trickle Bed Reactor: Mal-Distribution and Thermal Runaway Induced by Feed Disturbances," Chem. Eng. J. **161**, 257–268 (2010).
Sun, C. G., F. H. Yin, A. Afacan, K. Nandakumar and K. T. Chuang, "Modelling and Simulation of Flow Maldistribution in Random Packed Columns With Gas–Liquid Countercurrent Flow," Chem. Eng. Res. Design **78**(A3), 378–388 (2000).
Sundaresan, S., "Liquid Distribution in Trickle-Bed Reactors," Energy Fuels **8**(3), 531–535 (1994).
Sundaresan, S., "Modelling the Hydrodynamics of Multiphase Flow Reactors: Current Status and Challenges," AIChE J. **46**(6), 1102–1105 (2000).
Szady, M. J. and S. Sundaresan, "Effect of Boundaries on Trickle-Bed Hydrodynamics," AIChE J. **37**(8), 1237–1241 (1991).
Takeda, K., "Mathematical Modelling of Pulverised Coal Combustion in a Blast Furnace," PhD Thesis, Imperial College, London (1994).
Teruel, F. E. and Rizwan-uddina, "A New Turbulence Model for Porous Media Flows. Part I: Constitutive Equations and Model Closure," Int J. Heat Mass Transf. **52**(19–20), 4264–4272 (2009). www.sciencedirect.com/science/article/pii/S0017931010004199
Tryggvason, G., B. Bunner, A. Esmaeeli, D. Juric, N. Al-Rawahi, W. Tauber, J. Han, S. Nas and Y. J. Janz, "A Front-Tracking Method for the Computations of Multiphase Flow," J. Comp. Phys. **169**, 708–759 (2001).
Tryggvason, G., M. Sussman and M. Y. Hussaini, "Immersed Methods Boundary for Fluid Interfaces," in "Computational Methods for Multiphase Flow," A. Prosperetti and G. Tryggvason, Eds., Cambridge University Press, UK (2007).
Tung, V. X. and V. K. Dhir, "A Hydrodynamic Model for 2-Phase Flow Through Porous-Media," Int. J. Multiphase Flow **14**(1), 47–65 (1988).
van Antwerpen, W., C. G. du Toit and P. G. Rousseau, "A Review of Correlations to Model the Packing Structure and Effective Thermal Conductivity in Packed Beds of Mono-Sized Spherical Particles," Nucl. Eng. Design **240**(7), 1803–1818 (2010).
Vortmeyer, D. and J. Schuster, "Evaluation of Steady Flow Profiles in Rectangular and Circular Packed-Beds by a Variational Method," Chem. Eng. Sci. **38**(10), 1691–1699 (1983).
Wammes, W. J. A., S. J. Mechielsen and K. R. Westerterp, "The Transition Between Trickle Flow and Pulse Flow in a Cocurrent Gas–Liquid Trickle-Bed Reactor at Elevated Pressures," Chem. Eng. Sci. **45**(10), 3149–3158 (1990).
Xu, R. N. and P. X. Jiang, "Numerical Simulation of Fluid Flow in Microporous Media," Int. J. Heat Fluid Flow **29**(5), 1447–1455 (2008).
Zhukova, T. B., V. N. Pisarenko and V. V. Kafarov, "Modelling and Design of Industrial Reactors With a Stationary Bed of Catalyst and Two-Phase Gas–Liquid Flow—A Review," Int. Chem. Eng. **30**, 57–102 (1990).
Zimmerman, S. P. and K. M. Ng, "Liquid Distribution in Trickling Flow Trickle-Bed Reactors," Chem. Eng. Sci. **41**(4), 861–866 (1986).

Manuscript received May 31, 2011; revised manuscript received September 1, 2011; accepted for publication September 7, 2011.